



UNIVERSITÀ DEGLI STUDI DI PERUGIA
DIPARTIMENTO DI FISICA E GEOLOGIA
XXXII DOTTORATO DI RICERCA IN FISICA

ACADEMIC YEAR 2018/2019

DOCTORAL THESIS

Hadronic decays
of the J/ψ meson

Candidate:

Alessio Mangoni

Supervisors:

Prof. Simone Pacetti

Prof. Livio Fanò

Contents

Introduction	6
1 The J/ψ meson	8
1.1 The discovery of the J/ψ	8
1.2 J/ψ properties	11
1.3 Experiments	13
1.3.1 The BESIII experiment	13
1.4 J/ψ production in e^+e^- annihilation	15
1.5 J/ψ decay mechanisms	18
1.6 Value of $ \psi_{J/\psi}(0) ^2$	21
1.7 J/ψ decays into leptons	22
1.8 J/ψ decays into three photons	23
1.9 J/ψ decays into baryons	25
1.9.1 Effective Lagrangian for $J/\psi \rightarrow B\bar{B}$	30
2 J/ψ decays into mesons	34
2.1 The $J/\psi \rightarrow \pi^+\pi^-$ decay	34
2.1.1 Introduction	34
2.1.2 Electromagnetic branching ratio	35
2.1.3 Theoretical background	38

2.1.4	The coupling constants $g_{\eta\gamma}^{J/\psi}$, $g_{\eta'\gamma}^{J/\psi}$ and $g_{f_1\gamma}^{J/\psi}$	45
2.1.5	The coupling constants $g_{\eta\gamma}^{\pi\pi}$, $g_{\eta'\gamma}^{\pi\pi}$ and $g_{f_1\gamma}^{\pi\pi}$	47
2.1.6	The imaginary part of $A^{gg\gamma}$	50
2.2	The decay $J/\psi \rightarrow K^+K^-$	52
3	J/ψ decays into baryons	54
3.1	The $J/\psi \rightarrow B\bar{B}$ decay	54
3.1.1	Introduction	54
3.1.2	Theoretical background	57
3.1.3	Experimental data	61
3.1.4	Results	64
3.1.5	The case of complex R	71
3.1.6	Discussion	74
3.2	The decays of the J/ψ and $\psi(2S)$ into $\Lambda\bar{\Lambda}$ and $\Sigma^0\bar{\Sigma}^0$	75
3.2.1	Theoretical background	75
3.2.2	Results	78
	Conclusions	82
A	Notations and experimental data	84
A.1	Notations	84
A.2	Experimental data	85
B	Decay width and branching ratio	87
B.1	Phase space	87
B.2	Decay width	89
B.3	Branching ratio	90
	Acknowledgements	95

Introduction

This dissertation is devoted to the study of the J/ψ meson and its hadronic decays. Since their discovery $c\bar{c}$ mesons, the so-called charmonia, have been representing unique tools to expand our knowledge on the dynamic of the strong interaction at various energy ranges, for example one of the most challenging questions of our times is to understand the strong interaction in the confinement domain [1].

The J/ψ meson high production rate in electron-positron collisions and very large radiative decay rate make it a perfect laboratory for studying exotic hadrons composed of light quarks and gluons, which are the keys to understanding the nature of the strong interaction [2].

In this work we propose mainly phenomenological and theoretical models that allow, together with the use of the available experimental data, the calculation of form factors (FFs) and decay amplitudes.

In the first chapter we give an overview of the J/ψ meson, including details of its discover and its properties. We calculate and report also some useful results about the J/ψ meson. In this chapter we talk about the BESIII collaboration, as one of the most important experiment for the study of the J/ψ meson.

The second and the third chapter are dedicated to the J/ψ decays, respectively, into mesons and baryons, showing our recent results that have been published in refereed journals [3–5]. In particular in the second chapter we focus our attention on the J/ψ decay into a pair of pions, showing that this process does not proceed only electromagnetically as believed so far, due to the presence of a non-negligible mixed strong-EM contribution to the total branching

ratio.

In the third chapter we consider mainly the decay of the J/ψ meson into a pair of baryon-antibaryon, where we separate, for the first time, the single strong, electromagnetic and strong-EM contributions to the total BR and the relative Feynman amplitudes, obtaining also the relative phase between the strong and the electromagnetic ones.

At the end of this thesis there are two appendices, in the first we include notations and some experimental data, while in the second we report some calculations about decay widths and branching ratios.

Chapter 1

The J/ψ meson

1.1 The discovery of the J/ψ

The quark model starts in 1964 with the proposal of the quarks existence [6–8] for a description of the fundamental structure of hadrons in terms of the $SU(3)$ symmetry group. In the same year, various models of strong interaction symmetry were proposed [9, 10]. Bjorken and Glashow, in the framework of the “eightfold way” idea by Gell-Mann [11–14], proposed the existence of a new quark called “charm” (c) [15]. This was the fourth after the “up” (u), “down” (d) and “strange” (s) quarks. The existence of a fourth quark was proposed also in a work of some years later [16], where it was necessary to explain some anomalies in the kaon decays. A first suggestion for the order of magnitude of the charm quark mass was proposed in 1974 by Gaillard and Lee [17], who found a value of around 1-2 GeV.

The new quark allowed the possibility of the presence of bound states composed by the quark-antiquark pair. In 1974, in the so-called “November Revolution” the first $c\bar{c}$ bound state, known today as J/ψ meson, was discovered simultaneously by the team of Samuel Ting [18] at Brookhaven (they called it J), from the reaction

$$p + \text{Be} \rightarrow e^+ + e^- + X$$

and by the team of Burton Richter [19] at SLAC (they called it ψ), with the processes

$$e^+e^- \rightarrow e^+e^-, \text{ hadrons, } \mu^+\mu^-,$$

in both cases as a resonance. There were subsequent confirmations about the anomalous

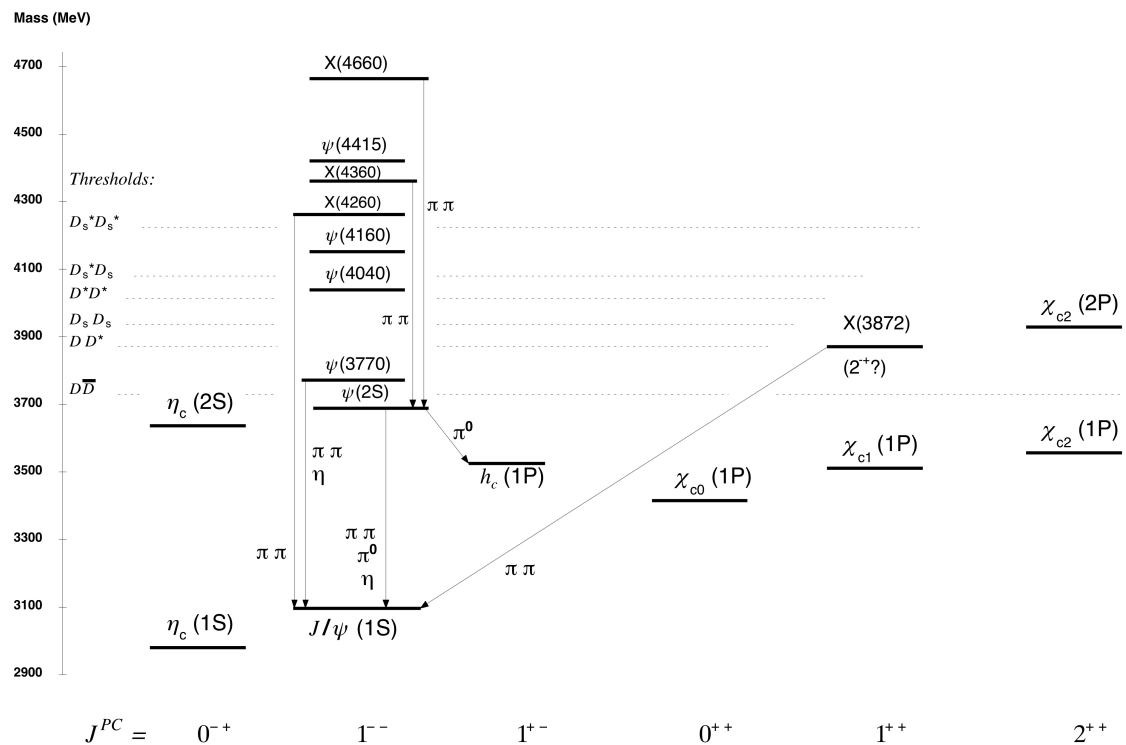


Figure 1.1: The level of charmonia [20].

increase in the cross section also at other experiments [21, 22]. Samuel Ting and Burton Richter received subsequently the Nobel prize in 1976 for their pioneering work in the discovery [23]. The discovery had a great impact in the community, for many reasons such as its simultaneous discovery in two different laboratories on two entirely different type of machines [24].

This resonance, the J/ψ meson, has a particularly small decay width, of the order of 10^2 keV, which suggests that decays to lighter hadrons are suppressed. This fact is related to

the phenomenological OZI¹ rule [7, 25–27], which postulates that processes having Feynman diagrams with disconnected quark lines are suppressed relative to connected ones.

The $c\bar{c}$ bound states are called “charmonium” [29] in analogy with positronium, the electron-

Table 1.1: Principal charmonium states properties [28].

Name	$I^G(J^{PC})$	$n^{2S+1}L_J$	Mass (MeV)	Width (MeV)
$\eta_c(1S)$	$0^+(0^{-+})$	1^1S_0	2983.9 ± 0.5	32.0 ± 0.8
$J/\psi(1S)$	$0^-(1^{--})$	1^3S_1	3096.900 ± 0.006	$(92.9 \pm 2.8) \times 10^{-3}$
$\chi_{c0}(1P)$	$0^+(0^{++})$	1^3P_0	3414.71 ± 0.30	10.8 ± 0.6
$\chi_{c1}(1P)$	$0^+(1^{++})$	1^3P_1	3510.67 ± 0.05	0.84 ± 0.04
$h_c(1P)$	$?^?(1^{+-})$	1^1P_1	3525.38 ± 0.11	0.7 ± 0.4
$\chi_{c2}(1P)$	$0^+(2^{++})$	1^3P_2	3556.17 ± 0.07	1.97 ± 0.09
$\eta_c(2S)$	$0^+(0^{-+})$	2^1S_0	3637.6 ± 1.2	$11.3^{+3.2}_{-2.9}$
$\psi(2S)$	$0^-(1^{--})$	2^3S_1	3686.097 ± 0.025	$(294 \pm 8) \times 10^{-3}$
$\psi(3770)$	$0^-(1^{--})$	1^3D_1	3773.13 ± 0.35	27.2 ± 1.0
$\chi_{c1}(3872)$	$0^+(1^{++})$		3871.69 ± 0.17	< 1.2
$\chi_{c2}(3930)$	$0^+(2^{++})$	2^3P_2	3927.2 ± 2.6	24 ± 6
$\psi(4040)$	$0^-(1^{--})$	3^3S_1	4039 ± 1	80 ± 10
$\psi(4160)$	$0^-(1^{--})$	2^3D_1	4191 ± 5	70 ± 10
$\psi(4360)$	$0^-(1^{--})$		4368 ± 13	96 ± 7
$\psi(4415)$	$0^-(1^{--})$	4^3S_1	4421 ± 4	62 ± 20
$\psi(4660)$	$0^-(1^{--})$		4643 ± 9	72 ± 11

positron (e^+e^-) bound state, whose bound-state level structure was similar and the J/ψ was the first charmonium to be discovered.

In 1976 a second sharp peak in the cross section for the $e^+e^- \rightarrow$ hadrons process was found [30], this was the discovery of the $\psi'(3685)$ charmonium. The spectroscopy of the charmonium family is shown in Fig. 1.1, while in Table 1.1 are reported some values of the principal charmonium states [31].

At that time, the charm quark was found in charm-anticharm bound states. Subsequently, also the lightest charmed mesons, named D mesons, were discovered [32]. The D^0 meson was

¹by S. Okubo, G. Zweig and J. Iizuka.

found as a resonance in $K^\pm\pi^\mp$ decays [33], while soon after were also discovered the D^+ , D^- and the excited state D^* [34].

1.2 J/ψ properties

The J/ψ meson has the following quantum numbers

$$I^G(J^{PC}) = 0^-(1^{--}),$$

the parity and charge conjugation eigenvalues are related to the orbital angular momentum (L) and spin (S) as follows

$$P = (-1)^{L+1}, \quad C = (-1)^{L+S}.$$

The J/ψ meson has the same quantum numbers of the photon, as was early investigated [35], in particular with the study of the $\mu^+\mu^-$ leptonic final state, where it was seen an interference with the non-resonant amplitude. Moreover the observation that decays into an odd number of pions were preferred led to the determination of a negative G -parity [36].

The J/ψ mass and decay width are determined experimentally and have the following values

$$M_{J/\psi} = (3.096916 \pm 0.000011) \text{ GeV}, \quad \Gamma_{J/\psi} = (92.9 \pm 2.8) \text{ keV},$$

taken from the Particle Data Group (PDG) [28]. For this reasons the J/ψ is indicated also with the $J/\psi(3100)$ notation, where the particle mass (in MeV) is indicated in parenthesis, or also $J/\psi(1S)$. The J/ψ meson is hindered to decay into mesons which contain a c quark due to its lightness, moreover, as anticipated, the small value of its decay width leads to a suppression of the decays into lighter hadrons.

Its mass has been measured firstly with high precision around 1980 [37–39], with methods that overcome the limitations due to the calibration of the absolute energy scale [40, 41]. On the other hand the J/ψ decay width has not been measured directly due to the high energy

spread of e^+e^- and $p\bar{p}$ accelerators, but should be inferred from the integrated leptonic reaction rate and the leptonic BR, assuming lepton universality. The first measures of the J/ψ decay width had a relative error of about 10% [42, 43].

The charmonium can be considered a non-relativistic system, contrary to what happens in a meson formed by light quarks. In a $c\bar{c}$ bound state the velocity v of the quark charm, in the center of mass (CM) system, is such that [31] $v^2/c^2 \sim 0.2$ or [44] $v^2/c^2 \sim 0.3$, where c is the speed of light in vacuum². Consequently, the charmonium spectrum can be simply described by the Schrödinger equation

$$\left[-\frac{\hbar^2}{2\mu} \vec{\nabla}^2 + V(\vec{r}) \right] \Psi(\vec{r}) = E \Psi(\vec{r}),$$

where $\mu \sim 2m_c$, being m_c the mass of the charm quark, and with a conventional quarkonium potential composed by the standard color Coulomb potential plus a linear term [45] of the type

$$V(r) = -\frac{a}{r} + kr, \quad (1.1)$$

called “Cornell potential”, where a and k can be found using a fitting procedure on the available data. In Ref. [46] authors found the following best fit values

$$a = 0.520, \quad k = 0.183 \text{ GeV}^2.$$

Corrections to the potential can also include, for example, terms for the fine structure or hyperfine interactions [47]. A potential model which incorporates the asymptotic freedom and linear quark confinement in a unified manner with the feature of a minimal number of parameters can be found in Ref. [48], while various potential models, from many authors, are reported in Refs. [49–55]. The standard potential shown in Eq. (1.1) is similar to that of positronium (e^+e^- bound state), except for the presence of the confinement term, linear in r .

² $c = 299\,792\,458 \text{ m/s}$ [28].

1.3 Experiments

The investigation of the properties and decays of the J/ψ meson is strongly related to its production in a particle accelerator. In particular, the simplest and cleanest way to produce J/ψ mesons is using an e^+e^- collider where the CM energy is fixed at the one corresponding to the J/ψ mass. The first e^+e^- colliders are SPEAR at Stanford [56–59], ADONE at Frascati [60–62], DORIS at Hamburg [63–65] and DCI at Orsay [66, 67]. Some of the detectors that provided measurements of the J/ψ decays are [68–74]:

- Mark I (SPEAR);
- DASP (DORIS);
- DESY (DORIS);
- PLUTO (DORIS);
- Crystal Ball (SPEAR);
- Mark II (SPEAR);
- DM2 (DCI);
- Mark III (SPEAR);
- BES (BEPC).

1.3.1 The BESIII experiment

One of the most important experiment for the study of the J/ψ meson operates at the Beijing Electron–Positron Collider II (BEPCII), an e^+e^- collider located in Beijing, People’s Republic of China at the Institute of High Energy Physics (IHEP). It uses the third generation of the Beijing Electron Spectrometer (BESIII) for the studies of light quarks, charm quarks

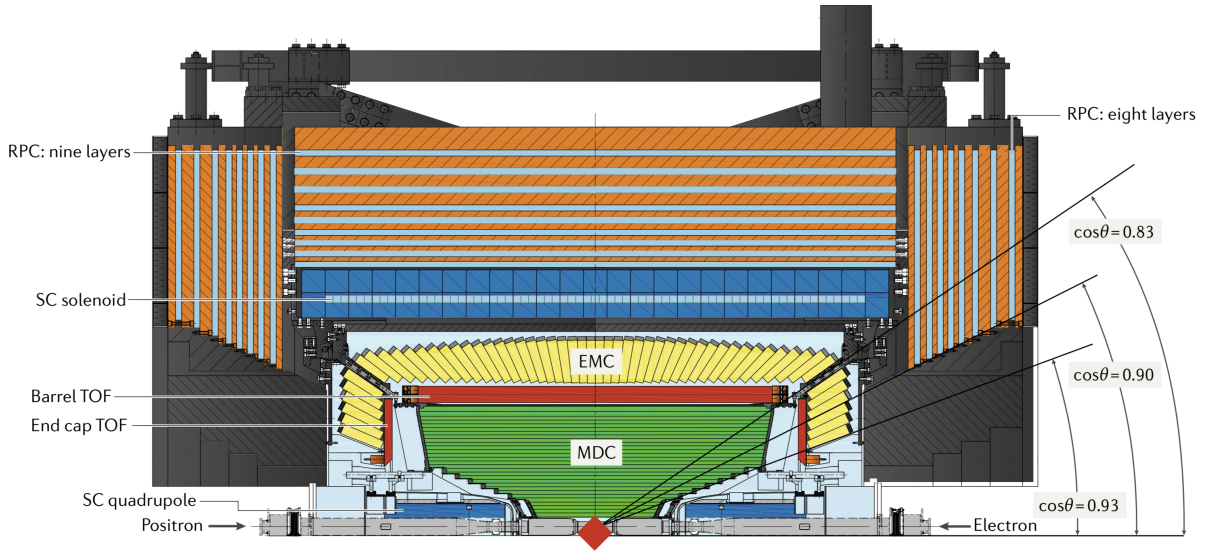


Figure 1.2: The BESIII detector [76].

and τ physics, being considered a so-called “charm-tau” factory [75]. In Fig. 1.2 is reported a scheme of the BESIII detector.

The physics program of the BESIII experiment includes: tests of electroweak interactions, studies of light hadron spectroscopy and decay properties, studies of the production and decay properties of the main charmonia, studies of charm and τ physics, search for glueballs, quark-hybrids, multi-quark states and other exotic states, precision measurements of QCD parameters and CKM parameters and search for new physics [77]. The BESIII experiment has the capability of adjusting the e^+e^- CM energy to the peaks of resonances and to just above or below the energy thresholds for particle–antiparticle pair formation [76]. In 2019 the collaboration has about 500 members from 72 institutions in 15 countries.

An e^+e^- collider has the advantage that the virtual photon produced by e^+e^- annihilation has the same quantum number of the J/ψ , allowing its direct production and, therefore, precise measurements of its mass and widths. BEPCII is a double ring machine with a design luminosity of about $1 \times 10^{33} \text{ cm}^{-2} \text{ s}^{-1}$ and a CM energy in the range (2.0–4.6) GeV [77]. Some of its parameters are reported in Table 1.2.

In 2019 the BESIII detector finished accumulating a sample of 10 billion J/ψ that is the world's largest data sample produced directly from e^+e^- annihilations. With 1.3 billion J/ψ events collected in 2009 and 2012, BESIII has reported many studies and the latest improvements have considerably boosted the sensitivity [2].

Table 1.2: Principal parameters of BEPCII [77].

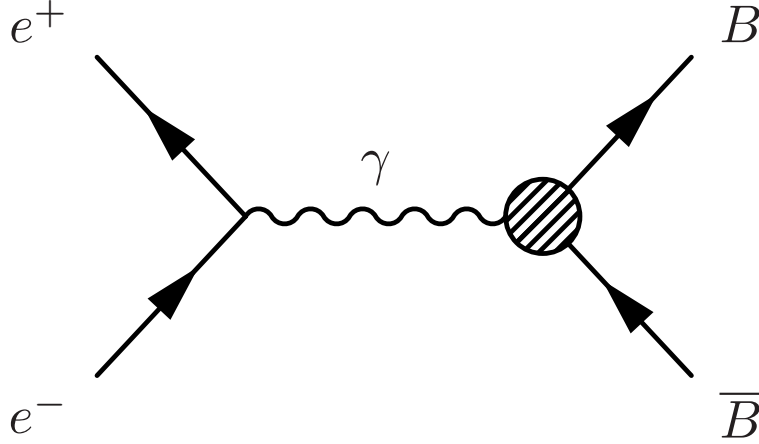
Parameters	BEPCII
Center of mass Energy	$(2.0 \div 4.6)$ GeV
Peak luminosity at 2×1.89 GeV	$\sim 10^{33} \text{ cm}^{-2} \text{ s}^{-1}$
Circumference	237.5 m
Number of rings	2
RF frequency	499.8 MHz
Number of bunches	2×93
Beam current	2×0.91 A
Bunch spacing	$2.4/8 \text{ m ns}^{-1}$
Bunch length (σ_z)	1.5 cm
Bunch width (σ_x)	$\sim 380 \text{ } \mu\text{m}$
Bunch height (σ_y)	$\sim 5.7 \text{ } \mu\text{m}$
Relative energy spread	5×10^{-4}
Crossing angle	± 11 mrad

1.4 J/ψ production in e^+e^- annihilation

Concerning the baryon-antibaryon production from an e^+e^- collider, we can find a relation between the continuum and the resonant amplitudes, where the considered intermediate state is the J/ψ meson. Consider firstly the generic process

$$e^-(k_1)e^+(k_2) \rightarrow B(p_1)\bar{B}(p_2),$$

where in parenthesis are shown the particle four-momenta and in Fig. 1.3 is reported the corresponding Feynman diagram. The amplitude can be written in terms of two FFs, \mathcal{F}_1^B

Figure 1.3: Feynman diagram for the process $e^+e^- \rightarrow B\bar{B}$.

and \mathcal{F}_2^B , that are functions of q^2 , being $q = p_1 + p_2 = k_1 + k_2$, as

$$-i\mathcal{A}(e^+e^- \rightarrow B\bar{B}) = \bar{v}(k_2)ie\gamma^\mu u(k_1) \left(\frac{-i\eta_{\mu\nu}}{q^2} \right) \bar{u}(p_1)ie\Gamma^\nu v(p_2),$$

where u (v) is the e^- (e^+) spinor, γ^μ are the Dirac matrices, Γ^μ is the baryonic vertex term and η is the Minkowski metric tensor with the $(+, -, -, -)$ signature. We have

$$\begin{aligned} \mathcal{A}(e^+e^- \rightarrow B\bar{B}) &= -e^2 \bar{v}(k_2)\gamma^\mu u(k_1) \left(\frac{\eta_{\mu\nu}}{q^2} \right) \bar{u}(p_1)\Gamma^\nu v(p_2) \\ &= -\frac{e^2}{q^2} \bar{v}(k_2)\gamma^\mu u(k_1) \bar{u}(p_1) \left(\gamma_\mu \mathcal{F}_1^B + i\frac{\sigma_{\mu\nu}q^\nu}{2M_B} \mathcal{F}_2^B \right) v(p_2), \end{aligned}$$

where $\bar{v}(k_2)\gamma_\mu u(k_1)$ is the leptonic four-current and $\bar{u}(p_1)\Gamma^\mu v(p_2)$ is the baryonic four-current

$$\Gamma^\mu = \gamma^\mu \mathcal{F}_1^B + i\frac{\sigma^{\mu\nu}q_\nu}{2M_B} \mathcal{F}_2^B, \quad (1.2)$$

being M_B the baryon mass. In the case of the non-resonant process

$$e^+e^- \rightarrow \gamma^* \rightarrow B\bar{B}$$

the two functions \mathcal{F}_1^B and \mathcal{F}_2^B are, respectively, the Dirac and Pauli FFs, called f_1^B and f_2^B .

The previous amplitude becomes

$$\mathcal{A}(e^+e^- \rightarrow B\bar{B}) = -e^2 \bar{v}(k_2) \gamma^\mu u(k_1) \left(\frac{\eta_{\mu\nu}}{q^2} \right) \bar{u}(p_1) \left(\gamma^\mu f_1^B + i \frac{\sigma^{\mu\nu} q_\nu}{2M_B} f_2^B \right) v(p_2).$$

In the case of the resonant process with the J/ψ meson, i.e.,

$$e^+e^- \rightarrow \gamma^* \rightarrow J/\psi \rightarrow B\bar{B},$$

the \mathcal{F} functions include the J/ψ propagator

$$\mathcal{F}_j^B = -i \frac{G_j^{\gamma*} G_j^{B\bar{B}}}{q^2 - M_{J/\psi}^2 + i M_{J/\psi} \Gamma_{J/\psi}}, \quad j = 1, 2,$$

where G_j^γ and $G_j^{B\bar{B}}$ represent, respectively, the coupling constant of the J/ψ with the photon and of the J/ψ with the baryon-antibaryon pair. Finally in the case of the process

$$e^+e^- \rightarrow \gamma^* \rightarrow J/\psi \rightarrow \gamma^* \rightarrow B\bar{B},$$

the FFs are

$$\begin{aligned} \mathcal{F}_j^{B\gamma} &= \left(-i \frac{G_j^{\gamma*} G_j^\gamma f_j}{q^2 - M_{J/\psi}^2 + i M_{J/\psi} \Gamma_{J/\psi}} \right) \left(\frac{-i}{q^2} \right) \\ &= - \frac{|G_j^\gamma|^2 f_j}{q^2 (q^2 - M_{J/\psi}^2 + i M_{J/\psi} \Gamma_{J/\psi})}, \quad j = 1, 2. \end{aligned}$$

Summing up all the three contributions (the continuum, the strong-resonant and the EM-resonant) we obtain the total FFs

$$\begin{aligned} \mathcal{F}_j^{\text{tot}} &= f_j^B + \mathcal{F}_j^B + \mathcal{F}_j^{B\gamma} = f_j^B - i \left(\frac{G_j^{\gamma*} G_j^{B\bar{B}} - i |G_j^\gamma|^2 f_j / q^2}{q^2 - M_{J/\psi}^2 + i M_{J/\psi} \Gamma_{J/\psi}} \right) \\ &= f_j^B \left[1 - \left(\frac{|G_j^\gamma|^2 / q^2 + i G_j^{\gamma*} G_j^{B\bar{B}} / f_j^B}{q^2 - M_{J/\psi}^2 + i M_{J/\psi} \Gamma_{J/\psi}} \right) \right], \quad j = 1, 2. \end{aligned}$$

Around the mass of the J/ψ meson we can write

$$\begin{aligned}\mathcal{F}_j^{\text{tot}} &= f_j^B \left[1 - \left(\frac{|G_j^\gamma|^2/M_{J/\psi}^2 + iG_j^{\gamma*}G_j^{B\bar{B}}/f_j^B}{q^2 - M_{J/\psi}^2 + iM_{J/\psi}\Gamma_{J/\psi}} \right) \right] \\ &= f_j^B \left[1 - \left(\frac{|C_j^\gamma| + |C_j|e^{i\varphi}}{q^2 - M_{J/\psi}^2 + iM_{J/\psi}\Gamma_{J/\psi}} \right) \right],\end{aligned}$$

with

$$|C_j^\gamma| \equiv \frac{|G_j^\gamma|^2}{q^2}, \quad C_j \equiv |C_j|e^{i\varphi} \equiv \frac{iG_j^{\gamma*}G_j^{B\bar{B}}}{f_j^B}, \quad \varphi = \arg \left(\frac{iG_j^{\gamma*}G_j^{B\bar{B}}}{f_j^B} \right),$$

where φ is the relative phase between C_j^γ and C_j , being C_j^γ a real quantity. The Feynman amplitude for the complete process (continuum, EM-resonant and strong-resonant) can be written as

$$\mathcal{A} = -\frac{e^2}{q^2} \bar{v}(k_2) \gamma^\mu u(k_1) \bar{u}(p_1) \left(\gamma_\mu \mathcal{F}_1^{\text{tot}} + i \frac{\sigma_{\mu\nu} q^\nu}{2M_B} \mathcal{F}_2^{\text{tot}} \right) v(p_2).$$

In the high energy limit, $q^2 \gg \Lambda_{\text{QCD}}^2$, the baryonic four-current $\bar{u}(p_1) \Gamma^\mu v(p_2)$ tends to $\bar{u}(p_1) \gamma^\mu G_M v(p_2)$, where G_M is the Sachs magnetic FF. The Feynman amplitude becomes

$$\mathcal{A} = -\frac{e^2}{q^2} \bar{v}(k_2) \gamma^\mu u(k_1) \bar{u}(p_1) \gamma_\mu v(p_2) G_M \left[1 - \left(\frac{|C_j^\gamma| + |C_j|e^{i\varphi}}{q^2 - M_{J/\psi}^2 + iM_{J/\psi}\Gamma_{J/\psi}} \right) \right],$$

and we can conclude that the continuum amplitude and the EM amplitude have opposite signs.

1.5 J/ψ decay mechanisms

The theory that describes the strong interaction, the quantum chromodynamics (QCD), is a very powerful theory at high energy. In the region of low and medium energy, calculations based on first principles are very difficult due to the non-perturbative contribution and often models are needed. In particular, charmonium states are on the boundary between perturbative and non-perturbative regimes so their decays, especially the hadronic ones, could be used to study QCD. Generally, the hadronic decays of the J/ψ meson can be parametrized using

three principal contributions, whose Feynman diagrams are shown in Fig. 1.4. At leading order, these are characterized by: a three-gluon (ggg), a two-gluon-plus-one-photon ($gg\gamma$) and a one-photon (γ) intermediate states, respectively [78, 79]. The former is related to the purely strong amplitude, while the latter is related to the purely electromagnetic (EM) one. It can be easily observed that in the case of the $gg\gamma$ contribution, see panel (b) of Fig. 1.4, a photon replaces one of the three gluons of the ggg one, shown in panel (a) of the same figure. Consider the generic decay

$$J/\psi \rightarrow \text{hadrons},$$

we can write its Feynman amplitude as the sum [80, 81]

$$\mathcal{A}(J/\psi \rightarrow \text{hadrons}) = \mathcal{A}^{ggg} + \mathcal{A}^{gg\gamma} + \mathcal{A}^{\gamma}. \quad (1.3)$$

The intermediate state with three photons, that has the same structure of the three-gluon one, is neglected being of order α^2 with respect to that with a single photon, being α the fine-structure constant³. These three contributions can also interfere, being, in general, complex quantities. Consider, for example, the case of G -parity conserving or violating decays. G -parity is a multiplicative quantum number defined as the product of charge conjugation and the isospin rotation by π radians around the y -axis, therefore the corresponding operator can be written as

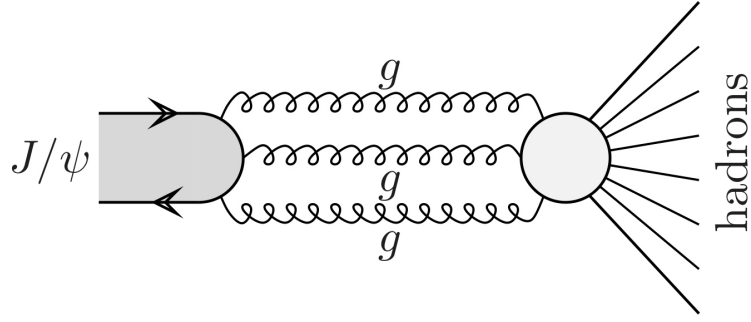
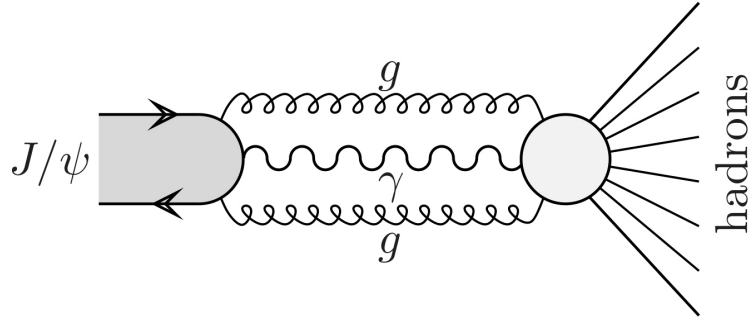
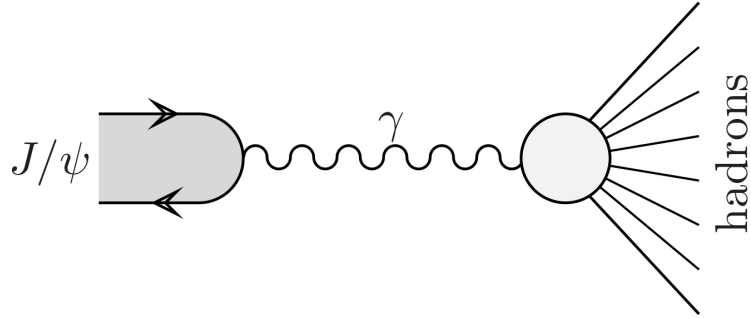
$$\hat{G} = e^{-i\pi\hat{I}_y}\hat{C}.$$

In the case of G -parity conserving decays, the first term on the right side of Eq. (1.3), i.e. \mathcal{A}^{ggg} , could be dominant ($\propto \alpha_S^3$, being α_S the QCD coupling constant), while it would be suppressed in presence of G -parity violation.

We report some experimental values of the J/ψ main decays, from PDG [28],

$$\text{BR}(J/\psi \rightarrow \text{hadrons}) = (87.7 \pm 0.5)\%,$$

³ $\alpha = 7.297\,352\,5664(17) \times 10^{-3}$ [28].

(a) The purely strong, $(ggg)^*$, intermediate state.(b) The mixed strong-EM, $(gg\gamma)^*$, intermediate state.(c) The purely EM, $(\gamma)^*$, intermediate state.Figure 1.4: The three principal contributions to the decay $J/\psi \rightarrow \text{hadrons}$.

$$\text{BR}(J/\psi \rightarrow e^+e^-) = (5.971 \pm 0.032)\%,$$

$$\text{BR}(J/\psi \rightarrow \mu^+\mu^-) = (5.961 \pm 0.033)\%.$$

The three-gluon and two-gluon-plus-one-photon decay widths are [29, 82–89]

$$\begin{aligned}\Gamma(J/\psi \rightarrow ggg) &= \frac{160}{81}(\pi^2 - 9) \frac{\alpha_S^3}{M_{J/\psi}^2} |\psi_{J/\psi}(0)|^2 \left(1 + 4.9 \frac{\alpha_S}{\pi}\right), \\ \Gamma(J/\psi \rightarrow gg\gamma) &= \frac{128}{9}(\pi^2 - 9) \frac{\alpha_S^2 \alpha Q_c^2}{M_{J/\psi}^2} |\psi_{J/\psi}(0)|^2 \left(1 - 0.9 \frac{\alpha_S}{\pi}\right).\end{aligned}$$

The EM decay width into leptons is [90, 91]

$$\Gamma(J/\psi \rightarrow l^+ l^-) = 16\pi \frac{\alpha^2 Q_c^2}{M_{J/\psi}^2} |\psi_{J/\psi}(0)|^2 \left(1 - \frac{16}{3} \frac{\alpha_S}{\pi}\right), \quad (1.4)$$

while the three-photons decay width is

$$\Gamma(J/\psi \rightarrow \gamma\gamma\gamma) = \frac{64}{3}(\pi^2 - 9) \frac{\alpha^3 Q_c^6}{M_{J/\psi}^2} |\psi_{J/\psi}(0)|^2 \left(1 - 12.6 \frac{\alpha_S}{\pi}\right). \quad (1.5)$$

In the previous expressions the corrections to α_S at the first order are also included.

It is common to define the ratio, called R , between the mixed strong-EM amplitude related to the $gg\gamma$ contribution shown in Fig. 1.4, panel (b), and the purely strong one, panel (a). This ratio can be calculated in the framework of perturbative QCD (pQCD), in fact it scales as the ratio of the EM to the strong coupling constant [78] and the result is

$$\lim_{q^2 \rightarrow +\infty} R(q^2) = -\frac{4}{5} \frac{\alpha}{\alpha_S(q^2)}. \quad (1.6)$$

1.6 Value of $|\psi_{J/\psi}(0)|^2$

The value of the modulus squared of the radial wave function of the J/ψ at the origin, $|\psi_{J/\psi}(0)|^2$, can be calculated from Eq. (1.4), since it is the expression where quantities are measured with more accuracy. Using numerical values from Ref. [28], one obtains

$$|\psi_{J/\psi}(0)|^2 = (0.0447 \pm 0.0014) \text{ GeV}^3.$$

1.7 J/ψ decays into leptons

The value of the BR for the decays of the J/ψ meson into a pair of leptons, l^+l^- , from PDG [28], is

$$\text{BR}(J/\psi \rightarrow l^+l^-) = (11.932 \pm 0.032)\%.$$

We can perform this computation by considering the generic process $c\bar{c} \rightarrow l^+l^-$ and write

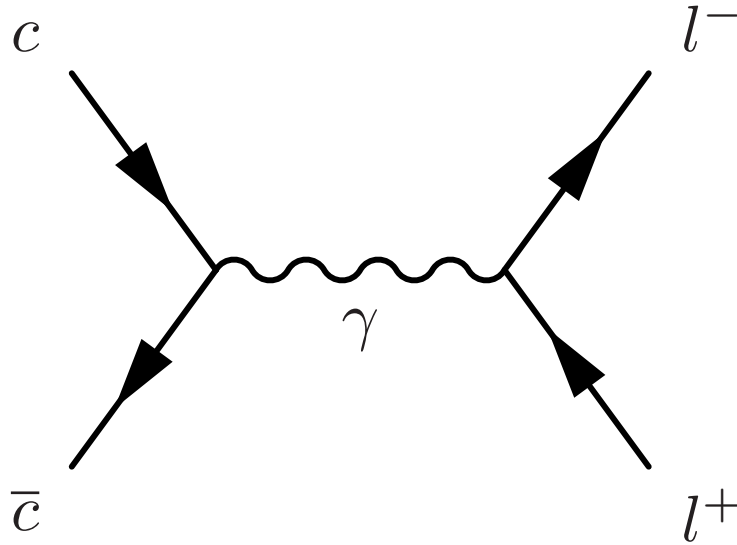


Figure 1.5: Feynman diagram for the EM scattering process $c\bar{c} \rightarrow l^+l^-$.

the amplitude of the Feynman diagram showed in Fig. 1.5,

$$\mathcal{A} = ie^2 Q_c \bar{u}(k_1) \gamma^\mu v(k_2) \frac{\eta_{\mu\nu}}{q^2} \bar{v}(p_2) \gamma^\nu u(p_1),$$

where k_1 , k_2 and p_1 , p_2 are, respectively, the four-momenta of the leptons and of the charm quarks, in the CM frame where $p_1 = p_2 \equiv p = (m_c, 0, 0, 0)$ with m_c mass of the charm quark, while q is the photon four-momentum, e is the elementary charge⁴ and Q_c is the charm quark charge in units of e ($Q_c = 2/3$), with $q^2 = (k_1 + k_2)^2 = (2p)^2 = 4m_c^2$. The mean squared

⁴ $e = 1.602\,176\,6208(98) \times 10^{-19}$ C [28].

modulus of the amplitude is

$$|\overline{\mathcal{A}}|^2 = \frac{\pi^2 \alpha^2 Q_c^2}{4m_c^4} \text{Tr} \left(\gamma_\mu (\not{p} + m_c) \gamma_\nu (\not{p} - m_c) \right) \text{Tr} \left(\gamma^\mu (\not{k}_2 - m) \gamma^\nu (\not{k}_1 + m) \right),$$

where m is the mass of the lepton⁵ and we have used the expression $e^2 = 4\pi\alpha$. The traces are

$$\text{Tr} \left(\gamma_\mu (\not{p} + m_c) \gamma_\nu (\not{p} - m_c) \right) = 8 \left(p_\mu p_\nu - m_c^2 \eta_{\mu\nu} \right),$$

$$\text{Tr} \left(\gamma^\mu (\not{k}_2 - m) \gamma^\nu (\not{k}_1 + m) \right) = 4 \left(k_1^\mu k_2^\nu + k_2^\mu k_1^\nu - k_1 \cdot k_2 \eta^{\mu\nu} - m^2 \eta^{\mu\nu} \right).$$

Neglecting m with respect to m_c , we obtain

$$|\overline{\mathcal{A}}|^2 = \frac{8\pi^2 \alpha^2 Q_c^2}{m_c^4} \left(2(k_1 \cdot p)(k_2 \cdot p) + m_c^2(k_1 \cdot k_2) \right) = 32\pi^2 \alpha^2 Q_c^2.$$

where we have used the following expressions

$$k_1 \cdot k_2 = 2m_c^2, \quad k_1 \cdot p = m_c^2, \quad k_2 \cdot p = m_c^2.$$

From Eq. (B.7) we have, finally,

$$\Gamma(J/\psi \rightarrow l^+ l^-) = \frac{64\pi}{9} \frac{\alpha^2}{M_{J/\psi}^2} |\psi_{J/\psi}(0)|^2,$$

with $m_c = M_{J/\psi}/2$, as reported in Eq. (1.4).

1.8 J/ψ decays into three photons

The $J/\psi \rightarrow \gamma\gamma\gamma$ decay was studied by various experiments, for example the Crystal Ball [92], and its BR can be calculated from a theoretical point of view. As done for the leptons final state, we can calculate the decay width of $J/\psi \rightarrow \gamma\gamma\gamma$ by considering the process $c\bar{c} \rightarrow \gamma\gamma\gamma$. In the CM frame we have the four-momenta of the charm quarks $p_1 =$

⁵ $m_e = 0.510\,998\,9461(31)$ MeV, $m_\mu = 938.272\,0813(58)$ MeV [28].

$p_2 \equiv p = (m_c, 0, 0, 0)$ with m_c mass of the charm quark. We denote with k_1, k_2, k_3 the four-momenta of the final state photons. Since there are three identical photons in the final state

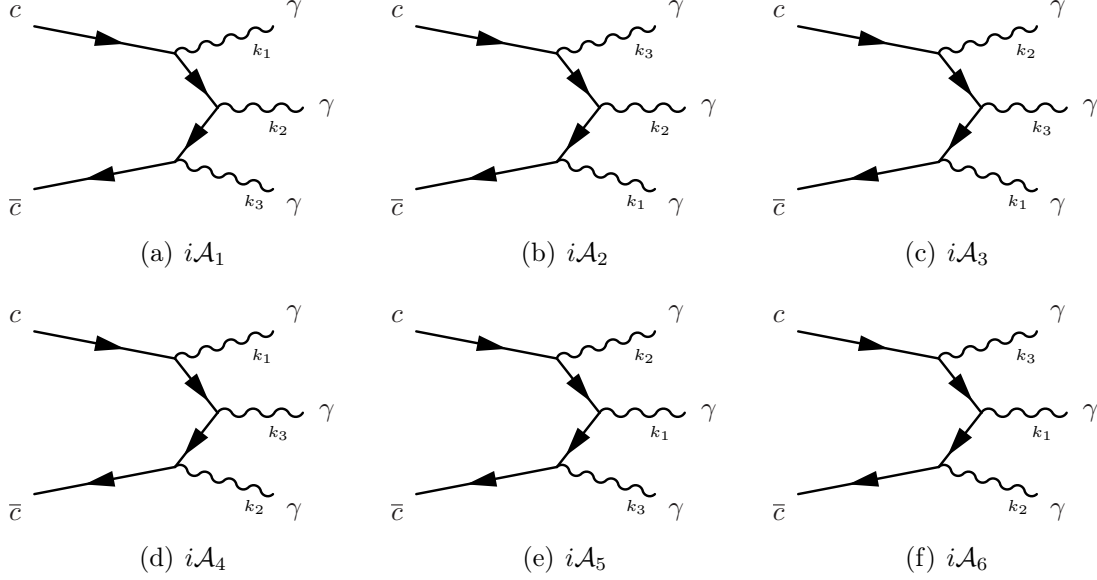


Figure 1.6: Feynman diagrams for the process $c\bar{c} \rightarrow \gamma\gamma\gamma$.

we have, at leading order, the $3! = 6$ Feynman diagrams shown in Fig. 1.6.

The squared moduli of the total amplitude is

$$\begin{aligned} |\overline{\mathcal{A}}|^2 &= \frac{1}{3!} \frac{1}{4} \sum_{\text{spin}} \sum_{\text{pol}} |\mathcal{A}|^2 = \frac{1024\pi^3 Q_c^6 \alpha^3}{3x^2(2m_c - x - z)^2 z^2} \left(2m_c^4 - 6m_c^3(x + z) \right. \\ &\quad + m_c^2(7x^2 + 13xz + 7z^2) - m_c(4x^3 + 9x^2z + 9xz^2 + 4z^3) \\ &\quad \left. + (x^2 + xz + z^2)^2 \right), \end{aligned}$$

where x, y and z are the energy of the photons, $Q_c = 2/3$ is the charm quark charge in units of the elementary charge e . The decay width is, using Eq. (B.3) and $m_c = M_{J/\psi}/2$,

$$\Gamma(J/\psi \rightarrow \gamma\gamma\gamma) = \frac{4096}{2187} (\pi^2 - 9) \frac{\alpha^3}{M_{J/\psi}^2} |\psi_{J/\psi}(0)|^2,$$

as reported in Eq. (1.5).

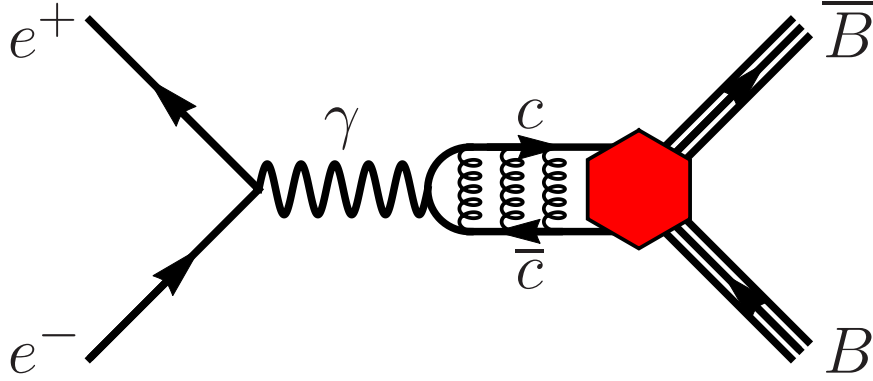


Figure 1.7: Feynman diagram of the process $e^+e^- \rightarrow \psi \rightarrow B\bar{B}$, the red hexagon represents the $\psi B\bar{B}$ coupling.

1.9 J/ψ decays into baryons

We consider the decay of a $c\bar{c}$ vector meson ψ (for example the J/ψ meson), produced via e^+e^- annihilation, into a baryon-antibaryon pair, $B\bar{B}$, i.e.,

$$e^-(k_1) + e^+(k_2) \rightarrow \psi(q) \rightarrow B(p_1) + \bar{B}(p_2), \quad (1.7)$$

where in parentheses are shown the four-momenta. The amplitude of the related Feynman diagram, shown in Fig. 1.7, is

$$\mathcal{A}(e^+e^- \rightarrow \psi \rightarrow B\bar{B}) = -ie^2 J_B^\mu D_\psi(q^2) \bar{v}(k_2) \gamma_\mu u(k_1),$$

where

$$J_B^\mu = \bar{u}(p_1) \Gamma^\mu v(p_2),$$

is the baryonic four-current, $D_\psi(q^2)$ is the ψ propagator, which includes the γ - ψ EM coupling, and $\bar{v}(k_2) \gamma_\mu u(k_1)$ is the leptonic four-current. The matrix Γ^μ , following Eq. (1.2), is [93]

$$\Gamma^\mu = \gamma^\mu f_1^B + \frac{i\sigma^{\mu\nu} q_\nu}{2M_B} f_2^B, \quad (1.8)$$

where M_B is the baryon mass and, f_1^B and f_2^B are constant FFs called, respectively, strong Dirac and Pauli couplings. The two FFs weight the vector and tensor part of the $\psi B\bar{B}$ vertex, where the latter contains also the anomalous magnetic moment. The strong electric and magnetic Sachs couplings [94], that have the same structure of the EM Sachs FFs, are

$$g_E^B = f_1^B + \frac{M_\psi^2}{4M_B^2} f_2^B, \quad g_M^B = f_1^B + f_2^B,$$

where M_ψ is the mass of the charmonium state⁶. The differential cross section of the process $e^+e^- \rightarrow \psi \rightarrow B\bar{B}$, in the e^+e^- CM frame, can be expressed in terms of the two Sachs couplings as follows

$$\frac{d\sigma}{d\cos\theta} = \frac{\pi\alpha^2\beta}{2M_\psi^2} \left(|g_M^B|^2 + \frac{4M_B^2}{M_\psi^2} |g_E^B|^2 \right) (1 + \alpha_B \cos^2\theta),$$

where β is the velocity⁷ of the baryon in final state, at the ψ mass, that can be written as

$$\beta = \sqrt{1 - \frac{4M_B^2}{M_\psi^2}},$$

being θ the scattering angle. Moreover, the polarization parameter α_B depends only on the modulus of the ratio g_E^B/g_M^B and is given by

$$\alpha_B = \frac{M_\psi^2 |g_M^B|^2 - 4M_B^2 |g_E^B|^2}{M_\psi^2 |g_M^B|^2 + 4M_B^2 |g_E^B|^2} = \frac{M_\psi^2 - 4M_B^2 |g_E^B/g_M^B|^2}{M_\psi^2 + 4M_B^2 |g_E^B/g_M^B|^2}, \quad (1.9)$$

with $\alpha_B \in [-1, 1]$.

The behavior of the polarization parameter α_B (as a function of the ratio $|g_E|/|g_M|$) and that of the ratio $|g_E|/|g_M|$ (as a function of α_B), in the particular case of $\psi = J/\psi$, are shown, respectively, in Fig. 1.8 and Fig. 1.9.

There three remarkable cases that can be discussed as examples:

- Maximum positive polarization ($\alpha_B = 1$)

⁶The four quantities f_1^B , f_2^B , g_E^B and g_M^B are in general complex numbers.

⁷We recall that $\beta = v/c$ therefore, in natural units where $c = 1$, $\beta = v$.

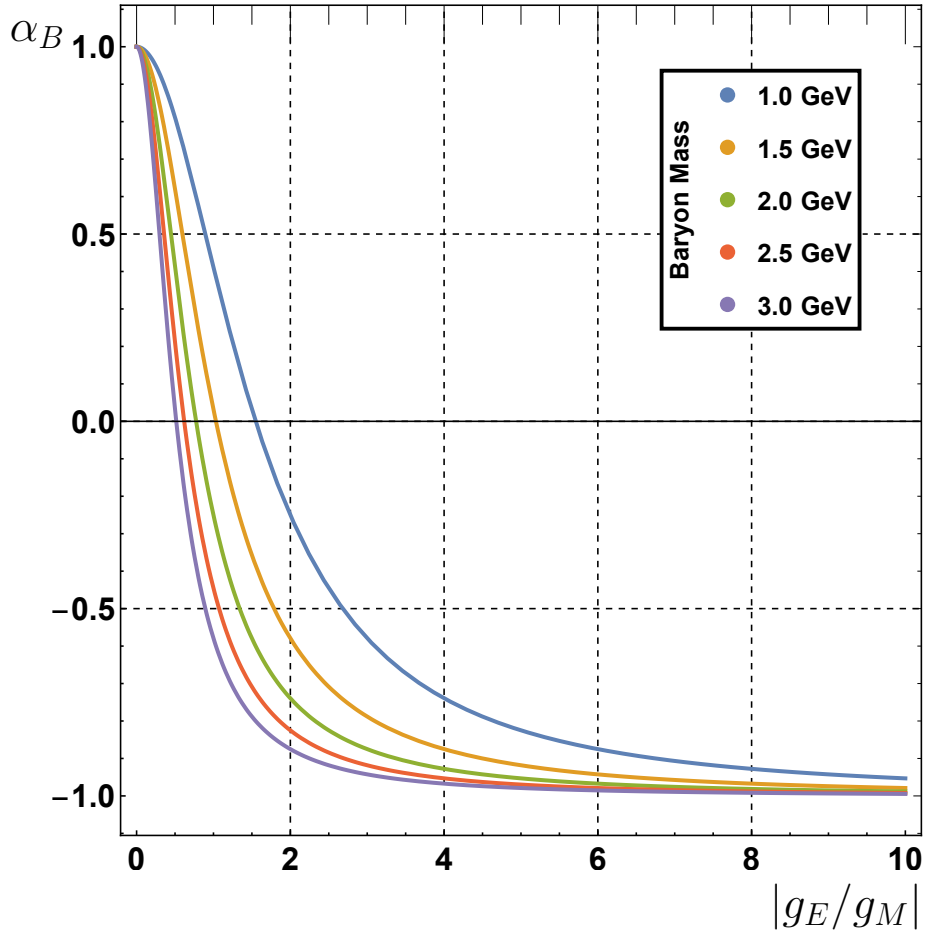


Figure 1.8: Polarization parameter α for $\psi = J/\psi$ and for various baryon masses from 1.0 GeV to 3.0 GeV, as a function of the ratio $|g_E|/|g_M|$.

the strong electric Sachs coupling vanishes, i.e.,

$$\alpha_B = 1 \quad \rightarrow \quad g_E^B = 0, \quad f_1^B = -\frac{M_\psi^2}{4M_B^2} f_2^B,$$

$$g_M^B = f_1^B \left(1 - \frac{4M_B^2}{M_\psi^2} \right) = f_2^B \left(1 - \frac{M_\psi^2}{4M_B^2} \right),$$

the relative phase between f_1^B and f_2^B is $i\pi$, and the ratio of the moduli is $M_\psi^2/(4M_B^2)$.

- Maximum negative polarization ($\alpha_B = -1$)

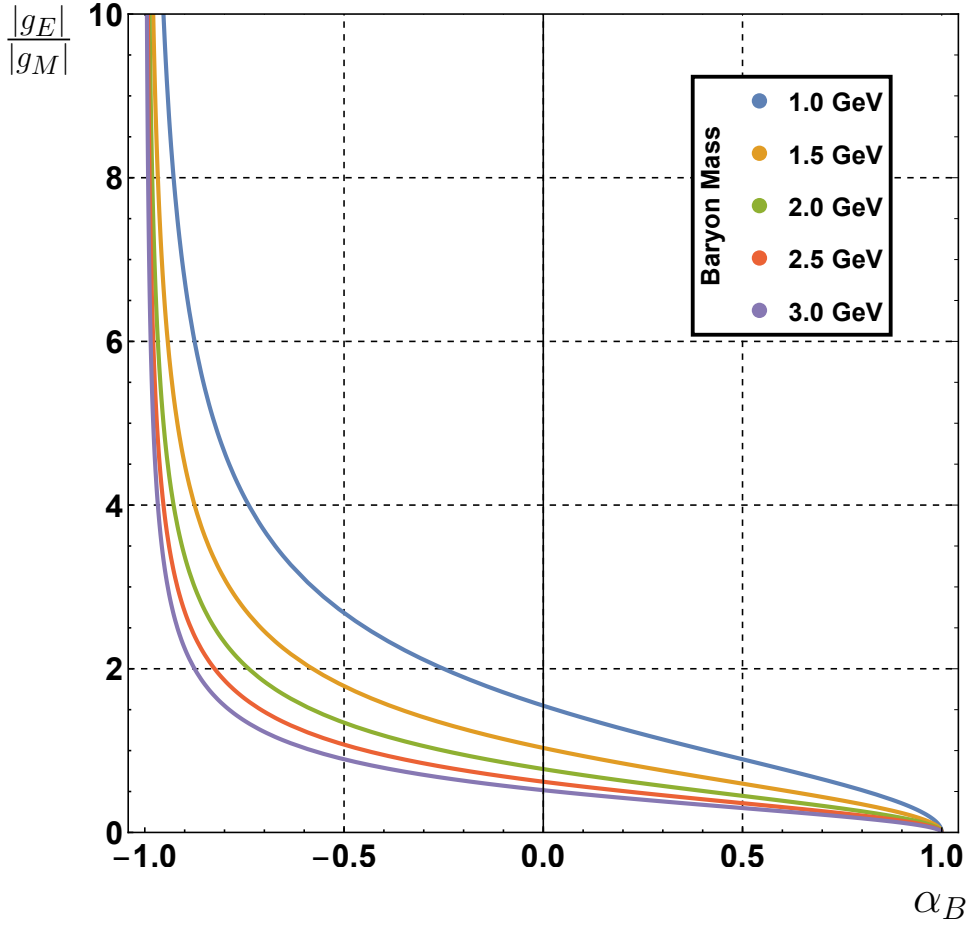


Figure 1.9: Ratio of the moduli of g_E and g_M for $\psi = J/\psi$ and for various baryon masses from 1.0 GeV to 3.0 GeV, as a function of the polarization parameter α .

$$\alpha_B = -1 \rightarrow g_M^B = 0, \quad f_1^B = -f_2^B,$$

$$g_E^B = f_1^B \left(1 - \frac{M_\psi^2}{4M_B^2} \right) = f_2^B \left(\frac{M_\psi^2}{4M_B^2} - 1 \right),$$

in this case the strong magnetic Sachs coupling vanishes, the relative phase between f_1^B and f_2^B is $-i\pi$ and the ratio of the moduli is one.

- No polarization ($\alpha_B = 0$)

the modulus of the ratio between the Sachs couplings become

$$\alpha_B = 0 \quad \rightarrow \quad \frac{|g_E^B|}{|g_M^B|} = \frac{M_\psi}{2M_B}.$$

The Feynman amplitude for the decay $\psi \rightarrow B\bar{B}$ can be written in terms of the strong magnetic and Dirac FFs as

$$\mathcal{A}(\psi \rightarrow B\bar{B}) = -i\epsilon_\psi^\mu \bar{u}(p_1)\Gamma_\mu v(p_2)$$

where the matrix Γ_μ is defined in Eq. (1.8), ϵ_ψ^μ is the polarization vector of the ψ meson, and the four-momenta follow the labelling of Eq. (1.7). The branching ratio (BR) is given by the standard form for the two-body decay

$$\mathcal{B}(\psi \rightarrow B\bar{B}) = \frac{1}{8\pi\Gamma_\psi} \overline{|\mathcal{A}(\psi \rightarrow B\bar{B})|^2} \frac{|\vec{p}_1|}{M_\psi^2}, \quad (1.10)$$

where Γ_ψ is the total width of the ψ meson. Using the mean value of the modulus squared of the amplitude, written in terms of the Sachs couplings,

$$\overline{|\mathcal{A}(\psi \rightarrow B\bar{B})|^2} = \frac{4}{3}M_\psi^2 \left(|g_M^B|^2 + \frac{2M_B^2}{M_\psi^2} |g_E^B|^2 \right).$$

we obtain the BR

$$\mathcal{B}(\psi \rightarrow B\bar{B}) = \frac{M_\psi\beta}{12\pi\Gamma_\psi} \left(|g_M^B|^2 + \frac{2M_B^2}{M_\psi^2} |g_E^B|^2 \right). \quad (1.11)$$

Since it does not depend on α_B , it cannot be used to determine the polarization parameter. The previous expression for the BR can be written as the sum of the moduli squared of two amplitudes

$$\text{BR}(\psi \rightarrow B\bar{B}) = |A_M^B|^2 + |A_E^B|^2, \quad (1.12)$$

where, comparing with Eq. (1.11),

$$A_M^B = \sqrt{\frac{M_\psi \beta}{12\pi\Gamma_\psi}} g_M^B, \quad A_E^B = \sqrt{\frac{M_\psi \beta}{6\pi\Gamma_\psi}} \frac{M_B}{M_\psi} g_E^B.$$

It follows that the polarization parameter of Eq. (1.9) can be also written as

$$\alpha_B = \frac{1 - 2|A_E^B|^2/|A_M^B|^2}{1 + 2|A_E^B|^2/|A_M^B|^2}.$$

1.9.1 Effective Lagrangian for $J/\psi \rightarrow B\bar{B}$

The spin-1/2 baryons are the proton (p), the neutron (n), the sigma baryons (Σ^\pm, Σ^0), the lambda particle (Λ) and the Ξ baryons (Ξ^-, Ξ^0). Some of their properties are shown in Table 1.3. They are organized into an octet of SU(3) and we can consider the following

Table 1.3: Mass and properties of spin-1/2 baryons from PDG [28].

Baryon	Mass M	Quark content
p	938.2720813(58) MeV	$u u d$
n	939.5654133(58) MeV	$u d d$
Σ^0	1192.642(24) MeV	$u d s$
Σ^+	1189.37(7) MeV	$u u s$
Σ^-	1197.449(30) MeV	$d d s$
Λ	1115.683(6) MeV	$u d s$
Ξ^0	1314.86(20) MeV	$u s s$
Ξ^-	1321.71(7) MeV	$d s s$

baryon matrix

$$\mathcal{B} = \begin{pmatrix} \Lambda/\sqrt{6} + \Sigma^0/\sqrt{2} & \Sigma^+ & p \\ \Sigma^- & \Lambda/\sqrt{6} - \Sigma^0/\sqrt{2} & n \\ \Xi^- & \Xi^0 & -2\Lambda/\sqrt{6} \end{pmatrix}.$$

Since the J/ψ meson is a $c\bar{c}$ bound state it behaves as a singlet with respect to the SU(3) symmetry group, therefore the leading order Lagrangian density for the decay $J/\psi \rightarrow B\bar{B}$

should have the invariant form [95]

$$\mathcal{L}^0 \propto \text{Tr} (B\bar{B}) .$$

Terms describing SU(3) symmetry breaking effects can be included to obtain a more complete Lagrangian density [96]. We consider, in particular, two types of symmetry breaking sources: the quark mass difference and the EM interaction. The first one can be parametrized by introducing the “spurion” matrix [95, 97, 98]

$$S_m = \frac{g_m}{3} \begin{pmatrix} 1 & 0 & 0 \\ 0 & 1 & 0 \\ 0 & 0 & -2 \end{pmatrix} ,$$

where g_m is the effective coupling constant. This matrix describes the mass breaking effect due to the s and u, d quarks mass difference related to the term

$$\frac{2m_u + m_s}{3} \bar{q}q + \frac{m_u - m_s}{\sqrt{3}} \bar{q}\lambda_8 q ,$$

where the SU(2) isospin symmetry is assumed, so that: $m_u = m_d$. The S_m matrix is proportional to the 8-th Gell-Mann matrix. The EM breaking effect is related to the fact that the photon-quark coupling constant is proportional to the electric charge, related to the term [96]

$$\mathcal{H}_{\text{em}} = \frac{e}{2} A^\mu \bar{q} \gamma_\mu \left(\lambda_3 + \frac{\lambda_8}{\sqrt{3}} \right) q ,$$

where e is the elementary charge, A^μ is the electromagnetic four-potential and λ_3 is the 3-rd Gell-Mann matrix. This effect can be parametrized using the spurion matrix

$$S_e = \frac{g_e}{3} \begin{pmatrix} 2 & 0 & 0 \\ 0 & -1 & 0 \\ 0 & 0 & -1 \end{pmatrix} ,$$

where g_e is the EM effective coupling constant.

The most general SU(3)-invariant effective Lagrangian density, which accounts for these effects, is

$$\begin{aligned}\mathcal{L} = & g \text{Tr}(B\bar{B}) + d \text{Tr}(\{\mathcal{B}, \bar{\mathcal{B}}\}S_e) + f \text{Tr}([\mathcal{B}, \bar{\mathcal{B}}]S_e) \\ & + d' \text{Tr}(\{\mathcal{B}, \bar{\mathcal{B}}\}S_m) + f' \text{Tr}([\mathcal{B}, \bar{\mathcal{B}}]S_m),\end{aligned}\quad (1.13)$$

where g, d, f, d', f' are coupling constants.

By considering single $B\bar{B}$ final states, the complete Lagrangian density can be written as the sum of seven contributions

$$\mathcal{L} = \mathcal{L}_{\Sigma^0\Lambda} + \mathcal{L}_p + \mathcal{L}_n + \mathcal{L}_{\Sigma^+} + \mathcal{L}_{\Sigma^-} + \mathcal{L}_{\Xi^0} + \mathcal{L}_{\Xi^-},$$

with the following sub-Lagrangian density, for the Σ^0 and Λ hyperons,

$$\begin{aligned}\mathcal{L}_{\Sigma^0\Lambda} = & \left(g + \frac{1}{3}dg_e + \frac{2}{3}d'g_m\right) \Sigma^0\bar{\Sigma}^0 + \left(g - \frac{1}{3}dg_e - \frac{2}{3}d'g_m\right) \Lambda\bar{\Lambda} \\ & + \left(\frac{\sqrt{3}}{3}dg_e\right) \Sigma^0\bar{\Lambda} + \left(\frac{\sqrt{3}}{3}dg_e\right) \Lambda\bar{\Sigma}^0,\end{aligned}\quad (1.14)$$

for the nucleons

$$\begin{aligned}\mathcal{L}_p = & \left(g + \frac{1}{3}dg_e + fg_e - \frac{1}{3}d'g_m + f'g_m\right) p\bar{p}, \\ \mathcal{L}_n = & \left(g - \frac{2}{3}dg_e - \frac{1}{3}d'g_m + f'g_m\right) n\bar{n},\end{aligned}$$

for the charged Σ hyperons

$$\begin{aligned}\mathcal{L}_{\Sigma^+} = & \left(g + \frac{1}{3}dg_e + fg_e + \frac{2}{3}d'g_m\right) \Sigma^+\bar{\Sigma}^-, \\ \mathcal{L}_{\Sigma^-} = & \left(g + \frac{1}{3}dg_e - fg_e + \frac{2}{3}d'g_m\right) \Sigma^-\bar{\Sigma}^+,\end{aligned}$$

and, finally, for the Ξ hyperons

$$\begin{aligned}\mathcal{L}_{\Xi^0} &= \left(g - \frac{2}{3}dg_e - \frac{1}{3}d'g_m - f'g_m \right) \Xi^0 \bar{\Xi}^0, \\ \mathcal{L}_{\Xi^-} &= \left(g + \frac{1}{3}dg_e - fg_e - \frac{1}{3}d'g_m - f'g_m \right) \Xi^- \bar{\Xi}^+.\end{aligned}$$

Chapter 2

J/ψ decays into mesons

In this chapter we present our results concerning the decays of the J/ψ into mesons. In Table 2.1 we report some of the larger BR of $J/\psi \rightarrow$ mesons from PDG [28].

Table 2.1: Branching ratios data from PDG [28] for some of the larger BR of the J/ψ decays into mesons.

Decay process	Branching ratio	Error
$J/\psi \rightarrow 2(\pi^+\pi^-)\pi^0$	$(3.37 \pm 0.26) \times 10^{-2}$	7.72%
$J/\psi \rightarrow 3(\pi^+\pi^-)\pi^0$	$(2.9 \pm 0.6) \times 10^{-2}$	20.69%
$J/\psi \rightarrow \pi^+\pi^-\pi^0\pi^0\pi^0$	$(2.71 \pm 0.29) \times 10^{-2}$	10.70%
$J/\psi \rightarrow \pi^+\pi^-\pi^0$	$(2.10 \pm 0.08) \times 10^{-2}$	3.81%
$J/\psi \rightarrow 2(\pi^+\pi^-\pi^0)$	$(1.61 \pm 0.21) \times 10^{-2}$	13.04%
$J/\psi \rightarrow \pi^+\pi^-\pi^0 K^+ K^-$	$(1.20 \pm 0.30) \times 10^{-2}$	25.00%

2.1 The $J/\psi \rightarrow \pi^+\pi^-$ decay

2.1.1 Introduction

The decay of the J/ψ meson into a pair of pions is an example of a G -parity violating decay. The J/ψ meson, having negative C -parity, $C_{J/\psi} = -1$, and isospin $I_{J/\psi} = 0$, has

negative G -parity $G_{J/\psi}$, being $G_{J/\psi} = C_{J/\psi}(-1)^{I_{J/\psi}} = -1$. The G -parity of a system of two pions, being a multiplicative quantum number, is positive ($G_{\pi\pi} = (-1)^2$). Therefore, the decay $J/\psi \rightarrow \pi^+\pi^-$ does not conserve G -parity. Strong interaction preserves G -parity as a consequence of its charge conjugation and isospin conservation. Electromagnetic and weak interactions can violate G -parity, being not invariant under G transformations. In this case of G -parity violation only two out of three contributions of Eq. (1.3) appear in the decay amplitude and we can write

$$\mathcal{A}(J/\psi \rightarrow \pi^+\pi^-) = \mathcal{A}^{gg\gamma} + \mathcal{A}^\gamma. \quad (2.1)$$

This fact can be generalized: when a decay violates isospin the purely strong amplitude is suppressed by the small dimensionless factor

$$\frac{m_u - m_d}{\sqrt{q^2}},$$

where m_u and m_d are the masses of u and d quarks and q^2 is the typical square momentum in the process.

The BR of J/ψ decay into a pair of pions can be decomposed as

$$\begin{aligned} \text{BR}(J/\psi \rightarrow \pi^+\pi^-) &= \text{BR}^{ggg}(J/\psi \rightarrow \pi^+\pi^-) + \text{BR}^{gg\gamma}(J/\psi \rightarrow \pi^+\pi^-) \\ &+ \text{BR}^\gamma(J/\psi \rightarrow \pi^+\pi^-) + \text{interference terms}, \end{aligned} \quad (2.2)$$

where

$$\mathcal{B}_X(J/\psi \rightarrow \pi^+\pi^-) \propto |\mathcal{A}_X(J/\psi \rightarrow \pi^+\pi^-)|^2,$$

with $X = ggg, gg\gamma, \gamma$.

2.1.2 Electromagnetic branching ratio

The EM contribution $\text{BR}^\gamma(J/\psi \rightarrow \pi^+\pi^-)$, corresponding to the intermediate state of the third Feynman diagram of Fig. 1.4, can be computed in terms of the “dressed” $e^+e^- \rightarrow \pi^+\pi^-$

and “bare” $e^+e^- \rightarrow \mu^+\mu^-$ cross sections, evaluated at the mass of the J/ψ , as [99,100]

$$\text{BR}^\gamma(J/\psi \rightarrow \pi^+\pi^-) = \mathcal{B}(J/\psi \rightarrow \mu^+\mu^-) \frac{\sigma(e^+e^- \rightarrow \pi^+\pi^-)}{\sigma^0(e^+e^- \rightarrow \mu^+\mu^-)} \bigg|_{q^2=M_{J/\psi}^2}, \quad (2.3)$$

where σ^0 stands for the bare cross section, i.e., the cross section corrected for the vacuum-

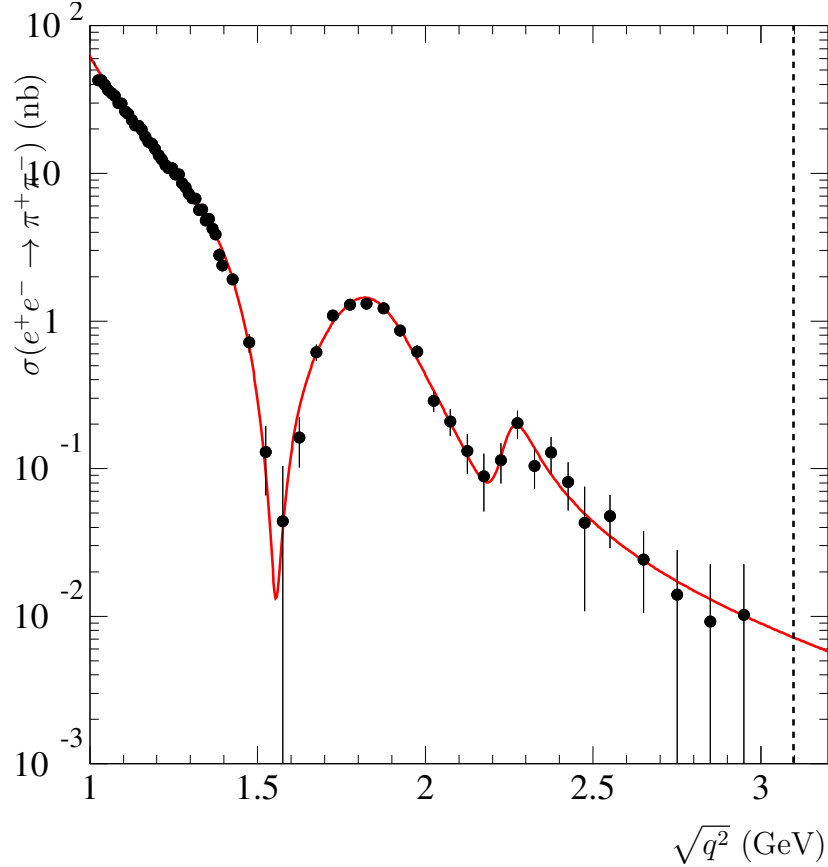


Figure 2.1: BABAR data on the $e^+e^- \rightarrow \pi^+\pi^-$ cross section and the fit (red line) from [101]. The vertical dashed line shows the J/ψ mass.

polarization contribution. It is a common belief the hypothesis of $\text{BR}^\gamma(h)$ -dominance in the J/ψ decays that violate G -parity, i.e., the fact that these decays proceed almost purely electromagnetically, with a negligible mixed strong-EM BR contribution, $\text{BR}^{gg\gamma}(J/\psi \rightarrow \pi^+\pi^-)$. Under this hypothesis the total BR should be given by the only EM one. This fact can

be verified, for example, for all the hadronic final states, h , with even numbers of pions as $h = 2(\pi^+\pi^-)$, $h = 2(\pi^+\pi^-\pi^0)$ and $h = 3(\pi^+\pi^-)$, for which $\text{BR}^\gamma(h) \simeq \mathcal{B}_{\text{PDG}}(h)$, as discussed in Ref. [100] using data from Refs. [102, 103].

For the decay $J/\psi \rightarrow \pi^+\pi^-$, using the value of the cross section $\sigma(e^+e^- \rightarrow \pi^+\pi^-)$ at the J/ψ mass, extrapolated from the BABAR data [101] with a fit based on the Gounaris-Sakurai formula [104] (see Fig. 2.1) the BR due to the one-photon exchange mechanism is

$$\text{BR}^\gamma(\pi^+\pi^-) = (4.7 \pm 1.7) \times 10^{-5}, \quad (2.4)$$

to be compared with [28]

$$\mathcal{B}_{\text{PDG}}(\pi^+\pi^-) = (14.7 \pm 1.4) \times 10^{-5}. \quad (2.5)$$

In this case the purely electromagnetic BR, Eq. (2.4), differs from the PDG value, Eq. (2.5), by almost 4.3 standard deviations. This result unavoidably means that there must be a further contribution beyond the purely EM one. Since the purely strong three-gluon amplitude, \mathcal{A}^{ggg} , is suppressed by G -parity conservation, the remaining amplitude that, contrary to what commonly expected, could play an important role is the one related to the second diagram of Fig. 1.4, i.e., $\mathcal{A}^{gg\gamma}$. Moreover, having two sizable amplitudes, \mathcal{A}^γ and $\mathcal{A}^{gg\gamma}$, there could also be a constructive interference term that would help in reconciling the prediction and the measured value for the total BR. The amplitude is the one in Eq. (2.1) where the two terms, purely EM and mixed strong-EM, are to be considered both relevant. The total BR, from Eq. (2.2), becomes

$$\begin{aligned} \mathcal{B}(J/\psi \rightarrow \pi^+\pi^-) &= \text{BR}^\gamma(J/\psi \rightarrow \pi^+\pi^-) + \text{BR}^{gg\gamma}(J/\psi \rightarrow \pi^+\pi^-) \\ &+ \mathcal{I}(J/\psi \rightarrow \pi^+\pi^-), \end{aligned} \quad (2.6)$$

where $\mathcal{I}(J/\psi \rightarrow \pi^+\pi^-)$ accounts for the interference term.

2.1.3 Theoretical background

The calculation of the amplitude $\mathcal{A}^{gg\gamma}(J/\psi \rightarrow \pi^+\pi^-)$ in the framework of QCD is quite difficult because the hadronization of the two-gluon plus one-photon intermediate state into $\pi^+\pi^-$ occurs at the few-GeV energy regime where QCD is still not perturbative. We find a lower limit for $\text{BR}^{gg\gamma}(J/\psi \rightarrow \pi^+\pi^-)$, as reported in Ref. [3], and show that, within the errors, it is of the same order of $\text{BR}^\gamma(J/\psi \rightarrow \pi^+\pi^-)$.

First of all we can decompose the BR contribution $\text{BR}^{gg\gamma}$ as

$$\begin{aligned} \text{BR}^{gg\gamma} = \text{BR}_{\text{Re}}^{gg\gamma} + \text{BR}_{\text{Im}}^{gg\gamma} &= \frac{1}{2M_{J/\psi}\Gamma_{J/\psi}} \times \left(\int d\rho_2 \overline{(\text{Re}(\mathcal{A}^{gg\gamma}))^2} \right. \\ &\quad \left. + \int d\rho_2 \overline{(\text{Im}(\mathcal{A}^{gg\gamma}))^2} \right), \end{aligned} \quad (2.7)$$

in order to highlight the contributions due to the real and imaginary parts of $\mathcal{A}^{gg\gamma}$, where $d\rho_2$ is the element of the two-body phase space, $M_{J/\psi}$ and $\Gamma_{J/\psi}$ are the mass and the width of the J/ψ meson.

It is possible to use the Cutkosky rule [105] to calculate the imaginary part of the amplitude $\mathcal{A}^{gg\gamma}$ by considering all possible on-shell intermediate states that can contribute to the decay chain $J/\psi \rightarrow (gg\gamma)^* \rightarrow \pi^+\pi^-$. Taking into account the mechanism where the two gluons hadronize into a set \mathcal{P} of $C = +1$ mesons h_j , the decay proceeds as

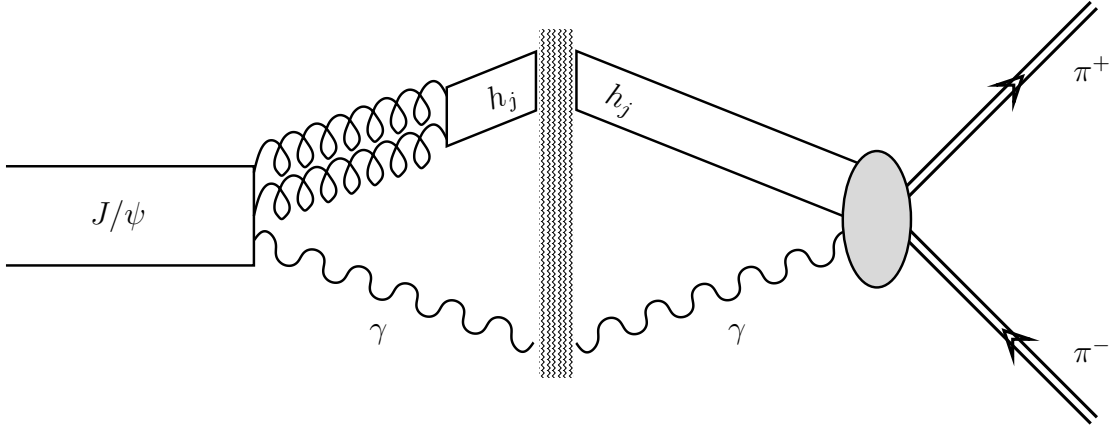
$$J/\psi \rightarrow \sum_{h_j \in \mathcal{P}} (h_j\gamma)^* \rightarrow \pi^+\pi^-.$$

The elements h_j of the set \mathcal{P} are only light unflavored mesons, that then couple strongly (OZI-allowed process) with the $\pi^+\pi^-$ final state.

Using the Cutkosky rule [105], sketched in Fig. 2.2, the imaginary part of $\mathcal{A}^{gg\gamma}$ is given in terms of a series on the intermediate states $h_j\gamma$, i.e.,

$$\text{Im}(\mathcal{A}^{gg\gamma}) = \frac{1}{2} \sum_j \sum_{\text{pol}} d\rho \mathcal{A}^*(J/\psi \rightarrow h_j\gamma) \mathcal{A}(\pi^+\pi^- \rightarrow h_j\gamma), \quad (2.8)$$

where the internal-sum runs over the photon polarizations and the integration is on the phase

Figure 2.2: Application of the Cutkosky rule for the decay $J/\psi \rightarrow (gg\gamma)^* \rightarrow \pi^+\pi^-$.

space

$$d\rho = \frac{p^0}{4\pi M_{J/\psi}} \frac{d\Omega}{4\pi}, \quad (2.9)$$

being p^μ the four-momentum of the photon. The selection of all the possible intermediate channels is experimentally driven. As a first estimate of the contribution that each channel

Table 2.2: Branching ratios of a selection of intermediate decays [28].

Meson M	J^{PC}	$10^3 \times \mathcal{B}(J/\psi \rightarrow h_j \gamma)$	$10^3 \times \mathcal{B}(h_j \rightarrow \pi^+ \pi^- \gamma)$
η	0^{-+}	1.104 ± 0.034	42.2 ± 0.8
$\eta'(958)$	0^{++}	5.13 ± 0.17	289 ± 50
$f_2(1270)$	2^{++}	1.64 ± 0.12	no data
$f_1(1285)$	1^{++}	0.61 ± 0.08	$(\rho^0) 53 \pm 12$
$f_0(1500)$	0^{++}	0.109 ± 0.024	no data
$f_2'(1525)$	2^{++}	$0.57^{+0.08}_{-0.05}$	no data
$f_0(1710)$	0^{++}	0.38 ± 0.05	no data
$f_4(2050)$	4^{++}	2.7 ± 0.7	no data
$f_0(2100)$	0^{++}	0.62 ± 0.10	no data
$\eta(2225)$	0^{-+}	$0.314^{+0.050}_{-0.019}$	no data

can give, one could consider the product of the BRs, i.e., $\mathcal{B}(J/\psi \rightarrow h_j \gamma) \times \mathcal{B}(\pi^+ \pi^- \rightarrow h_j \gamma)$. Table 2.2 reports all the BRs listed in Ref. [28]. While there are ten candidates on the J/ψ

side, only three sets of data are available on the $\pi^+\pi^-$ side. The most prominent contribution is the one due to the η' meson, followed by that due to the η . A further contribution that could be considered is the one due to the axial vector meson $f_1(1285)$, for which the combined strength is compatible with that of the η meson. In light of that, the imaginary part of the amplitude $\mathcal{A}^{gg\gamma}$, from Eq (2.8), has three main contributions, i.e.,

$$\begin{aligned} \text{Im}(\mathcal{A}^{gg\gamma}) &\simeq \frac{1}{2} \oint d\rho \mathcal{A}^*(J/\psi \rightarrow \eta\gamma) \mathcal{A}(\pi^+\pi^- \rightarrow \eta\gamma) \\ &+ \frac{1}{2} \oint d\rho \mathcal{A}^*(J/\psi \rightarrow \eta'\gamma) \mathcal{A}(\pi^+\pi^- \rightarrow \eta'\gamma) \\ &+ \frac{1}{2} \oint d\rho \mathcal{A}^*(J/\psi \rightarrow f_1\gamma) \mathcal{A}(\pi^+\pi^- \rightarrow f_1\gamma) \\ &\simeq \text{Im}(\mathcal{A}_{\eta'\gamma}) + \text{Im}(\mathcal{A}_{\eta\gamma}) + \text{Im}(\mathcal{A}_{f_1\gamma}), \end{aligned} \quad (2.10)$$

where f_1 stands for the $f_1(1285)$ meson and the approximate identity is due to the truncation of the series.

The first amplitude in the right-hand-side of Eq (2.8), considering the decay

$$J/\psi(P) \rightarrow h_j(k) + \gamma(p),$$

where in parentheses are reported the particle four-momenta, can be written as [106, 107]

$$\mathcal{A}(J/\psi \rightarrow \eta\gamma) = g_{\eta\gamma}^{J/\psi} p_\tau P_\lambda \epsilon_\delta(J/\psi) \epsilon_\sigma(\gamma) \varepsilon^{\tau\lambda\delta\sigma}, \quad (2.11)$$

$$\mathcal{A}(J/\psi \rightarrow f_1\gamma) = g_{f_1\gamma}^{J/\psi} p_\tau \epsilon_\lambda(f_1) \epsilon_\delta(J/\psi) \epsilon_\sigma(\gamma) \varepsilon^{\tau\lambda\delta\sigma},$$

where $g_{\eta\gamma}^{J/\psi}$ and $g_{f_1\gamma}^{J/\psi}$ are the coupling constants, $\epsilon_\delta(J/\psi)$, $\epsilon_\sigma(\gamma)$ and $\epsilon_\lambda(f_1)$ are the J/ψ , photon and axial vector polarization vectors, and $\varepsilon^{\tau\lambda\delta\sigma}$ is the Levi-Civita symbol.

The second amplitude in the right-hand-side of Eq. (2.8) concerns the $\pi^+\pi^-$ annihilation process

$$\pi^+(k_1) + \pi^-(k_2) \rightarrow h_j(k) + \gamma(p). \quad (2.12)$$

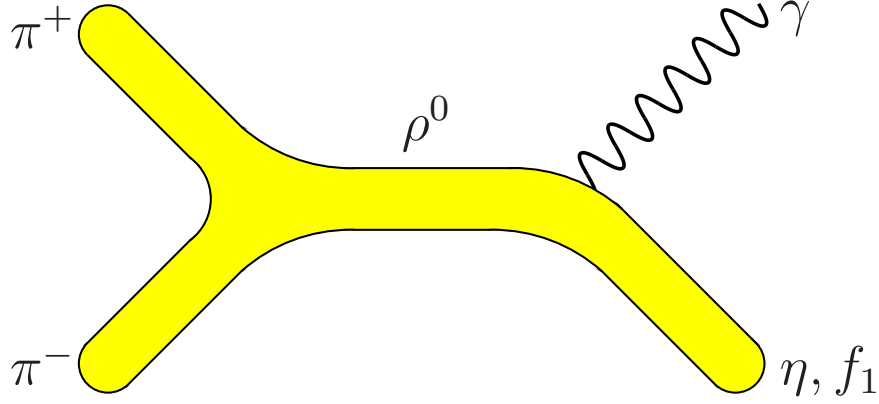


Figure 2.3: Feynman diagram for $\pi^+\pi^- \rightarrow \eta\gamma$ and $\pi^+\pi^- \rightarrow f_1\gamma$ mediated by the ρ^0 meson.

The amplitude for this process can be computed in terms of effective meson fields, as described by the Feynman diagram of Fig. 2.3. Here the coupling between the $\pi^+\pi^-$ initial state and the $h_j\gamma$ final state is assumed to be mediated by the ρ^0 vector meson. Such an assumption is supported by the strong affinity of the two-pion system with quantum numbers $J^{PC} = 1^{--}$ and the ρ^0 , experimentally confirmed by the BR $\mathcal{B}(\rho^0 \rightarrow \pi^+\pi^-) = 1$ [28]. It follows that the amplitudes read [106, 107]

$$\mathcal{A}(\pi\pi \rightarrow \eta\gamma) = g_{\eta\gamma}^{\pi\pi} \frac{d_\alpha p_\beta \epsilon_\mu(\gamma) q_\nu \varepsilon^{\alpha\beta\mu\nu}}{M_\rho^2 - q^2 - iM_\rho\Gamma_\rho}, \quad (2.13)$$

$$\mathcal{A}(\pi\pi \rightarrow f_1\gamma) = g_{f_1\gamma}^{\pi\pi} \frac{d_\alpha p_\beta \epsilon_\mu(\gamma) \epsilon_\nu(f_1) \varepsilon^{\alpha\beta\mu\nu}}{M_\rho^2 - q^2 - iM_\rho\Gamma_\rho},$$

where $g_{\eta(f_1)\gamma}^{\pi^+\pi^-}$ is the $\pi^+\pi^-\eta(f_1)\gamma$ coupling constant, $d = k_1 - k_2$, while $q = k_1 + k_2$, M_ρ and Γ_ρ are the four-momentum, the mass and the width of the ρ^0 meson.

The imaginary term at denominator, $iM_\rho\Gamma_\rho$, can be omitted, because its contribution to the resulting BR is of the order of 0.01% and then it is negligible with respect to the experimental uncertainty. Moreover, the negligibility of this term allows to recover the reality of $\text{Im}(\mathcal{A}^{gg\gamma})$, by also validating the truncation of the Cutkosky series.

In the CM system we can write the four-momenta

$$\begin{aligned} P = q &= (M_{J/\psi}, 0, 0, 0), \quad p = (p^0, \vec{p}) = p^0(1, \sin(\theta), 0, \cos(\theta)), \\ k &= (k^0, -\vec{p}), \quad k_{1,2} = (M_{J/\psi}/2, 0, 0, \pm\omega), \end{aligned} \quad (2.14)$$

with the scalar products

$$\begin{aligned} p^2 &= 0, \quad P^2 = M_{J/\psi}^2, \quad (k_1 - k_2) \cdot P = 0, \quad (k_1 - k_2) \cdot p = -2p^0\omega \cos \theta, \\ P \cdot \epsilon(J/\psi) &= 0, \quad p \cdot P = p^0 M_{J/\psi}, \end{aligned} \quad (2.15)$$

where θ is the scattering angle of the photon and ω is the modulus of the pion three-momenta.

We have also the following relations for the energies

$$\begin{aligned} E_\gamma &= p^0 = |\vec{p}| = \frac{M_{J/\psi}}{2} \left(1 - \frac{M_\eta^2}{M_{J/\psi}^2} \right), \\ E_{h_j} &= k^0 = \sqrt{M_{h_j}^2 + (p^0)^2} = \frac{M_{J/\psi}}{2} \left(1 + \frac{M_{h_j}^2}{M_{J/\psi}^2} \right). \end{aligned}$$

We calculate explicitly only the case of $h = \eta$, since the others can be obtained by replacing the masses and the coupling constants with the corresponding new ones.

We define the quantity

$$Z_\eta \equiv \sum_{\text{pol}} \mathcal{A}(\pi^+\pi^- \rightarrow \eta\gamma) \mathcal{A}^*(J/\psi \rightarrow \eta\gamma),$$

and, using the amplitudes of Eq. (2.11) and Eq. (2.13), we compute

$$\begin{aligned}
Z_\eta &= \frac{g_{\eta\gamma}^{\pi\pi} g_{\eta\gamma}^{J/\psi}}{M_\rho^2 - M_{J/\psi}^2} d_\alpha p_\beta q_\nu P_\lambda p_\tau \epsilon_\delta(J/\psi) \varepsilon^{\beta\alpha\nu\mu} \varepsilon^{\tau\lambda\delta\sigma} \sum_{\text{pol}} \epsilon_\mu(\gamma) \epsilon_\sigma(\gamma) \\
&= -\frac{g_{\eta\gamma}^{\pi\pi} g_{\eta\gamma}^{J/\psi}}{M_\rho^2 - M_{J/\psi}^2} (k_1 - k_2)_\alpha p_\beta q_\nu P_\lambda p_\tau \epsilon_\delta(J/\psi) \varepsilon^{\beta\alpha\nu\mu} \varepsilon^{\tau\lambda\delta\sigma} \eta_{\mu\sigma} \\
&= \frac{g_{\eta\gamma}^{\pi\pi} g_{\eta\gamma}^{J/\psi}}{M_\rho^2 - M_{J/\psi}^2} (k_1 - k_2)_\alpha p_\beta P_\nu P_\lambda p_\tau \epsilon_\delta(J/\psi) \begin{vmatrix} \eta^{\beta\tau} & \eta^{\alpha\tau} & \eta^{\nu\tau} \\ \eta^{\beta\lambda} & \eta^{\alpha\lambda} & \eta^{\nu\lambda} \\ \eta^{\beta\delta} & \eta^{\alpha\delta} & \eta^{\nu\delta} \end{vmatrix},
\end{aligned}$$

where we have used the well-known relation

$$\sum_{\text{pol}} \epsilon_\mu(\gamma) \epsilon_\sigma(\gamma) = -\eta_{\mu\sigma}.$$

Moreover

$$\begin{aligned}
Z_\eta &= \frac{g_{\eta\gamma}^{\pi\pi} g_{\eta\gamma}^{J/\psi}}{M_\rho^2 - M_{J/\psi}^2} \left\{ p^2 \left[(k_1 - k_2) \cdot P \right] \left[P \cdot \epsilon(J/\psi) \right] - p^2 P^2 \left[(k_1 - k_2) \cdot \epsilon(J/\psi) \right] \right. \\
&\quad + P^2 \left[(k_1 - k_2) \cdot p \right] \left[p \cdot \epsilon(J/\psi) \right] - (p \cdot P) \left[(k_1 - k_2) \cdot p \right] \left[P \cdot \epsilon(J/\psi) \right] \\
&\quad \left. + (p \cdot P)^2 \left[(k_1 - k_2) \cdot \epsilon(J/\psi) \right] - (p \cdot P) \left[(k_1 - k_2) \cdot P \right] \left[p \cdot \epsilon(J/\psi) \right] \right\}.
\end{aligned}$$

By using the definitions of Eq. (2.1.3) and the results of Eq. (2.1.3) we obtain

$$\begin{aligned}
Z_\eta &= \frac{g_{\eta\gamma}^{\pi\pi} g_{\eta\gamma}^{J/\psi}}{M_\rho^2 - M_{J/\psi}^2} \left[M_{J/\psi}^2 \left(-2p^0 \omega \cos \theta \right) \left(p^0 \epsilon_0(J/\psi) + p^1 \epsilon_1(J/\psi) + p^3 \epsilon_3(J/\psi) \right) \right. \\
&\quad \left. + (p^0)^2 M_{J/\psi}^2 \left(2\omega \epsilon_3(J/\psi) \right) \right], \\
Z_\eta &= \frac{2g_{\eta\gamma}^{\pi\pi} g_{\eta\gamma}^{J/\psi} M_{J/\psi}^2 (p^0)^2 \omega}{M_{J/\psi}^2 - M_\rho^2} \left[\epsilon_0(J/\psi) \cos \theta + \epsilon_1(J/\psi) \sin \theta \cos \theta \right. \\
&\quad \left. + \epsilon_3(J/\psi) (1 - \cos^2 \theta) \right].
\end{aligned}$$

By integrating over the solid angle

$$\begin{aligned} \int d\Omega Z_\eta &= \frac{2g_{\eta\gamma}^{\pi\pi} g_{\eta\gamma}^{J/\psi} M_{J/\psi}^2 (p^0)^2 \omega}{M_{J/\psi}^2 - M_\rho^2} \left(\epsilon_3(J/\psi) \int d\Omega \sin^2 \theta \right) \\ &= \frac{16\pi g_{\eta\gamma}^{\pi\pi} g_{\eta\gamma}^{J/\psi} M_{J/\psi}^2 (p^0)^2 \epsilon_3(J/\psi)}{3(M_{J/\psi}^2 - M_\rho^2)} \sqrt{\frac{M_{J/\psi}^2}{4} - M_\pi^2}, \end{aligned}$$

where $\epsilon_3(J/\psi) = \epsilon_3^{(\sigma)}(J/\psi)$ is the numerical third component ($\mu = 3$) of the generic σ -th polarization four-vector of the J/ψ meson.

Finally, the imaginary parts can be written as

$$\begin{aligned} \text{Im}(\mathcal{A}^{\eta\gamma}) &= \sqrt{\frac{M_{J/\psi}^2}{4} - M_\pi^2} \frac{g_{\eta\gamma}^{\pi\pi} g_{\eta\gamma}^{J/\psi} M_{J/\psi}^4 \epsilon_3(J/\psi)}{48\pi (M_{J/\psi}^2 - M_\rho^2)} \left(1 - \frac{M_\eta^2}{M_{J/\psi}^2} \right)^3, \\ \text{Im}(\mathcal{A}^{f_1\gamma}) &= \sqrt{\frac{M_{J/\psi}^2}{4} - M_\pi^2} \frac{g_{f_1\gamma}^{\pi\pi} g_{f_1\gamma}^{J/\psi} M_{J/\psi}^4 \epsilon_3(J/\psi)}{48\pi M_{f_1}^2 (M_{J/\psi}^2 - M_\rho^2)} \left(1 - \frac{M_{f_1}^2}{M_{J/\psi}^2} \right)^3 \left(1 + \frac{M_{f_1}^2}{M_{J/\psi}^2} \right). \end{aligned}$$

These expressions and that due to the $\eta'\gamma$ intermediate state, which has the same structure of $\text{Im}(\mathcal{A}^{\eta\gamma})$, have to be summed up to obtain the complete imaginary part of $\mathcal{A}^{gg\gamma}$, see Eq. (2.10).

The corresponding contribution to the BR, $\text{BR}_{\text{Im}}^{gg\gamma}$, as given in Eq. (2.7), is

$$\text{BR}_{gg\gamma}^{\text{Im}} = \frac{\sqrt{M_{J/\psi}^2 - 4M_\pi^2}}{16\pi M_{J/\psi}^2 \Gamma_{J/\psi}} \frac{(M_{J/\psi}^2 - 4M_\pi^2)^{3/2}}{4(48\pi)^3 M_{J/\psi}^6 \Gamma_{J/\psi}} \left| \sum_{h=\eta, \eta', f_1} g_{h\gamma}^{\pi\pi} g_{h\gamma}^{J/\psi} K_h \right|^2, \quad (2.16)$$

where the average over the polarization states of the J/ψ meson has been performed and the kinematical factor K_h reads

$$K_h = \begin{cases} (M_{J/\psi}^2 - M_h^2)^3 & h = \eta, \eta' \\ \frac{(M_{J/\psi}^2 - M_h^2)^3}{M_h^2} \left(1 + \frac{M_h^2}{M_{J/\psi}^2} \right) & h = f_1 \end{cases}. \quad (2.17)$$

The quantity of Eq. (2.16) represents a lower limit for $\text{BR}^{gg\gamma}$, because the contribution due to the real part of the amplitude, $\text{BR}_{\text{Re}}^{gg\gamma}$, as shown in Eq. (2.7), is positive. The values of the six coupling constants $g_{h\gamma}^{\pi\pi}$ and $g_{h\gamma}^{J/\psi}$ ($h = \eta, \eta', f_1$) have to be extracted from the data.

2.1.4 The coupling constants $g_{\eta\gamma}^{J/\psi}$, $g_{\eta'\gamma}^{J/\psi}$ and $g_{f_1\gamma}^{J/\psi}$

The experimental value of the modulus of the coupling constant $g_{h\gamma}^{J/\psi}$, with $h = \eta, \eta', f_1$, can be extracted from the rate of the corresponding radiative decay

$$J/\psi(P) \rightarrow h(k) + \gamma(p),$$

where, in parentheses, are reported the four-momenta, consistently with previous definitions. We show explicitly the calculus for the $h = \eta$ case, since the other cases are quite similar. From Eq. (2.11) we can write

$$\begin{aligned} \overline{|\mathcal{A}(J/\psi \rightarrow \eta\gamma)|^2} &= \frac{1}{3} \sum_{\text{pol}} |g_{\eta\gamma}^{J/\psi}|^2 |P_\lambda p_\tau \epsilon_\delta(J/\psi) \epsilon_\sigma(\gamma) \varepsilon^{\tau\lambda\delta\sigma}|^2 \\ &= \frac{1}{3} |g_{\eta\gamma}^{J/\psi}|^2 P_\lambda P_{\lambda'} p_\tau p_{\tau'} \sum_{\text{pol}} \epsilon_\delta(J/\psi) \epsilon_{\delta'}(J/\psi) \\ &\quad \times \sum_{\text{pol}} \epsilon_\sigma(\gamma) \epsilon_{\sigma'}(\gamma) \varepsilon^{\tau\lambda\delta\sigma} \varepsilon^{\tau'\lambda'\delta'\sigma'}, \end{aligned}$$

and

$$\begin{aligned} \overline{|\mathcal{A}(J/\psi \rightarrow \eta\gamma)|^2} &= \frac{1}{3} |g_{\eta\gamma}^{J/\psi}|^2 P_\lambda P_{\lambda'} p_\tau p_{\tau'} \varepsilon^{\tau\lambda\delta\sigma} \varepsilon^{\tau'\lambda'\delta'\sigma} = \frac{2}{3} |g_{\eta\gamma}^{J/\psi}|^2 P_\lambda P_{\lambda'} p_\tau p_{\tau'} \\ &\quad \times (\eta^{\tau\lambda'} \eta^{\lambda\tau'} - \eta^{\tau\tau'} \eta^{\lambda\lambda'}) = \frac{2}{3} |g_{\eta\gamma}^{J/\psi}|^2 (P_\lambda P^\tau p_\tau p^\lambda - P_\lambda P^\lambda p_\tau p^\tau) \\ &= \frac{2}{3} |g_{\eta\gamma}^{J/\psi}|^2 \left((p \cdot P)^2 - p^2 P^2 \right) = \frac{2}{3} |g_{\eta\gamma}^{J/\psi}|^2 \left((p \cdot P)^2 - p^2 P^2 \right). \end{aligned}$$

By using the following scalar products

$$p \cdot P = p^0 M_{J/\psi} = \frac{M_{J/\psi}^2}{2} \left(1 - \frac{M_\eta^2}{M_{J/\psi}^2} \right) = \frac{1}{2} (M_{J/\psi}^2 - M_\eta^2) ,$$

$$P^2 = M_{J/\psi}^2 , \quad p^2 = 0 ,$$

we obtain

$$\overline{|\mathcal{A}(J/\psi \rightarrow \eta\gamma)|^2} = \frac{1}{6} |g_{\eta\gamma}^{J/\psi}|^2 (M_{J/\psi}^2 - M_\eta^2)^2 .$$

Using Eq. (B.4) we arrive, after some further calculations, to the obtained radiative decay width

$$\Gamma(J/\psi \rightarrow h\gamma) = \frac{K_h}{96\pi M_{J/\psi}^3} |g_{h\gamma}^{J/\psi}|^2 ,$$

where K_h is the kinematical factor defined in Eq. (2.17).

It follows that the modulus of the coupling constant can be extracted as

$$|g_{h\gamma}^{J/\psi}| = \sqrt{\frac{96\pi M_{J/\psi}^3 \Gamma(J/\psi \rightarrow h\gamma)}{K_h}} .$$

Finally, by using the experimental values of radiative decay widths $\Gamma(J/\psi \rightarrow \eta\gamma)$, $\Gamma(J/\psi \rightarrow \eta'\gamma)$ and $\Gamma(J/\psi \rightarrow f_1\gamma)$ [28], reported in Table 2.3, the coupling constants are

$$|g_{h\gamma}^{J/\psi}| = \begin{cases} (1.070 \pm 0.023) \times 10^{-3} \text{ GeV}^{-1} & h = \eta \\ (2.563 \pm 0.055) \times 10^{-3} \text{ GeV}^{-1} & h = \eta' \\ (1.191 \pm 0.080) \times 10^{-3} & h = f_1 \end{cases} . \quad (2.18)$$

We observe that, as a consequence of the structure of the amplitudes shown in Eq. (2.11), the coupling constant of the axial vector is adimensional, while those of the pseudoscalar mesons have the dimension of inverse energy. Looking at their structure we see that they differ only by the interchange of the J/ψ four-momentum P_λ with the adimensional polarization vector

Table 2.3: Decay widths from Ref. [28].

Decay processes	Decay widths Γ (GeV)
$J/\psi \rightarrow \eta\gamma$	$(1.026 \pm 0.044) \times 10^{-7}$
$J/\psi \rightarrow \eta'\gamma$	$(4.78 \pm 0.14) \times 10^{-7}$
$J/\psi \rightarrow f_1\gamma$	$(5.67 \pm 0.76) \times 10^{-8}$

of f_1 .

2.1.5 The coupling constants $g_{\eta\gamma}^{\pi\pi}$, $g_{\eta'\gamma}^{\pi\pi}$ and $g_{f_1\gamma}^{\pi\pi}$

There are no data on the cross section of the process $\pi^+\pi^- \rightarrow h\gamma$, with $h = \eta, \eta'$ and f_1 , so that the coupling constant $g_{h\gamma}^{\pi\pi}$, appearing in Eq. (2.13), can not be directly measured. Nevertheless, the same coupling constants must regulate the amplitudes of the decay

$$h(k) \rightarrow \pi^+(k_1) + \pi^-(k_2) + \gamma(\tilde{p}), \quad h = \eta, \eta', f_1.$$

as a consequence of the crossing symmetry. This decay is obtained by moving the photon from the final to the initial state of the original reaction of Eq. (2.12), with the Feynman diagram of Fig. 2.3, and then by making a time-reversal transformation.

For the case $h = \eta$, the other cases are very similar, we can write

$$\begin{aligned} d\Gamma(\eta \rightarrow \pi^+\pi^-\gamma) &= \frac{1}{2M_\eta} \overline{|\mathcal{A}(\eta \rightarrow \pi^+\pi^-\gamma)|^2} d\rho_3 \\ &= \frac{1}{(2\pi)^3} \frac{1}{32M_\eta^3} \overline{|\mathcal{A}(\pi^+\pi^- \rightarrow \eta\gamma)|^2} dq^2 dq_1^2, \end{aligned} \quad (2.19)$$

where $d\rho_3$ is the three-body phase space and with

$$q \equiv k - \tilde{p} = k_1 + k_2, \quad q_1 \equiv k_1 + \tilde{p} = k - k_2. \quad (2.20)$$

For the amplitude $\overline{|\mathcal{A}(\pi^+\pi^- \rightarrow \eta\gamma)|^2}$ we consider the process

$$\eta(k) + \gamma(p) \rightarrow \rho^0(\tilde{q}) \rightarrow \pi^+(k_1) + \pi^-(k_2),$$

where $p = -\tilde{p}$ and $\tilde{q} = k + p = q$. From Eq. (2.13) we can write

$$\begin{aligned}
|\overline{\mathcal{A}(\pi\pi \rightarrow \eta\gamma)}|^2 &= \sum_{\text{pol}} |g_{\eta\gamma}^{\pi\pi}|^2 \left| d_\alpha \frac{1}{M_\rho^2 - q^2 - iM_\rho\Gamma_\rho} p_\beta q_\nu \epsilon_\mu(\gamma) \varepsilon^{\beta\alpha\nu\mu} \right|^2 \\
&= \frac{|g_{\eta\gamma}^{\pi\pi}|^2 d_\alpha d_{\alpha'} p_\beta p_{\beta'} q_\nu q_{\nu'}}{(q^2 - M_\rho^2)^2 + \Gamma_\rho^2 M_\rho^2} \sum_{\text{pol}} \epsilon_\mu(\gamma) \epsilon_{\mu'}(\gamma) \varepsilon^{\beta\alpha\nu\mu} \varepsilon^{\beta'\alpha'\nu'\mu'} \\
&= - \frac{|g_{\eta\gamma}^{\pi\pi}|^2 (k_1 - k_2)_\alpha (k_1 - k_2)_{\alpha'} p_\beta p_{\beta'} q_\nu q_{\nu'} \varepsilon^{\beta\alpha\nu\mu} \varepsilon^{\beta'\alpha'\nu'\mu'} \eta_{\mu\mu'}}{(q^2 - M_\rho^2)^2 + \Gamma_\rho^2 M_\rho^2} \\
&= \frac{|g_{\eta\gamma}^{\pi\pi}|^2 (k_1 - k_2)_\alpha (k_1 - k_2)_{\alpha'} p_\beta p_{\beta'} q_\nu q_{\nu'}}{(q^2 - M_\rho^2)^2 + \Gamma_\rho^2 M_\rho^2} \begin{vmatrix} \eta^{\beta\beta'} & \eta^{\alpha\beta'} & \eta^{\nu\beta'} \\ \eta^{\beta\alpha'} & \eta^{\alpha\alpha'} & \eta^{\nu\alpha'} \\ \eta^{\beta\nu'} & \eta^{\alpha\nu'} & \eta^{\nu\nu'} \end{vmatrix},
\end{aligned}$$

from which we obtain

$$\begin{aligned}
|\overline{\mathcal{A}(\pi\pi \rightarrow \eta\gamma)}|^2 &= \frac{|g_{\eta\gamma}^{\pi\pi}|^2}{(q^2 - M_\rho^2)^2 + \Gamma_\rho^2 M_\rho^2} \left\{ p^2 q^2 (k_1 - k_2)^2 - p^2 [(k_1 - k_2) \cdot q]^2 \right. \\
&\quad + (p \cdot q) [(k_1 - k_2) \cdot p] [(k_1 - k_2) \cdot q] - q^2 [(k_1 - k_2) \cdot p]^2 \\
&\quad \left. + (p \cdot q) [(k_1 - k_2) \cdot p] [(k_1 - k_2) \cdot q] - (p \cdot q)^2 (k_1 - k_2)^2 \right\}.
\end{aligned}$$

Using the definitions of Eq. (2.20), we have the following relations

$$\begin{aligned}
k_1^2 &= k_2^2 = M_\pi^2, \quad k^2 = M_\eta^2, \quad p^2 = \tilde{p}^2 = 0, \\
p \cdot (k_1 - k_2) &= M_\pi^2 - q_1^2 + \frac{1}{2}(M_\eta^2 - q^2), \quad q \cdot (k_1 - k_2) = 0, \\
p \cdot q &= \frac{1}{2}(q^2 - M_\eta^2), \quad (k_1 - k_2)^2 = 4M_\pi^2 - q^2,
\end{aligned}$$

therefore Eq. (2.21) becomes

$$\begin{aligned} \overline{|\mathcal{A}(\pi\pi \rightarrow \eta\gamma)|^2} &= \frac{|g_{\eta\gamma}^{\pi\pi}|^2 \left(-q^2 \left((k_1 - k_2) \cdot p \right)^2 - (p \cdot q)^2 (k_1 - k_2)^2 \right)}{(q^2 - M_\rho^2)^2 + \Gamma_\rho^2 M_\rho^2} \\ &= |g_{\eta\gamma}^{\pi\pi}|^2 \frac{(q^2 - 4M_\pi^2)(q^2 - M_\eta^2)^2 - q^2(q^2 + 2q_1^2 - 2M_\pi^2 - M_\eta^2)^2}{4 \left[(q^2 - M_\rho^2)^2 + \Gamma_\rho^2 M_\rho^2 \right]}. \end{aligned}$$

Finally, with an analogous procedure for $h = \eta', f_1$, from Eq. (2.19), we obtain the decay width

$$\begin{aligned} \Gamma(h \rightarrow \pi^+\pi^-\gamma) &= \int \overline{|\mathcal{A}(h \rightarrow \pi^+\pi^-\gamma)|^2} d\rho_3 \\ &= \frac{1}{(2\pi)^3} \frac{|g_{h\gamma}^{\pi\pi}|^2}{128M_h^3} \int_{q_{\min}^2}^{q_{\max}^2} dq^2 \int_{q_{1\min}^2(q^2)}^{q_{1\max}^2(q^2)} dq_1^2 I_h(q^2, q_1^2), \end{aligned} \quad (2.21)$$

where the integration variables and the corresponding limits are: $q^2 \equiv (k - \tilde{p})^2 = (k_1 + k_2)^2$, $q_1^2 \equiv (k_1 + \tilde{p})^2 = (k - k_2)^2$,

$$\begin{aligned} q_{\min}^2 &= 4M_\pi^2, & q_{\max}^2 &= M_h^2, \\ q_{1\min, \max}^2(q^2) &= \frac{M_h^4}{4q^2} - \left(\sqrt{\frac{q^2}{4} - M_\pi^2} \pm \frac{M_h^2 - q^2}{2\sqrt{q^2}} \right)^2, \end{aligned}$$

with $h = \eta, \eta', f_1$. The functions $I_h(q^2, q_1^2)$ have two different forms, for the case of pseudoscalar mesons we have

$$I_h(q^2, q_1^2) = \frac{(q^2 - 4M_\pi^2)(q^2 - M_h^2)^2}{(q^2 - M_\rho^2)^2 + \Gamma_\rho^2 M_\rho^2} - \frac{q^2(q^2 + 2q_1^2 - 2M_\pi^2 - M_h^2)^2}{(q^2 - M_\rho^2)^2 + \Gamma_\rho^2 M_\rho^2}, \quad h = \eta, \eta',$$

while for the axial vector meson it reads

$$I_{f_1}(q^2, q_1^2) = \frac{1}{3M_{f_1}^2} \left[\frac{(q^2 - 4M_\pi^2)(q^2 - M_{f_1}^2)^2}{(q^2 - M_\rho^2)^2 + \Gamma_\rho^2 M_\rho^2} - \frac{(q^2 - 2M_{f_1}^2)(q^2 + 2q_1^2 - 2M_\pi^2 - M_{f_1}^2)^2}{(q^2 - M_\rho^2)^2 + \Gamma_\rho^2 M_\rho^2} \right].$$

Table 2.4: Decay widths from Ref. [28].

Decay processes	Decay widths Γ (GeV)
$\eta \rightarrow \pi^+\pi^-\gamma$	$(5.53 \pm 0.32) \times 10^{-8}$
$\eta' \rightarrow \pi^+\pi^-\gamma$	$(5.76 \pm 0.10) \times 10^{-5}$
$f_1 \rightarrow \pi^+\pi^-\gamma$	$(1.20 \pm 0.28) \times 10^{-4}$

The phase-space integrals are

$$\tilde{I}_h = \int_{q_{\min}^2}^{q_{\max}^2} dq^2 \int_{q_{1\min}^2(q^2)}^{q_{1\max}^2(q^2)} dq_1^2 I_h(q^2, q_1^2) = \begin{cases} (5.840 \pm 0.011) \times 10^{-5} \text{ GeV}^6 & h = \eta \\ (2.719 \pm 0.019) \times 10^{-1} \text{ GeV}^6 & h = \eta' \\ (6.403 \pm 0.052) \text{ GeV}^4 & h = f_1 \end{cases},$$

and also in this case the contribution due to the axial vector meson has a different dimension, E^4 instead of E^6 , as a consequence of the different structure of the amplitude, see Eq. (2.13).

Finally, the corresponding coupling constants can be extracted by means of

$$|g_{h\gamma}^{\pi\pi}| = (2\pi M_h)^{3/2} \sqrt{\frac{128\Gamma(h \rightarrow \pi^+\pi^-\gamma)}{\tilde{I}_h}} = \begin{cases} (2.223 \pm 0.047) \text{ GeV}^{-1} & h = \eta \\ (2.431 \pm 0.060) \text{ GeV}^{-1} & h = \eta' \\ 3.55 \pm 0.41 & h = f_1 \end{cases}.$$

where we have used the experimental data show in Table 2.4.

2.1.6 The imaginary part of $A^{gg\gamma}$

We calculate the contribution to the BR due to the imaginary part of the $gg\gamma$ amplitude, $\text{BR}_{\text{Im}}^{gg\gamma}$, using Eq. (2.16) which contains the sum of the three amplitudes related to the intermediate mesons η , η' and f_1 . We notice that there are also effects due to interference terms

having three amplitudes¹.

We assume that the relative phase of the amplitudes of the two pseudoscalar contributions, being due to the η meson and to its first excitation η' , is zero, so they are simply summed up with constructive interference. On the other hand, the relative phase between the axial vector and pseudoscalar mesons amplitudes is unknown.

The single contributions obtained from Eq. (2.16) are

$$\begin{aligned} \text{BR}_{\text{Im}}^{gg\gamma}(\eta) &= (1.176 \pm 0.080) \times 10^{-6}, \\ \text{BR}_{\text{Im}}^{gg\gamma}(\eta') &= (5.34 \pm 0.38) \times 10^{-6}, \\ \text{BR}_{\text{Im}}^{gg\gamma}(f_1) &= (0.74 \pm 0.20) \times 10^{-6}. \end{aligned}$$

It is useful to note that they follow the same hierarchy of the relative BRs shown in Table. 2.2, with the main contribution given by the pseudoscalar meson η' . The total pseudoscalar contribution, due to the η and η' particles, is

$$\text{BR}_{\text{Im}}^{gg\gamma}(\eta + \eta') = \left(\sqrt{\text{BR}_{\text{Im}}^{gg\gamma}(\eta)} + \sqrt{\text{BR}_{\text{Im}}^{gg\gamma}(\eta')} \right)^2 = (1.152 \pm 0.066) \times 10^{-5}. \quad (2.22)$$

Concerning the introduction of the f_1 contribution we obtain the following two extreme cases

$$\begin{aligned} \text{BR}_{\text{Im}}^{gg\gamma}(\eta + \eta' - f_1) &= (0.643 \pm 0.074) \times 10^{-5}, \\ \text{BR}_{\text{Im}}^{gg\gamma}(\eta + \eta' + f_1) &= (1.81 \pm 0.12) \times 10^{-5}, \end{aligned} \quad (2.23)$$

due to destructive and constructive interference respectively.

These values represent lower limits for $\text{BR}^{gg\gamma}$ and they represent the 13% and the 37% of the purely EM BR contribution that is

$$\text{BR}^\gamma(\pi^+\pi^-) = (4.7 \pm 1.7) \times 10^{-5},$$

¹The possibility of ortogonality, i.e., amplitudes with a $\pm\pi/2$ relative phase, is predicted by the fact that there are three contributions.

as given in Eq. (2.4). This fact leaves open the possibility that the total $\text{BR}^{gg\gamma}$ contribution would be of the same order of BR^γ .

Finally, using Eq. (2.6) and the value of Eq. (2.22) for $\text{BR}_{\text{Im}}^{gg\gamma}$ that represents an average of the two possibilities of Eq.(2.23), together with the experimental datum for BR^γ , as given in Eq. (2.4), we obtain

$$\begin{aligned} \mathcal{B}(\pi^+\pi^-) &= \text{BR}^\gamma(\pi^+\pi^-) + \text{BR}^{gg\gamma}(\pi^+\pi^-) + \mathcal{I}(\pi^+\pi^-) \\ &= (5.9 \pm 1.7) \times 10^{-5} + \text{BR}_{\text{Re}}^{gg\gamma}(\pi^+\pi^-) + \mathcal{I}(\pi^+\pi^-), \end{aligned} \quad (2.24)$$

to be compared with the PDG datum [28] of Eq. (2.5)

$$\text{BR}_{\text{PDG}}(\pi^+\pi^-) = (14.7 \pm 1.4) \times 10^{-5}.$$

2.2 The decay $J/\psi \rightarrow K^+K^-$

The method discussed in the previous section, for the case of the J/ψ decay into pions, can be used for any other similar processes. One of particular interest is the decay

$$J/\psi \rightarrow K^+K^-.$$

In fact in this case we can use simply $h_1 = \eta$ and $h_2 = \eta'$ as intermediate states for the application of the Cutkosky rule, see Eq. (2.8). The procedure is identical to that described in the previous section, in this case we consider the following decay chain

$$J/\psi \rightarrow \sum_j \eta_j \gamma \rightarrow K^+K^-,$$

where $\eta_1 = \eta$ and $\eta_2 = \eta'$. The coupling constant that appears in the amplitude of the first decay, $J/\psi \rightarrow \eta_j \gamma$, is obtained by using the measured decay rate $\Gamma(J/\psi \rightarrow \eta_j \gamma)$ and is the same of the $\pi^+\pi^-$ case. Concerning the amplitude of the second part of the process, the $\eta_j \gamma \rightarrow K^+K^-$, we assume that the K^+K^- final state system, having $J^{PC} = 1^{--}$, resonates

almost completely in the ϕ vector meson, that plays the same role of the $\rho^0(770)$ in the case of pions, therefore we consider the scattering

$$\eta_j \gamma \rightarrow \phi \rightarrow K^+ K^-.$$

The obtained value for $\text{BR}_{\text{Im}}^{gg\gamma}$ is

$$\text{BR}_{\text{Im}}^{gg\gamma}(J/\psi \rightarrow K^+ K^-) = (2.3 \pm 0.1) \times 10^{-7},$$

to be compared with the total BR from PDG [28]

$$\text{BR}_{\text{PDG}}(K^+ K^-) = (28.6 \pm 2.1) \times 10^{-5}$$

and with the EM BR_γ . The latter can be calculated using data from Ref. [108], and it is

$$\text{BR}_\gamma(K^+ K^-) = (13.8 \pm 0.7) \times 10^{-5}.$$

We can conclude that the contribution to the total BR of $J/\psi \rightarrow K^+ K^-$ due to the imaginary part of the mixed strong-EM amplitude is totally negligible, being three order of magnitude lower than both the purely EM and the total BRs.

Chapter 3

J/ψ decays into baryons

In this chapter we present our results concerning the decays of the J/ψ into baryons. In Table 3.1 we report some of the larger BR of $J/\psi \rightarrow$ baryons from PDG [28].

Table 3.1: Branching ratios data from PDG [28] for some of the larger BR of the J/ψ decays into baryons.

Decay process	Branching ratio	Error
$J/\psi \rightarrow p\bar{p}$	$(2.121 \pm 0.029) \times 10^{-3}$	1.37%
$J/\psi \rightarrow n\bar{n}$	$(2.09 \pm 0.16) \times 10^{-3}$	7.66%
$J/\psi \rightarrow \Lambda\bar{\Lambda}$	$(1.89 \pm 0.09) \times 10^{-3}$	4.76%
$J/\psi \rightarrow \Sigma^+\bar{\Sigma}^-$	$(1.50 \pm 0.24) \times 10^{-3}$	16.00%
$J/\psi \rightarrow \Sigma^0\bar{\Sigma}^0$	$(1.172 \pm 0.032) \times 10^{-3}$	2.73%
$J/\psi \rightarrow \Xi^0\bar{\Xi}^0$	$(1.17 \pm 0.04) \times 10^{-3}$	3.42%

3.1 The $J/\psi \rightarrow B\bar{B}$ decay

3.1.1 Introduction

Particles directly produced at e^+e^- colliders decay with relatively high probability into a baryon–antibaryon, $B\bar{B}$, pair [79]. In this kind of collider, electrons and positrons annihilate,

producing a resonance, such as the J/ψ meson, that could decay into entangled $B\bar{B}$ pairs. For example in the case of $e^+e^- \rightarrow J/\psi \rightarrow \Lambda\bar{\Lambda}$, see Fig. 3.1, the J/ψ , produced at rest in a single photon annihilation process, subsequently decays into a $\Lambda\bar{\Lambda}$ pair [109].

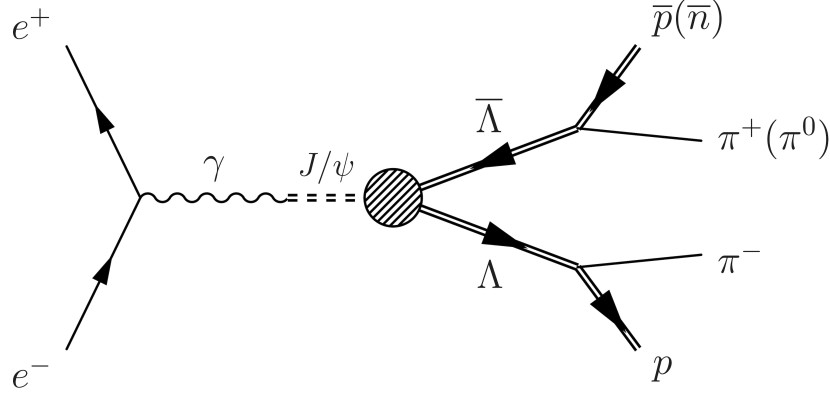


Figure 3.1: Feynman diagram for a typical process $e^+e^- \rightarrow J/\psi \rightarrow \Lambda\bar{\Lambda}$.

The decays of the J/ψ meson into a $B\bar{B}$ pair proceed via strong and EM interactions. The Feynman amplitude, from Eq. (1.3), can be written as a sum of three sub-amplitudes

$$\mathcal{A}_{B\bar{B}} = \mathcal{A}_{B\bar{B}}^{ggg} + \mathcal{A}_{B\bar{B}}^{\gamma} + \mathcal{A}_{B\bar{B}}^{gg\gamma},$$

where $\mathcal{A}_{B\bar{B}}^{ggg}$ is the purely strong, $\mathcal{A}_{B\bar{B}}^{\gamma}$ is the purely EM and $\mathcal{A}_{B\bar{B}}^{gg\gamma}$ is the mixed strong-EM sub-amplitude. The corresponding Feynman diagrams are shown in Fig. 3.2.

Usually, as in the meson cases, the mixed strong-EM contribution is not considered since it is assumed to be negligible with respect to the strong and EM ones [110]. The calculation in the framework of QCD of this mixed contribution is a hard task, as stated in sub-section 2.1.3, also because the hadronization process of the $gg\gamma$ into the final baryon-antibaryon pair does occur at the non-perturbative regime of QCD.

Furthermore, as we have shown in section 2.1, in the cases where the purely strong contribution is suppressed, for example in G -parity violating decays, the contribution of the mixed strong-EM term (related to $|\mathcal{A}^{gg\gamma}|$) cannot be neglected [3].

The BR of the $J/\psi \rightarrow B\bar{B}$ decays contains the interference term between the sum of the

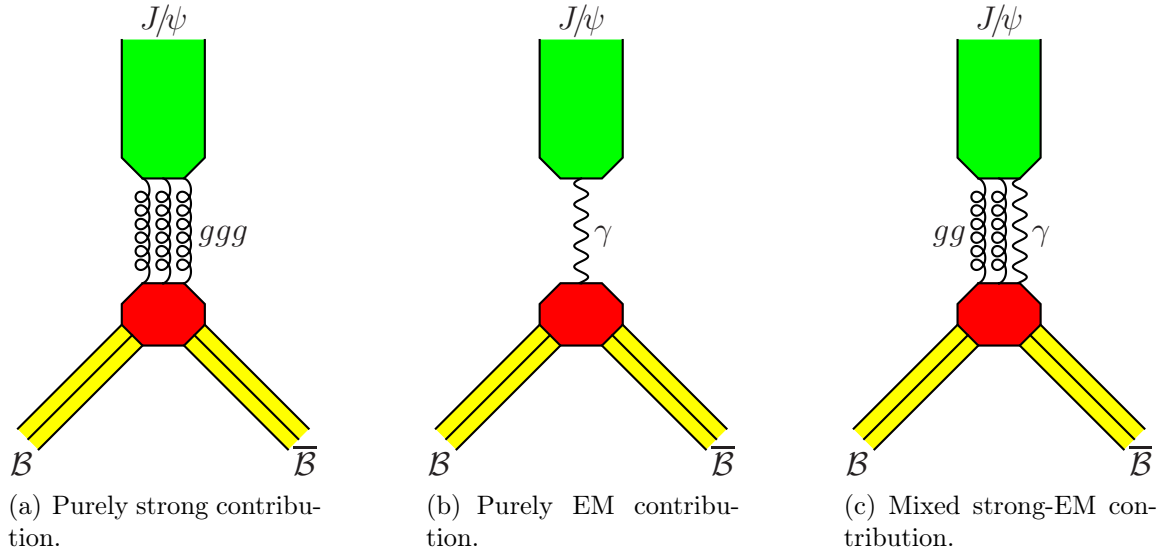


Figure 3.2: Feynman diagrams for the three sub-amplitude of the decay $J/\psi \rightarrow B\bar{B}$.

purely strong and mixed sub-amplitudes, $(\mathcal{A}_{B\bar{B}}^{ggg} + \mathcal{A}_{B\bar{B}}^{gg\gamma})$, for which we assume the same phase [78], and the purely EM sub-amplitude, $\mathcal{A}_{B\bar{B}}^{\gamma}$. In principle, we can obtain the relative phase between these two contributions $(\mathcal{A}_{B\bar{B}}^{ggg} + \mathcal{A}_{B\bar{B}}^{gg\gamma})$ and $\mathcal{A}_{B\bar{B}}^{\gamma}$, called φ , by studying the J/ψ -resonance line-shape in processes as $e^+e^- \rightarrow J/\psi \rightarrow B\bar{B}$.

From a theoretical point of view, all sub-amplitudes should become real at a sufficiently high energy [111–113], i.e., at a fully perturbative QCD regime. On the other hand, it is quite difficult to establish whether such a regime, which entails maximum (positive or negative) interference, is attained already at the J/ψ mass.

A recent measurement [114] of the relative phase φ , performed by exploiting the decay of the J/ψ meson into nucleon-antinucleon, gave

$$\varphi = (88.7 \pm 8.1)^\circ,$$

which is in agreement with the no-interference case.

In order to describe the decay amplitude of the J/ψ meson into baryon-antibaryon pairs of the spin-1/2 flavour SU(3) octet we define a model [5] based on the effective Lagrangian density

discussed in sub-section 1.9.1. These baryons ($p, n, \Sigma^\pm, \Sigma^0, \Lambda, \Xi^-, \Xi^0$) can be organized in the baryon matrix

$$\mathcal{B} = \begin{pmatrix} \Lambda/\sqrt{6} + \Sigma^0/\sqrt{2} & \Sigma^+ & p \\ \Sigma^- & \Lambda/\sqrt{6} - \Sigma^0/\sqrt{2} & n \\ \Xi^- & \Xi^0 & -2\Lambda/\sqrt{6} \end{pmatrix}.$$

3.1.2 Theoretical background

The BR for the decay of the J/ψ meson into a baryon-antibaryon pair $B\bar{B}$ can be written as

$$\text{BR}_{B\bar{B}} = \frac{|\vec{p}|}{8\pi M_{J/\psi}^2 \Gamma_{J/\psi}} \left| \mathcal{A}_{B\bar{B}}^{ggg} + \mathcal{A}_{B\bar{B}}^{gg\gamma} + \mathcal{A}_{B\bar{B}}^{\gamma} \right|^2,$$

see Eq. (1.10), where \vec{p} is the three-momentum of the baryon (antibaryon) in the $B\bar{B}$ center of mass frame (J/ψ rest frame).

As a consequence of the amplitude decomposition, the BR can be written as the sum of four contributions, i.e.,

$$\text{BR}_{B\bar{B}} \equiv \text{BR}_{B\bar{B}}^{ggg} + \text{BR}_{B\bar{B}}^{gg\gamma} + \text{BR}_{B\bar{B}}^{\gamma} + \text{BR}^{\text{int}}, \quad (3.1)$$

where the symbol $\text{BR}_{B\bar{B}}^{\lambda}$ stands for the BR due to the λ intermediate state, with $\lambda = ggg, gg\gamma, \gamma$, while the last term accounts for the interference among the sub-amplitudes.

This term, as already stated, depends only on the relative phase φ between the sub-amplitudes $(\mathcal{A}_{B\bar{B}}^{ggg} + \mathcal{A}_{B\bar{B}}^{gg\gamma})$ and $\mathcal{A}_{B\bar{B}}^{\gamma}$, because we assume that purely strong, $\mathcal{A}_{B\bar{B}}^{ggg}$, and the mixed strong-EM sub-amplitude, $\mathcal{A}_{B\bar{B}}^{gg\gamma}$, have the same phase, i.e., they are relatively real and positive [78]. Using the effective Lagrangian density of Eq. (1.13), the total decay amplitude can be parametrized in terms of the phase φ and the coupling constants belonging to the set $\mathcal{C} = \{G_0, D_e, D_m, F_e, F_m\}$. Such five coupling constants are linear combinations of those appearing explicitly as coefficients of the traces in Eq. (1.13), i.e., g, d, f, d', f' .

In particular, G_0 is related to the coupling constant g ; D_e, F_e to d, g , which refer to the EM breaking effects, and D_m, F_m to d', g' , describing the mass difference breaking effects.

We define two more subsets of coupling constants

$$\mathcal{C}_{\text{strong}} = \{G_0, D_m, F_m\}, \quad \mathcal{C}_{\text{EM}} = \{D_e, F_e\}, \quad \mathcal{C} = \mathcal{C}_{\text{strong}} \cup \mathcal{C}_{\text{EM}},$$

with, as said before, the strong and EM coupling constants of these two subsets, respectively relatively real and positive [95]. This assumption does not affect the results because the EM and mass difference effects, parametrized by D_m , F_m , D_e and F_e , represent sub-leading contributions with respect to G_0 , and hence the eventual presence of non-vanishing imaginary parts would leave almost unchanged the dominant strong coupling. A similar hypothesis is made also in other works, see for example Refs. [97, 115]. It follows that the only non-zero relative phase is φ , the one between strong and EM interactions. Moreover, since such a phase is mainly due to the dominant coupling constant G_0 , we assume that φ does not depend on the $B\bar{B}$ final state.

To account for the presence of the mixed strong-EM sub-amplitude $\mathcal{A}_{B\bar{B}}^{gg\gamma}$, we introduce a new parameter R , that represents the ratio between the mixed strong-EM and the purely strong sub-amplitude

$$R = \frac{\mathcal{A}_{B\bar{B}}^{gg\gamma}}{\mathcal{A}_{B\bar{B}}^{ggg}}. \quad (3.2)$$

We assume that the dependence on the hadronization processes of the $gg\gamma$ and the ggg intermediate states cancels out in the ratio of the two sub-amplitudes, so that the new parameter R has the same value for each $B\bar{B}$ final state, like the relative phase φ and the five coupling constants of the set \mathcal{C} . Being proportional to the baryon charge [80, 112], the sub-amplitude $\mathcal{A}_{B\bar{B}}^{gg\gamma}$, and hence the parameter R are non-vanishing only for charged baryons. Asymptotically, when QCD is in perturbative regime, for $q^2 \gg \Lambda_{\text{QCD}}^2$, from Eq. (1.6) the ratio R becomes real and it can be written as

$$R_{\text{pQCD}}(q^2) \equiv \left. \frac{\mathcal{A}_{B\bar{B}}^{gg\gamma}}{\mathcal{A}_{B\bar{B}}^{ggg}} \right|_{\text{pQCD}} = \lim_{q^2 \rightarrow +\infty} R(q^2) = -\frac{4}{5} \frac{\alpha}{\alpha_S(q^2)}. \quad (3.3)$$

Table 3.2: Amplitudes parametrization.

$B\bar{B}$	$\mathcal{A}_{B\bar{B}} = \mathcal{A}_{B\bar{B}}^{ggg} + \mathcal{A}_{B\bar{B}}^{gg\gamma} + \mathcal{A}_{B\bar{B}}^{\gamma}$
$\Sigma^0\bar{\Sigma}^0$	$(G_0 + 2D_m)e^{i\varphi} + D_e$
$\Lambda\bar{\Lambda}$	$(G_0 - 2D_m)e^{i\varphi} - D_e$
$\Lambda\bar{\Sigma}^0 + \text{c.c.}$	$\sqrt{3} D_e$
$p\bar{p}$	$(G_0 - D_m + F_m)(1 + R)e^{i\varphi} + D_e + F_e$
$n\bar{n}$	$(G_0 - D_m + F_m)e^{i\varphi} - 2 D_e$
$\Sigma^+\bar{\Sigma}^-$	$(G_0 + 2D_m)(1 + R)e^{i\varphi} + D_e + F_e$
$\Sigma^-\bar{\Sigma}^+$	$(G_0 + 2D_m)(1 + R)e^{i\varphi} + D_e - F_e$
$\Xi^0\bar{\Xi}^0$	$(G_0 - D_m - F_m)e^{i\varphi} - 2 D_e$
$\Xi^-\bar{\Xi}^+$	$(G_0 - D_m - F_m)(1 + R)e^{i\varphi} + D_e - F_e$

The realization of the perturbative regime at the J/ψ mass is not well established, as already discussed, so the value R_{pQCD} is not a good approximation for our parameter R . We do retain the reality of R , following Refs. [79, 80, 112], as the main working hypothesis.

In light of that, we write the amplitude $\mathcal{A}_{B\bar{B}}$ for a given decay $J/\psi \rightarrow B\bar{B}$ as a combination of the coupling constants of the set $\mathcal{C} = \{G_0, D_e, D_m, F_e, F_m\}$, of the parameter R and using the relative phase φ . The amplitudes for the $J/\psi \rightarrow B\bar{B}$ decays for the nine baryon-antibaryon pair of the spin-1/2 SU(3) octet are reported in Table 3.2.

The purely EM $\mathcal{A}_{B\bar{B}}^{\gamma}$ is the combination of the coupling constants of the subset \mathcal{C}_{EM} , the purely strong $\mathcal{A}_{B\bar{B}}^{ggg}$ is the combination of the coupling constants of the subset $\mathcal{C}_{\text{strong}}$ multiplied by the phase $e^{i\varphi}$ and the mixed strong-EM sub-amplitude $\mathcal{A}_{B\bar{B}}^{gg\gamma}$, which is present only for charged baryons, is given by $\mathcal{A}_{B\bar{B}}^{gg\gamma} = R \mathcal{A}_{B\bar{B}}^{ggg}$.

Considering the decay of the J/ψ meson into a pair of nucleons, i.e., $B\bar{B} = p\bar{p}, n\bar{n}$, we have the following sub-amplitudes

$$\begin{aligned}
\mathcal{A}_{p\bar{p}}^{\gamma} &= D_e + F_e, & \mathcal{A}_{p\bar{p}}^{ggg} &= (G_0 - D_m + F_m) e^{i\varphi}, \\
\mathcal{A}_{p\bar{p}}^{gg\gamma} &= R (G_0 - D_m + F_m) e^{i\varphi}, & \mathcal{A}_{n\bar{n}}^{\gamma} &= -2D_e, \\
\mathcal{A}_{n\bar{n}}^{ggg} &= (G_0 - D_m + F_m) e^{i\varphi}, & \mathcal{A}_{n\bar{n}}^{gg\gamma} &= 0,
\end{aligned} \tag{3.4}$$

where it can be seen that the neutron-antineutron final state has the same purely strong sub-amplitude of the proton-antiproton one, different purely EM and, being neutral, vanishing mixed sub-amplitude.

For the sigma baryons, i.e., $B\bar{B} = \Sigma^+\bar{\Sigma}^-, \Sigma^-\bar{\Sigma}^+, \Sigma^0\bar{\Sigma}^0$, we have the following sub-amplitudes

$$\begin{aligned}\mathcal{A}_{\Sigma^+\bar{\Sigma}^-}^\gamma &= D_e + F_e, & \mathcal{A}_{\Sigma^+\bar{\Sigma}^-}^{ggg} &= (G_0 + 2D_m) e^{i\varphi}, & \mathcal{A}_{\Sigma^+\bar{\Sigma}^-}^{gg\gamma} &= R(G_0 + 2D_m) e^{i\varphi}, \\ \mathcal{A}_{\Sigma^-\bar{\Sigma}^+}^\gamma &= D_e - F_e, & \mathcal{A}_{\Sigma^-\bar{\Sigma}^+}^{ggg} &= (G_0 + 2D_m) e^{i\varphi}, & \mathcal{A}_{\Sigma^-\bar{\Sigma}^+}^{gg\gamma} &= R(G_0 + 2D_m) e^{i\varphi}, \\ \mathcal{A}_{\Sigma^0\bar{\Sigma}^0}^\gamma &= D_e, & \mathcal{A}_{\Sigma^0\bar{\Sigma}^0}^{ggg} &= (G_0 + 2D_m) e^{i\varphi}, & \mathcal{A}_{\Sigma^0\bar{\Sigma}^0}^{gg\gamma} &= 0,\end{aligned}\quad (3.5)$$

they have, as expected, the same purely strong sub-amplitude, but different purely EM ones. The sub-amplitudes for the Λ particle are

$$\mathcal{A}_{\Lambda\bar{\Lambda}}^\gamma = -D_e, \quad \mathcal{A}_{\Lambda\bar{\Lambda}}^{ggg} = (G_0 - 2D_m) e^{i\varphi}, \quad \mathcal{A}_{\Lambda\bar{\Lambda}}^{gg\gamma} = 0, \quad (3.6)$$

while those for the Ξ baryons, i.e., $B\bar{B} = \Xi^0\bar{\Xi}^0, \Xi^-\bar{\Xi}^+$ are

$$\begin{aligned}\mathcal{A}_{\Xi^0\bar{\Xi}^0}^\gamma &= -2D_e, & \mathcal{A}_{\Xi^0\bar{\Xi}^0}^{ggg} &= (G_0 - D_m - F_m) e^{i\varphi}, & \mathcal{A}_{\Xi^0\bar{\Xi}^0}^{gg\gamma} &= 0, \\ \mathcal{A}_{\Xi^-\bar{\Xi}^+}^\gamma &= D_e - F_e, & \mathcal{A}_{\Xi^-\bar{\Xi}^+}^{ggg} &= (G_0 - D_m - F_m) e^{i\varphi}, & & \\ \mathcal{A}_{\Xi^-\bar{\Xi}^+}^{gg\gamma} &= R(G_0 - D_m - F_m) e^{i\varphi}.\end{aligned}\quad (3.7)$$

The generic total amplitude for the $J/\psi \rightarrow B\bar{B}$ decay is parametrized as

$$\mathcal{A}_{B\bar{B}} = \mathcal{A}_{B\bar{B}}^{ggg}(1 + R)e^{i\varphi} + \mathcal{A}_{B\bar{B}}^\gamma \equiv \mathcal{S}_{B\bar{B}} e^{i\varphi} + \mathcal{A}_{B\bar{B}}^\gamma, \quad (3.8)$$

where $\mathcal{S}_{B\bar{B}} = \mathcal{A}_{B\bar{B}}^{ggg}(1 + R)$ and $\mathcal{A}_{B\bar{B}}^\gamma$ are real quantities to be determined by a minimization procedure, fitting the model predictions of the BRs to the corresponding experimental values. The total amplitude is defined up to an arbitrary, ineffective overall phase. By setting this phase to have $\mathcal{S}_{B\bar{B}}$ always positive, hence $\mathcal{S}_{B\bar{B}} = |\mathcal{S}_{B\bar{B}}|$, the sub-amplitude $\mathcal{A}_{B\bar{B}}^\gamma$ could be positive or negative, i.e., $\mathcal{A}_{B\bar{B}}^\gamma = |\mathcal{A}_{B\bar{B}}^\gamma|$ or $\mathcal{A}_{B\bar{B}}^\gamma = |\mathcal{A}_{B\bar{B}}^\gamma|e^{\pm i\pi}$. So that, the amplitude can be

redefined up to an overall sign as

$$\mathcal{A}_{B\bar{B}} \rightarrow \mathcal{A}_{B\bar{B}} = |\mathcal{S}_{B\bar{B}}| e^{i\varphi_{B\bar{B}}} + |\mathcal{A}_{B\bar{B}}^\gamma|, \quad (3.9)$$

where $\varphi_{B\bar{B}} = \varphi$ if $\mathcal{A}_{B\bar{B}}^\gamma > 0$ and $\varphi_{B\bar{B}} = \varphi \pm \pi$ if $\mathcal{A}_{B\bar{B}}^\gamma < 0$. This form is useful in order to make comparisons with the moduli of sub-amplitudes and the relative phase that the BESIII Collaboration [114] has obtained by fitting the data with a phenomenological parametrization of the amplitude. The choice between $\varphi_{B\bar{B}} = \varphi + \pi$ and $\varphi_{B\bar{B}} = \varphi - \pi$, when $\mathcal{A}_{B\bar{B}}^\gamma$ is negative, is guided by the request that the total relative phase has to be in a given determination, for instance, $\varphi_{B\bar{B}} \in [0, 2\pi]$. Actually, since the experimental observable is the modulus squared of the amplitude $\mathcal{A}_{B\bar{B}}$, which depends only on the cosine of the relative phase, being

$$|\mathcal{A}_{B\bar{B}}|^2 = |\mathcal{S}_{B\bar{B}}|^2 + |\mathcal{A}_{B\bar{B}}^\gamma|^2 + 2|\mathcal{S}_{B\bar{B}}||\mathcal{A}_{B\bar{B}}^\gamma| \cos(\varphi_{B\bar{B}}),$$

the ambiguity between the two values $\varphi_{B\bar{B}}^{\text{exp}}$ and $2\pi - \varphi_{B\bar{B}}^{\text{exp}}$, with $\varphi_{B\bar{B}}^{\text{exp}} \in [0, \pi]$ and hence $2\pi - \varphi_{B\bar{B}}^{\text{exp}} \in [\pi, 2\pi]$, cannot be resolved. In other words, both values $\pm\varphi_{B\bar{B}}$, $|\mathcal{S}_{B\bar{B}}|$ and $|\mathcal{A}_{B\bar{B}}^\gamma|$ being equal, give the same modulus squared, because $|\mathcal{A}_{B\bar{B}}|^2 = |\mathcal{A}_{B\bar{B}}^*|^2$, where $\mathcal{A}_{B\bar{B}}^*$ is the complex conjugate of $\mathcal{A}_{B\bar{B}}$.

3.1.3 Experimental data

At present, data are available for eight out of the nine decays, their values are reported in Table 3.3. The decay $J/\psi \rightarrow \Sigma^- \bar{\Sigma}^+$ is the only one that has not yet been observed. From the BR of the decay $J/\psi \rightarrow (\Lambda \bar{\Sigma}^0 + \text{c.c.})$, which is purely EM, see the third row of Table 3.2, we can extract the modulus of D_e as

$$|D_e| = \sqrt{\frac{16\pi M_{J/\psi} \Gamma_{J/\psi} \text{BR}(J/\psi \rightarrow (\Lambda \bar{\Sigma}^0 + \text{c.c.}))}{3\beta_{\Lambda \bar{\Sigma}^0}}},$$

Table 3.3: Branching ratios data from PDG [28] and BESIII experiment [116].

Decay process	Branching ratio	Error
$J/\psi \rightarrow \Sigma^0 \bar{\Sigma}^0$	$(1.164 \pm 0.004) \times 10^{-3}$	0.34%
$J/\psi \rightarrow \Lambda \bar{\Lambda}$	$(1.943 \pm 0.003) \times 10^{-3}$	0.15%
$J/\psi \rightarrow \Lambda \bar{\Sigma}^0 + \text{c.c.}$	$(2.83 \pm 0.23) \times 10^{-5}$	8.13%
$J/\psi \rightarrow p \bar{p}$	$(2.121 \pm 0.029) \times 10^{-3}$	1.37%
$J/\psi \rightarrow n \bar{n}$	$(2.09 \pm 0.16) \times 10^{-3}$	7.66%
$J/\psi \rightarrow \Sigma^+ \bar{\Sigma}^-$	$(1.50 \pm 0.24) \times 10^{-3}$	16.00%
$J/\psi \rightarrow \Xi^0 \bar{\Xi}^0$	$(1.17 \pm 0.04) \times 10^{-3}$	3.42%
$J/\psi \rightarrow \Xi^- \bar{\Xi}^+$	$(9.7 \pm 0.8) \times 10^{-4}$	8.25%

where the velocity of the outgoing baryon in the J/ψ -CM system is defined as

$$\beta_{\Lambda \bar{\Sigma}^0} \equiv \sqrt{1 - \frac{2(M_{\Sigma^0}^2 + M_{\Lambda}^2)}{M_{J/\psi}^2} + \frac{(M_{\Sigma^0}^2 - M_{\Lambda}^2)^2}{M_{J/\psi}^4}}.$$

Using the experimental value of $\text{BR}_{\Lambda \bar{\Sigma}^0}$, given in the third row of Table 3.3, we obtain

$$|D_e| = (4.52 \pm 0.20) \times 10^{-4} \text{ GeV},$$

where the data on the masses are taken from PDG [28], see Table 1.3, the same data are used also in the following. Analogously, the EM BR of the decay of the J/ψ meson into proton-antiproton is given by

$$\text{BR}_{p\bar{p}}^\gamma = \frac{\beta_{p\bar{p}}}{16\pi M_{J/\psi} \Gamma_{J/\psi}} |D_e + F_e|^2,$$

whit

$$\beta_{p\bar{p}} = \sqrt{1 - \frac{4M_p^2}{M_{J/\psi}^2}}.$$

The EM BR is related to the $e^+e^- \rightarrow p\bar{p}$ non-resonant cross section at the J/ψ mass by the formula, see Eq.(2.3),

$$\text{BR}_{B\bar{B}}^\gamma = \text{BR}_{\mu\mu} \frac{\sigma_{e^+e^- \rightarrow B\bar{B}}(M_{J/\psi}^2)}{\sigma_{e^+e^- \rightarrow \mu^+\mu^-}^0(M_{J/\psi}^2)}, \quad (3.10)$$

where $\text{BR}_{\mu\mu}$ is the BR of the decay $J/\psi \rightarrow \mu^+\mu^-$, and $\sigma_{e^+e^- \rightarrow \mu^+\mu^-}^0(q^2)$ represents the bare $e^+e^- \rightarrow \mu^+\mu^-$ cross section, i.e., the cross section corrected for the vacuum-polarization

$$\sigma_{e^+e^- \rightarrow \mu^+\mu^-}^0(q^2) = \frac{4\pi\alpha^2}{3q^2}.$$

The modulus of the sum of the two parameters D_e and F_e has, therefore, the expression

$$|D_e + F_e| = \sqrt{\frac{12 \text{BR}_{\mu\mu} M_{J/\psi}^3 \Gamma_{J/\psi} \sigma_{e^+e^- \rightarrow p\bar{p}}(M_{J/\psi}^2)}{\alpha^2 \beta_{p\bar{p}}}}.$$

The most recent data on the $p\bar{p}$ cross section obtained by the BESIII Collaboration [117] give at the J/ψ mass the cross section

$$\sigma_{e^+e^- \rightarrow p\bar{p}}(M_{J/\psi}^2) = \frac{6912 \pi \alpha^2 (M_{J/\psi}^2 + 2M_p^2)}{M_{J/\psi}^{12} \text{GeV}^{-8}} \times \left[\ln^2 \left(\frac{M_{J/\psi}^2}{0.52^2 \text{GeV}^2} \right) + \pi^2 \right]^{-2}. \quad (3.11)$$

Using this result together with [28]

$$\text{BR}_{\mu\mu} = (5.961 \pm 0.033) \times 10^{-2},$$

for the $J/\psi \rightarrow \mu^+\mu^-$ BR, we obtain

$$\text{BR}_{p\bar{p}}^{\gamma, \text{exp}} = (8.46 \pm 0.79) \times 10^{-5}, \quad (3.12)$$

from which

$$|D_e + F_e| = (1.240 \pm 0.061) \times 10^{-3} \text{ GeV}.$$

The errors include both statistical and systematic contributions due to the cross section fit to the BESIII data.

3.1.4 Results

We need to perform a minimization, fitting the model predictions to the experimental data, in order to obtain the seven free parameters, five of them being part of the \mathcal{C} set, previously defined, plus the parameter R and the relative phase φ . We define the χ^2 function

$$\chi^2(\mathcal{C}; R, \varphi) = \sum_{B\bar{B}} \left(\frac{\text{BR}_{B\bar{B}}^{\text{th}} - \text{BR}_{B\bar{B}}^{\text{exp}}}{\delta \text{BR}_{B\bar{B}}^{\text{exp}}} \right)^2 + \left(\frac{\text{BR}_{p\bar{p}}^{\gamma, \text{th}} - \text{BR}_{p\bar{p}}^{\gamma, \text{exp}}}{\delta \text{BR}_{p\bar{p}}^{\gamma, \text{exp}}} \right)^2, \quad (3.13)$$

where the sum runs over the eight baryon-antibaryon pairs, $B\bar{B}$, for which experimental data are available, reported in Table 3.3 and the last term imposes the constraint of the EM BR reported in Eq. (3.12).

The numerical minimization is performed with respect to the five coupling constants of the set $\mathcal{C} = \{G_0, D_e, D_m, F_e, F_m\}$, the ratio R defined in Eq. (3.2), and the relative phase φ .

The best values of the parameters resulting from the numerical minimization are shown in Table 3.4. The errors have been obtained by means of a Monte Carlo Gaussian simulation.

Table 3.4: Values of the parameters from the χ^2 minimization.

G_0	$(5.73511 \pm 0.0059) \times 10^{-3} \text{ GeV}$
D_e	$(4.52 \pm 0.19) \times 10^{-4} \text{ GeV}$
D_m	$(-3.74 \pm 0.34) \times 10^{-4} \text{ GeV}$
F_e	$(7.91 \pm 0.62) \times 10^{-4} \text{ GeV}$
F_m	$(2.42 \pm 0.12) \times 10^{-4} \text{ GeV}$
φ	$1.27 \pm 0.14 = (73 \pm 8)^\circ$
R	$(-9.7 \pm 2.1) \times 10^{-2}$

Using the obtained parameters we can calculate the value of the BRs for each baryon-antibaryon final state. The BRs are reported in Table 3.5, where they are compared with the corresponding experimental values (see Table 3.3) used to perform the χ^2 minimization.

It is interesting to notice that the obtained value for the BR of the unobserved $J/\psi \rightarrow \Sigma^- \bar{\Sigma}^+$

Table 3.5: Branching ratios from PDG [28] (second column), from parameters of Table 3.4 (third column) and their difference in units of the total error (fourth column).

$B\bar{B}$	$\text{BR}_{B\bar{B}}^{\text{PDG}} \times 10^3$	$\text{BR}_{B\bar{B}} \times 10^3$	$\frac{\Delta\text{BR}}{\sum \sigma_{\text{BR}}}$
$\Sigma^0\bar{\Sigma}^0$	1.164 ± 0.004	1.160 ± 0.041	~ 0.09
$\Lambda\bar{\Lambda}$	1.943 ± 0.003	1.940 ± 0.055	~ 0.05
$\Lambda\bar{\Sigma}^0 + \text{c.c.}$	0.0283 ± 0.0023	0.0280 ± 0.0024	~ 0.06
$p\bar{p}$	2.121 ± 0.029	2.10 ± 0.16	~ 0.1
$n\bar{n}$	2.09 ± 0.16	2.10 ± 0.12	~ 0.04
$\Sigma^+\bar{\Sigma}^-$	1.50 ± 0.24	1.110 ± 0.086	~ 1
$\Sigma^-\bar{\Sigma}^+$	/	0.857 ± 0.051	/
$\Xi^0\bar{\Xi}^0$	1.17 ± 0.04	1.180 ± 0.072	~ 0.09
$\Xi^-\bar{\Xi}^+$	0.97 ± 0.08	0.979 ± 0.065	~ 0.06

decay, i.e.,

$$\text{BR}_{\Sigma^-\bar{\Sigma}^+} = (0.857 \pm 0.051) \times 10^{-3}, \quad (3.14)$$

represents a prediction of our model. Moreover, it is important to notice that only one of the obtained BRs is quite different from its corresponding PDG value, the BR of the $J/\psi \rightarrow \Sigma^+\bar{\Sigma}^-$ decay, in fact we found the value

$$\text{BR}_{\Sigma^+\bar{\Sigma}^-} = (1.110 \pm 0.086) \times 10^{-3}, \quad (3.15)$$

to be compared with the PDG value

$$\text{BR}_{\Sigma^+\bar{\Sigma}^-}^{\text{PDG}} = (1.50 \pm 0.24) \times 10^{-3}$$

that has also a large relative error of about the 16%. A recent independent preliminary analysis [118] confirms our prediction for the BR of the $J/\psi \rightarrow \Sigma^+\bar{\Sigma}^-$ decay. The analysis is actually only preliminary and the found value is $\text{BR}_{\Sigma^+\bar{\Sigma}^-} = (1.115 \pm 0.005^{\text{stat}}) \times 10^{-3}$.

The ratios between the input and best values of the BRs, that represent the nine free parameters of the χ^2 given in Eq. (3.13), are shown in Fig. 3.3. The minimum normalized χ^2

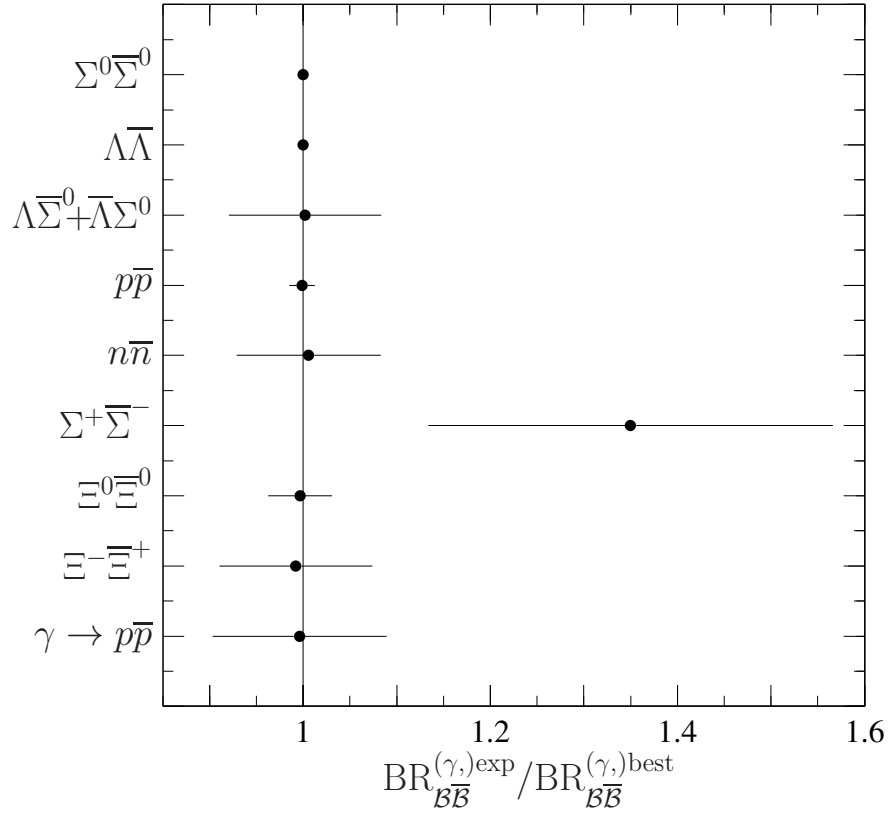


Figure 3.3: Ratios between the experimental input values of BRs and their best values obtained by minimizing the χ^2 of Eq. (3.13). The lower point, at the ordinate labelled width $\gamma \rightarrow p\bar{p}$, is the contribution due to EM BR of the proton, see Eq. (3.12).

is

$$\frac{\chi^2(\mathcal{C}^{\text{best}}, R^{\text{best}}, \varphi^{\text{best}})}{N_{\text{dof}}} = 1.33, \quad (3.16)$$

where the number of degrees of freedom is

$$N_{\text{dof}} = N_{\text{const}} - N_{\text{param}} = 2,$$

in fact we have nine constraints, $N_{\text{const}} = 9$, and seven free parameters, $N_{\text{param}} = 7$. It is possible to verify the significance of the mixed strong-EM contribution in the description of

the J/ψ decay mechanism by comparing the normalized χ^2 of Eq. (3.16), obtained in the case where R is considered as a free parameter, to that in which it is fixed at $R = 0$, i.e.,

$$\frac{\chi^2(\mathcal{C}'^{\text{best}}; R = 0, \varphi'^{\text{best}})}{N_{\text{dof}}} = \frac{16.44}{3} = 5.48, \quad (3.17)$$

where $\mathcal{C}'^{\text{best}}$ and φ'^{best} are the set of best values of the coupling constants and the best relative phase obtained in this case. Despite the quite low number of degrees of freedom and also the smallness of the best value obtained for R , see Table 3.4, this large χ^2 , see Eq. (3.17), represents a clear indication in favor of the necessity of the mixed strong-EM contribution. In fact the most suitable criterion to compare these two hypotheses, namely: free R and $R = 0$, is the one provided by the p -value, $p(\chi^2; N_{\text{dof}})$. The two p -values are

$$p(2.65; 2) = 0.266, \quad p(16.44; 3) = 9.21 \times 10^{-4}, \quad (3.18)$$

and represent the probabilities to obtain by chance $\chi^2 = 2.65$ and $\chi^2 = 16.44$, with two and three degrees of freedom respectively, if the model is correct.

As mentioned before, the knowledge of the seven coupling constants of Table 3.4 brings important information on the structure of the amplitudes for the considered $J/\psi \rightarrow B\bar{B}$ decays. In fact, using these values, from Eq. (3.1.2), Eq. (3.1.2), Eq. (3.6) and Eq. (3.1.2), we can calculate each individual sub-amplitude and, hence, the corresponding contribution to the total BR, under the assumptions concerning their relative phases. The resulting purely strong, purely EM and mixed strong-EM contributions to the total BR for the nine final states are reported in Table 3.6.

We calculate also the ratios of the moduli of the sub-amplitudes $|\mathcal{A}_{B\bar{B}}^\gamma/\mathcal{A}_{B\bar{B}}^{ggg}|$ and $|\mathcal{A}_{B\bar{B}}^{gg\gamma}/\mathcal{A}_{B\bar{B}}^{ggg}|$, i.e., the moduli of the purely EM and mixed strong-EM sub-amplitudes normalized to the modulus of the purely strong sub-amplitude, the approximate results are shown in Table 3.7. First of all we observe that, in all cases, since by assumption it does not depend on the $B\bar{B}$ final state, the strength of the mixed strong-EM sub-amplitude relative to the dominant three-gluon one represents about the 10% of the dominant contribution and becomes $\sim 1\%$

Table 3.6: Purely strong (second column), purely EM (third column) and mixed (fourth column) BRs.

$B\bar{B}$	$\text{BR}_{B\bar{B}}^{ggg} \times 10^3$	$\text{BR}_{B\bar{B}}^{\gamma} \times 10^5$	$\text{BR}_{B\bar{B}}^{gg\gamma} \times 10^5$
$\Sigma^0 \bar{\Sigma}^0$	1.100 ± 0.030	0.902 ± 0.076	0
$\Lambda \bar{\Lambda}$	2.020 ± 0.042	0.981 ± 0.083	0
$\Lambda \bar{\Sigma}^0 + \text{c.c.}$	0	2.83 ± 0.24	0
$p \bar{p}$	2.220 ± 0.085	8.52 ± 0.89	2.19 ± 0.93
$n \bar{n}$	2.220 ± 0.085	4.50 ± 0.38	0
$\Sigma^+ \bar{\Sigma}^-$	1.100 ± 0.030	6.86 ± 0.72	1.08 ± 0.46
$\Sigma^- \bar{\Sigma}^+$	1.090 ± 0.030	0.52 ± 0.20	1.07 ± 0.46
$\Xi^0 \bar{\Xi}^0$	1.260 ± 0.053	2.99 ± 0.25	0
$\Xi^- \bar{\Xi}^+$	1.240 ± 0.052	0.43 ± 0.16	1.22 ± 0.52

Table 3.7: Approximate values of moduli of the ratios between sub-amplitudes $\mathcal{A}_{B\bar{B}}^{\gamma}$ and $\mathcal{A}_{B\bar{B}}^{ggg}$ (second column), and between $\mathcal{A}_{B\bar{B}}^{gg\gamma}$ and $\mathcal{A}_{B\bar{B}}^{ggg}$ (third column).

$B\bar{B}$	$ \mathcal{A}_{B\bar{B}}^{\gamma}/\mathcal{A}_{B\bar{B}}^{ggg} $	$ \mathcal{A}_{B\bar{B}}^{gg\gamma}/\mathcal{A}_{B\bar{B}}^{ggg} $
$\Sigma^0 \bar{\Sigma}^0$	~ 0.09	0
$\Lambda \bar{\Lambda}$	~ 0.07	0
$p \bar{p}$	~ 0.20	~ 0.1
$n \bar{n}$	~ 0.14	0
$\Sigma^+ \bar{\Sigma}^-$	~ 0.25	~ 0.1
$\Sigma^- \bar{\Sigma}^+$	~ 0.07	~ 0.1
$\Xi^0 \bar{\Xi}^0$	~ 0.15	0
$\Xi^- \bar{\Xi}^+$	~ 0.06	~ 0.1

for the BR, see the fourth column of Table 3.6. More intriguing is the comparison between the mixed and the purely EM contributions, third and fourth columns of Table 3.6 for the BRs and, second and third columns of Table 3.7 for the sub-amplitudes. They are always of the same order, but while for the proton and Σ^+ the modulus of the purely EM sub-amplitude is about twice the modulus of the mixed sub-amplitude, in the cases of Σ^- and Ξ^- the hierarchy is inverted. Such different behavior could be due to the different quark structure of the two pairs of baryons.

The moduli of the sub-amplitudes $\mathcal{S}_{B\bar{B}}$ and $\mathcal{A}_{B\bar{B}}^\gamma$, together with the phase $\varphi_{B\bar{B}}$, defined in

Table 3.8: Moduli of sub-amplitudes $\mathcal{S}_{B\bar{B}}$, $\mathcal{A}_{B\bar{B}}^\gamma$ and phase $\varphi_{B\bar{B}}$, defined in Eq. (3.9).

$B\bar{B}$	$ \mathcal{S}_{B\bar{B}} \times 10^3$	$ \mathcal{A}_{B\bar{B}}^\gamma \times 10^4$	$\varphi_{B\bar{B}}$
$\Sigma^0 \bar{\Sigma}^0$	4.987 ± 0.065	4.52 ± 0.19	φ
$\Lambda \bar{\Lambda}$	6.483 ± 0.065	4.52 ± 0.19	$\pi - \varphi$
$\Lambda \bar{\Sigma}^0 + \text{c.c.}$	0	7.83 ± 0.33	φ
$p \bar{p}$	5.74 ± 0.14	12.43 ± 0.65	φ
$n \bar{n}$	6.351 ± 0.037	9.04 ± 0.38	$\pi - \varphi$
$\Sigma^+ \bar{\Sigma}^-$	4.50 ± 0.12	12.43 ± 0.65	φ
$\Sigma^- \bar{\Sigma}^+$	4.50 ± 0.12	3.39 ± 0.65	$\pi - \varphi$
$\Xi^0 \bar{\Xi}^0$	5.867 ± 0.037	9.04 ± 0.38	$\pi - \varphi$
$\Xi^- \bar{\Xi}^+$	5.30 ± 0.13	3.39 ± 0.65	$\pi - \varphi$

Eq. (3.8) and Eq. (3.9), are reported in Table 3.8. The five final states: $\Lambda \bar{\Lambda}$, $n \bar{n}$, $\Sigma^- \bar{\Sigma}^+$, $\Xi^0 \bar{\Xi}^0$, $\Xi^- \bar{\Xi}^+$, have negative $\mathcal{A}_{B\bar{B}}^\gamma$ sub-amplitudes and then $\varphi_{B\bar{B}} = \pi - \varphi$, this is a phenomenological finding due to the values that have been obtained for the coupling constants D_e and F_e with the fitting procedure, see Table 3.4, and to the SU(3) symmetry of the model, that determines the signs of the coupling constants in the definition of the sub-amplitudes, see Table 3.2. As an example, let us consider the $p \bar{p}$ and $n \bar{n}$ final states. Using the standard parametrization of Eq. (3.9), the total relative phase between the two sub-amplitudes $\mathcal{S}_{B\bar{B}} e^{i\varphi}$ and $\mathcal{A}_{B\bar{B}}^\gamma$ differ by 180° , i.e.,

$$\arg \left(\frac{\mathcal{S}_{p\bar{p}} e^{i\varphi}}{\mathcal{A}_{p\bar{p}}^\gamma} \right) = \varphi, \quad \arg \left(\frac{\mathcal{S}_{n\bar{n}} e^{i\varphi}}{\mathcal{A}_{n\bar{n}}^\gamma} \right) = \varphi \pm \pi.$$

The last result is a consequence of the negative value of $\mathcal{A}_{n\bar{n}}^\gamma = -2D_e$, with $D_e > 0$, see Table 3.4. As shown in the sixth row of Table 3.4 the best value of the relative phase between strong and EM sub-amplitudes is

$$\varphi = (73 \pm 8)^\circ$$

and it agrees with the result given in Refs. [95, 119] and with the value given in Ref. [114], i.e., $(88.7 \pm 8.1)^\circ$, obtained by studying the decays of the J/ψ meson into nucleon-antinucleon.

There is also a very good agreement between our result and the value found in Ref. [120], i.e., $(76 \pm 11)^\circ$. More in detail, by considering the relative sign between the sub-amplitudes $|\mathcal{S}_{B\bar{B}}|$ and $|\mathcal{A}_{B\bar{B}}^\gamma|$, defined in Eq. (3.9), we can distinguish between two values of the relative phase $\varphi_{B\bar{B}}$, see Table 3.8,

$$\begin{aligned}\varphi_{\Sigma^0\bar{\Sigma}^0, \Lambda\bar{\Sigma}^0, p\bar{p}, \Sigma^+\bar{\Sigma}^-} &= (73 \pm 8)^\circ, \\ \varphi_{\Lambda\bar{\Lambda}, n\bar{n}, \Sigma^-\bar{\Sigma}^+, \Xi^0\bar{\Xi}^0, \Xi^-\bar{\Xi}^+} &= (107 \pm 8)^\circ.\end{aligned}$$

The fact that the relative phase φ is closer to 90° rather than to 0° or 180° , as already discussed, disagrees with the pQCD predictions, in fact, in the perturbative regime, all QCD amplitudes should be real. It follows that the obtained relative phase could be interpreted as the indication of a non-complete realization of pQCD at this energy, at least for the examined J/ψ decays.

Another result that agrees with this conclusion is the value obtained for the ratio R , shown in the last row of Table 3.4, i.e.,

$$R = -0.097 \pm 0.021.$$

This value, in addition to confirming that the mixed strong-EM sub-amplitude is negligible with respect to purely strong one, is not compatible with that predicted by pQCD, see Eq. (3.3), which is indeed

$$R_{\text{pQCD}}(M_{J/\psi}^2) = -\frac{4}{5} \frac{\alpha}{\alpha_S(M_{J/\psi}^2)} \sim -0.030,$$

where we have used $\alpha_S(M_{J/\psi}^2) \sim 0.2$ [80]. Therefore, as anticipated, at the J/ψ mass the perturbative regime of QCD is still not reached. A similar conclusion is also suggested in Ref. [83].

Finally, we use the values in the second column of Table 3.6 to calculate the non-resonant $e^+e^- \rightarrow B\bar{B}$ Born cross sections at the J/ψ mass, $q^2 = M_{J/\psi}^2$. The results are reported in Table 3.9.

Table 3.9: Non-resonant $e^+e^- \rightarrow B\bar{B}$ Born cross sections at $q^2 = M_{J/\psi}^2$.

$e^+e^- \rightarrow B\bar{B}$	Cross section at the $q^2 = M_{J/\psi}^2$
$e^+e^- \rightarrow \Sigma^0\bar{\Sigma}^0$	(1.37 ± 0.12) pb
$e^+e^- \rightarrow \Lambda\bar{\Lambda}$	(1.49 ± 0.13) pb
$e^+e^- \rightarrow (\Lambda\bar{\Sigma}^0 + \text{c.c.})$	(4.30 ± 0.36) pb
$e^+e^- \rightarrow p\bar{p}$	(12.9 ± 1.4) pb
$e^+e^- \rightarrow n\bar{n}$	(6.84 ± 0.58) pb
$e^+e^- \rightarrow \Sigma^+\bar{\Sigma}^-$	(10.4 ± 1.1) pb
$e^+e^- \rightarrow \Sigma^-\bar{\Sigma}^+$	(0.79 ± 0.30) pb
$e^+e^- \rightarrow \Xi^0\bar{\Xi}^0$	(4.54 ± 0.38) pb
$e^+e^- \rightarrow \Xi^-\bar{\Xi}^+$	(0.65 ± 0.24) pb

Currently there are no data for the majority of these cross sections, so we cannot make direct comparisons. These results represent a prediction of our model that could be useful for future experiments. We remember that the EM BR for the proton-antiproton final state is the only exception, in fact we used its experimental value, given in Eq. (3.12) and extracted from the non-resonant $e^+e^- \rightarrow p\bar{p}$ cross section data [117], as a constraint in the numerical χ^2 minimization.

3.1.5 The case of complex R

We consider a complex ratio R by introducing a new parameter, the relative phase between the purely strong sub-amplitude and the mixed one, called φ_2 . In this case, from Eq. (3.2), we can write

$$R = \frac{\mathcal{A}_{B\bar{B}}^{gg\gamma}}{\mathcal{A}_{B\bar{B}}^{ggg}} = \left| \frac{\mathcal{A}_{B\bar{B}}^{gg\gamma}}{\mathcal{A}_{B\bar{B}}^{ggg}} \right| e^{i\varphi_2}. \quad (3.19)$$

The amplitudes for the decays $J/\psi \rightarrow B\bar{B}$, under this new hypothesis, are reported in Table 3.10. By performing the same fitting procedure used in the case of real R , we obtain the values shown in Table 3.11. The values of the seven parameters G_0 , D_e , D_m , F_e , F_m , φ and $|R|$ are very close to those obtained in the case of real R , shown in Table 3.15. The total BRs

Table 3.10: Amplitudes parameterization with a complex ratio R .

$B\bar{B}$	$\mathcal{A}_{B\bar{B}} = \mathcal{A}_{B\bar{B}}^{ggg} + \mathcal{A}_{B\bar{B}}^{gg\gamma} + \mathcal{A}_{B\bar{B}}^{\gamma}$
$\Sigma^0\bar{\Sigma}^0$	$(G_0 + 2D_m)e^{i\varphi} + D_e$
$\Lambda\bar{\Lambda}$	$(G_0 - 2D_m)e^{i\varphi} - D_e$
$\Lambda\bar{\Sigma}^0 + \text{c.c.}$	$\sqrt{3} D_e$
$p\bar{p}$	$(G_0 - D_m + F_m)(1 + R e^{i\varphi_2})e^{i\varphi} + D_e + F_e$
$n\bar{n}$	$(G_0 - D_m + F_m)e^{i\varphi} - 2D_e$
$\Sigma^+\bar{\Sigma}^-$	$(G_0 + 2D_m)(1 + R e^{i\varphi_2})e^{i\varphi} + D_e + F_e$
$\Sigma^-\bar{\Sigma}^+$	$(G_0 + 2D_m)(1 + R e^{i\varphi_2})e^{i\varphi} + D_e - F_e$
$\Xi^0\bar{\Xi}^0$	$(G_0 - D_m - F_m)e^{i\varphi} - 2D_e$
$\Xi^-\bar{\Xi}^+$	$(G_0 - D_m - F_m)(1 + R e^{i\varphi_2})e^{i\varphi} + D_e - F_e$

Table 3.11: Values of the parameters from the χ^2 minimization in the case of a complex ratio R .

G_0	$(5.73488 \pm 0.0040) \times 10^{-3} \text{ GeV}$
D_e	$(4.52 \pm 0.15) \times 10^{-4} \text{ GeV}$
D_m	$(-3.70 \pm 0.19) \times 10^{-4} \text{ GeV}$
F_e	$(7.88 \pm 0.28) \times 10^{-4} \text{ GeV}$
F_m	$(2.38 \pm 0.59) \times 10^{-4} \text{ GeV}$
φ	$1.29 \pm 0.11 = (74 \pm 6)^\circ$
φ_2	$3.59 \pm 0.81 = (206 \pm 46)^\circ$
$ R $	$(11.5 \pm 1.7) \times 10^{-2}$

calculated using these parameters are shown in Table 3.12, together with the corresponding PDG values. The purely strong, purely EM and mixed strong-EM BRs are reported in Table 3.13.

The numerical minimization gives the normalized χ^2

$$\frac{\chi^2(\mathcal{C}^{\text{best}}, |R|^{\text{best}}, \varphi^{\text{best}}, \varphi_2^{\text{best}})}{N_{\text{dof}}} = 2.59,$$

where, in this case,

$$N_{\text{dof}} = N_{\text{const}} - N_{\text{param}} = 1,$$

Table 3.12: Branching ratios from PDG [28] (second column), from parameters of Table 3.11 (third column).

$B\bar{B}$	$\text{BR}_{B\bar{B}}^{\text{PDG}} \times 10^3$	$\text{BR}_{B\bar{B}} \times 10^3$
$\Sigma^0 \bar{\Sigma}^0$	1.160 ± 0.041	1.160 ± 0.028
$\Lambda \bar{\Lambda}$	1.940 ± 0.055	1.940 ± 0.039
$\Lambda \bar{\Sigma}^0 + \text{c.c.}$	0.0283 ± 0.0023	0.0280 ± 0.0019
$p\bar{p}$	2.121 ± 0.029	2.20 ± 0.27
$n\bar{n}$	2.09 ± 0.16	2.08 ± 0.08
$\Sigma^+ \bar{\Sigma}^-$	1.50 ± 0.24	1.20 ± 0.14
$\Sigma^- \bar{\Sigma}^+$	/	0.91 ± 0.10
$\Xi^0 \bar{\Xi}^0$	1.17 ± 0.04	1.180 ± 0.049
$\Xi^- \bar{\Xi}^+$	0.97 ± 0.08	1.00 ± 0.12

Table 3.13: Purely strong (second column), purely EM (third column) and mixed (fourth column) BRs in the case of a complex ratio R .

$B\bar{B}$	$\text{BR}_{B\bar{B}}^{ggg} \times 10^3$	$\text{BR}_{B\bar{B}}^{\gamma} \times 10^5$	$\text{BR}_{B\bar{B}}^{gg\gamma} \times 10^5$
$\Sigma^0 \bar{\Sigma}^0$	1.100 ± 0.017	0.903 ± 0.061	0
$\Lambda \bar{\Lambda}$	2.010 ± 0.024	0.982 ± 0.066	0
$\Lambda \bar{\Sigma}^0 + \text{c.c.}$	0	2.83 ± 0.19	0
$p\bar{p}$	2.210 ± 0.043	8.47 ± 0.43	2.97 ± 0.87
$n\bar{n}$	2.210 ± 0.043	4.50 ± 0.30	0
$\Sigma^+ \bar{\Sigma}^-$	1.100 ± 0.017	6.82 ± 0.35	1.49 ± 0.44
$\Sigma^- \bar{\Sigma}^+$	1.090 ± 0.017	0.500 ± 0.094	1.47 ± 0.43
$\Xi^0 \bar{\Xi}^0$	1.260 ± 0.027	2.99 ± 0.20	0
$\Xi^- \bar{\Xi}^+$	1.240 ± 0.026	0.410 ± 0.077	1.67 ± 0.49

having, $N_{\text{const}} = 9$ and $N_{\text{param}} = 8$.

The obtained value for the relative phase between the purely strong sub-amplitude and the mixed strong-EM one, $\varphi_2 = (206 \pm 46)^\circ$ is compatible with our first hypothesis about the reality and negativity of R , corresponding to a relative phase φ_2 of 180° . In this case the p -value, see Eq. (3.18), is

$$p(2.59; 1) = 0.108.$$

In light of such full agreement and of the lower statistical significance we consider as our main results those obtained under the hypothesis of real R .

3.1.6 Discussion

We have calculated the purely strong, purely EM and mixed strong-EM contributions to the total BR, see Table 3.6, and hence the moduli of the corresponding sub-amplitudes, for each pair of baryons, see Table 3.7 and Table 3.8. The mixed strong-EM contribution is determined for the first time and it is proven to be crucial, in the framework of our model, for the correct description of the decay mechanism. We have obtained the relative phase between strong and EM sub-amplitudes, assuming that the strong and mixed strong-EM ones have the same phase and, finally, we have used the purely EM BRs to calculate the Born non-resonant cross sections of the annihilation processes $e^+e^- \rightarrow B\bar{B}$ at the J/ψ mass. The possibility of disentangling single contributions allows, for the first time, to determine the mixed strong-EM sub-amplitude for each charged $B\bar{B}$ final state. In particular, the mixed strong-EM sub-amplitude is about 10% of the corresponding purely strong sub-amplitude, for the charged final states, while it is, as supposed, zero for the neutral ones, see third column of Table 3.7. On the other hand the purely EM sub-amplitude is between 6% and 25% of the corresponding purely strong sub-amplitude, see second column of Table 3.7. Furthermore considering the four charged final states: $p\bar{p}$, $\Sigma^+\bar{\Sigma}^-$, $\Sigma^-\bar{\Sigma}^+$, $\Xi^-\bar{\Xi}^+$, for two of them, $\Sigma^-\bar{\Sigma}^+$ and $\Xi^-\bar{\Xi}^+$, the mixed strong-EM sub-amplitudes are larger than the corresponding purely EM ones, while the remaining two show an opposite trend.

The hypothesis of a complex ratio R has been considered and it has been shown that the resulting relative phase, φ_2 , between the purely strong and the mixed strong-EM sub-amplitudes is compatible with 180° , i.e., with a real and negative value of R .

Finally, our prediction for the neutron cross section, see fifth row of Table 3.9, i.e.,

$$\sigma_{e^+e^- \rightarrow n\bar{n}}(M_{J/\psi}^2) = (6.84 \pm 0.58) \text{ pb},$$

is in agreement with the “natural” expectation

$$\begin{aligned}\sigma_{e^+e^- \rightarrow n\bar{n}}^{\text{expected}}(M_{J/\psi}^2) &= \left(\frac{\mu_n}{\mu_p}\right)^2 \sigma_{e^+e^- \rightarrow p\bar{p}}(M_{J/\psi}^2) = \left(\frac{-1.913}{2.793}\right)^2 (12.9 \pm 1.4) \text{ pb} \\ &= (6.1 \pm 0.7) \text{ pb},\end{aligned}$$

which is obtained by scaling the proton cross section, reported in the fourth row of Table 3.9, by the square value of the ratio between neutron, μ_n , and proton, μ_p , magnetic moment.

3.2 The decays of the J/ψ and $\psi(2S)$ into $\Lambda\bar{\Lambda}$ and $\Sigma^0\bar{\Sigma}^0$

The decay mechanisms of the lightest charmonia can be studied almost only by means of effective models, since these decays happen at energy regimes that do not allow the use of pQCD. From Eq. (1.14) it can be seen that the Lagrangian for the particular decay to $\Lambda\bar{\Lambda}$ and $\Sigma^0\bar{\Sigma}^0$ can be described in terms of only two parameters. This fact can be seen also by looking at the first two rows of Table 3.2, where the number of parameters can be reduced by replacing them with some appropriate linear combination. For this reason in this chapter we pay attention to the J/ψ and $\psi(2S)$ charmonia, and study their decays into baryon-antibaryon pairs with $B\bar{B} = \Lambda\bar{\Lambda}, \Sigma^0\bar{\Sigma}^0$.

3.2.1 Theoretical background

The differential cross section of the process $e^+e^- \rightarrow \psi \rightarrow B\bar{B}$ has the well known $\cos\theta$ dependence [111]

$$\frac{dN}{d\cos\theta} \propto 1 + \alpha_B \cos^2\theta,$$

where α_B is the so-called polarization parameter and θ is the baryon scattering angle, i.e., the angle between the outgoing baryon and the beam direction in the e^+e^- center of mass frame.

In Fig. 3.4 and Fig. 3.5 are shown BESIII data [116] on the angular distributions of the

four decays: $J/\psi \rightarrow \Lambda\bar{\Lambda}$, $J/\psi \rightarrow \Sigma^0\bar{\Sigma}^0$, and $\psi(2S) \rightarrow \Lambda\bar{\Lambda}$, $\psi(2S) \rightarrow \Sigma^0\bar{\Sigma}^0$. Only the decay $J/\psi \rightarrow \Sigma^0\bar{\Sigma}^0$ has a negative polarization parameter α_B , as was already pointed out in Ref. [121]. These results represent a real finding compared with the first experiments where the opposite trend on the angular distribution of the J/ψ into $\Lambda\bar{\Lambda}$ and $\Sigma^0\bar{\Sigma}^0$ was not found, see for example Ref. [122].

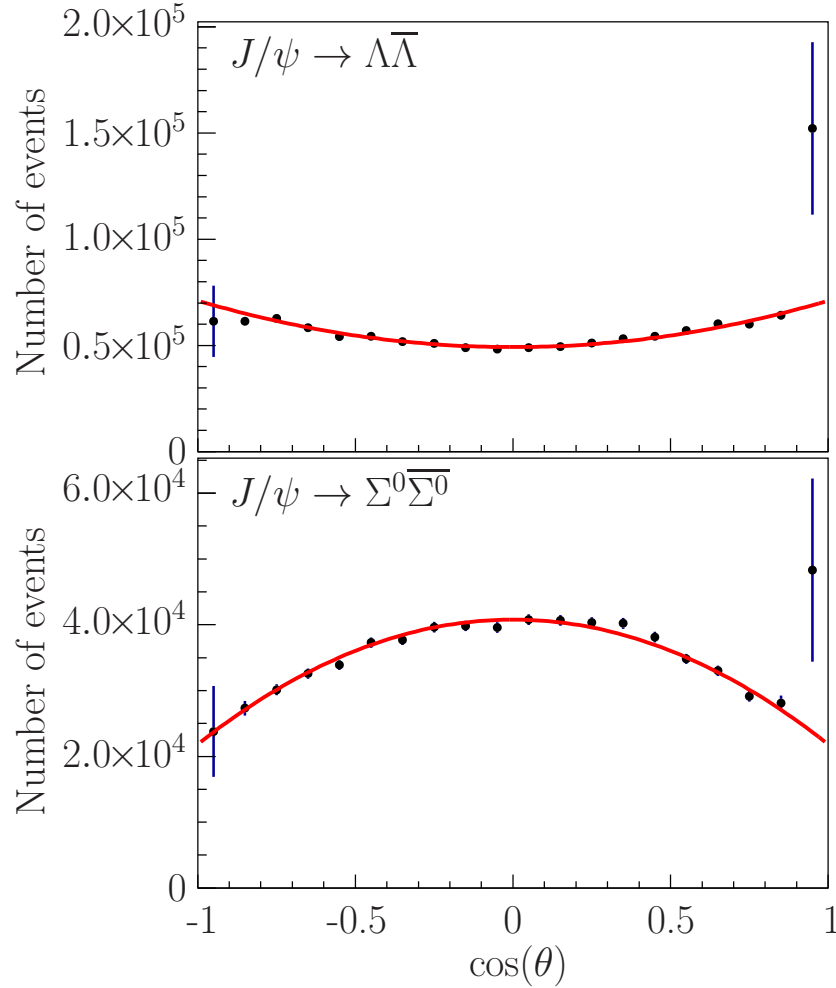


Figure 3.4: Angular distribution of the baryon for the J/ψ decays into $\Lambda\bar{\Lambda}$ (upper panel) and $\Sigma^0\bar{\Sigma}^0$ (lower panel).

Starting from Eq. (1.13) and, in particular, considering Eq. (1.14), it is possible to extract

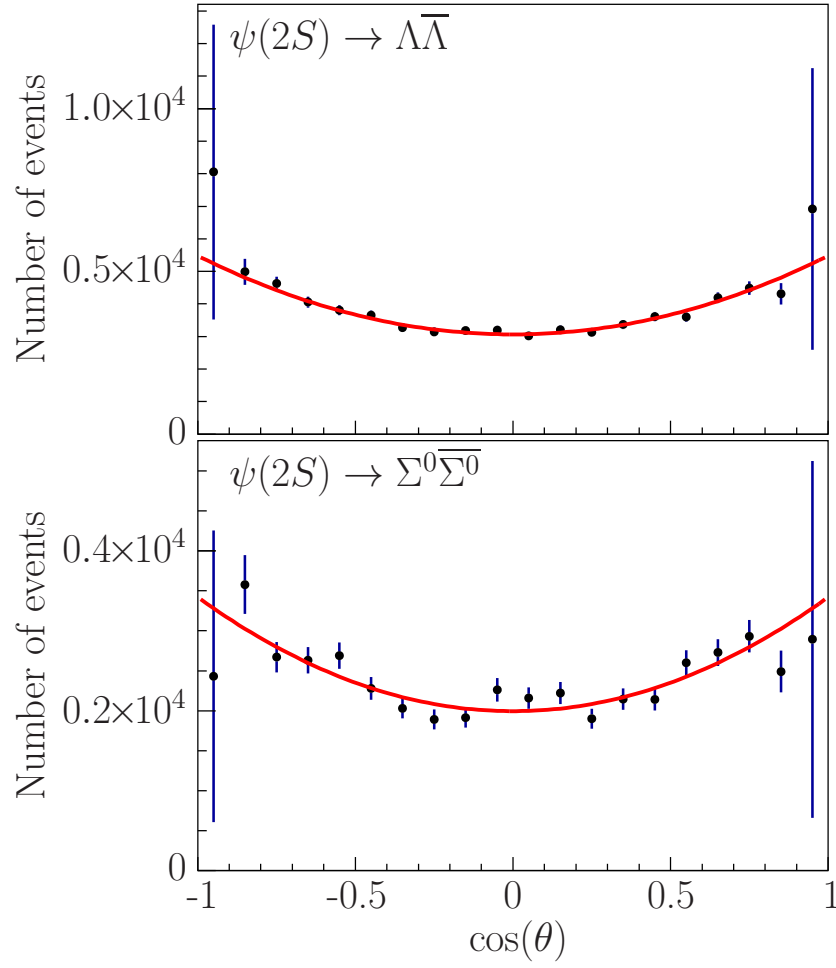


Figure 3.5: Angular distribution of the baryon for the $\psi(2S)$ decays into $\Lambda\bar{\Lambda}$ (upper panel) and $\Sigma^0\bar{\Sigma}^0$ (lower panel).

the Lagrangians describing only the J/ψ and $\psi(2S)$ decays into $\Lambda\bar{\Lambda}$ and $\Sigma^0\bar{\Sigma}^0$. We can write

$$\mathcal{L}_{\Sigma^0\bar{\Sigma}^0} = (G_0 + G_1) \Sigma^0\bar{\Sigma}^0, \quad \mathcal{L}_{\Lambda\bar{\Lambda}} = (G_0 - G_1) \Lambda\bar{\Lambda}, \quad (3.20)$$

where G_0 and G_1 are the following combinations of coupling constants

$$G_0 = g, \quad G_1 = \frac{d}{3} (2g_m + g_e).$$

By using the same structure of Eq. (1.12), the BRs can be expressed in terms of electric and magnetic amplitudes as

$$\text{BR}_{\psi \rightarrow \Sigma^0\bar{\Sigma}^0} = |A_E^\Sigma|^2 + |A_M^\Sigma|^2, \quad \text{BR}_{\psi \rightarrow \Lambda\bar{\Lambda}} = |A_E^\Lambda|^2 + |A_M^\Lambda|^2.$$

We can also decompose such amplitudes as combinations of leading, E_0 and M_0 , and sub-leading terms, E_1 and M_1 , see Eq. (3.20), with opposite relative signs, i.e.,

$$\begin{aligned} \text{BR}_{\psi \rightarrow \Sigma^0\bar{\Sigma}^0} &= |E_0 + E_1|^2 + |M_0 + M_1|^2 = |E_0|^2 + |E_1|^2 + 2|E_0||E_1|\cos(\rho_E) \\ &\quad + |M_0|^2 + |M_1|^2 + 2|M_0||M_1|\cos(\rho_M), \\ \text{BR}_{\psi \rightarrow \Lambda\bar{\Lambda}} &= |E_0 - E_1|^2 + |M_0 - M_1|^2 = |E_0|^2 + |E_1|^2 - 2|E_0||E_1|\cos(\rho_E) \\ &\quad + |M_0|^2 + |M_1|^2 - 2|M_0||M_1|\cos(\rho_M), \end{aligned}$$

where ρ_E and ρ_M are the phases of the ratios E_0/E_1 and M_0/M_1 .

3.2.2 Results

We use data from precise measurements [109, 116] of the BRs and polarization parameters, reported in Table 3.14. These BESIII data are in agreement with the results of other experiments [123–127]. We have to fix the relative phases ρ_E and ρ_M , since we have six free parameters (four moduli and two relative phases) and only four constraints (two BRs and two polarization parameters) for each charmonium state. We find that the values $\rho_E = 0$ and $\rho_M = \pi$ are phenomenologically favored by the data themselves. In fact, largely different

Table 3.14: Branching ratios and polarization parameters from Ref. [116]. In particular the value of α_B for the decay $J/\psi \rightarrow \Lambda\bar{\Lambda}$ is from Ref. [109].

Decay	BR	Pol. par. α_B
$J/\psi \rightarrow \Sigma^0\bar{\Sigma}^0$	$(11.64 \pm 0.04) \times 10^{-4}$	-0.449 ± 0.020
$J/\psi \rightarrow \Lambda\bar{\Lambda}$	$(19.43 \pm 0.03) \times 10^{-4}$	0.461 ± 0.009
$\psi(2S) \rightarrow \Sigma^0\bar{\Sigma}^0$	$(2.44 \pm 0.03) \times 10^{-4}$	0.71 ± 0.11
$\psi(2S) \rightarrow \Lambda\bar{\Lambda}$	$(3.97 \pm 0.03) \times 10^{-4}$	0.824 ± 0.074

choices would give negative, and hence unphysical, values for the moduli $|E_0|$, $|E_1|$, $|M_0|$ and $|M_1|$.

The results of the fitting procedure for $|E_0|$, $|E_1|$, $|M_0|$ and $|M_1|$ are reported in Table 3.15 and

Table 3.15: Moduli of the leading and sub-leading amplitudes.

Ampl.	J/ψ	$\psi(2S)$
$ E_0 $	$(2.16 \pm 0.02) \times 10^{-2}$	$(0.42 \pm 0.07) \times 10^{-2}$
$ E_1 $	$(0.42 \pm 0.02) \times 10^{-2}$	$(0.03 \pm 0.05) \times 10^{-2}$
$ M_0 $	$(3.15 \pm 0.02) \times 10^{-2}$	$(1.72 \pm 0.02) \times 10^{-2}$
$ M_1 $	$(0.90 \pm 0.02) \times 10^{-2}$	$(0.23 \pm 0.02) \times 10^{-2}$

Table 3.16: Moduli of the strong Sachs FFs.

FFs	J/ψ	$\psi(2S)$
$ g_E^\Sigma $	$(1.99 \pm 0.04) \times 10^{-3}$	$(0.6 \pm 0.1) \times 10^{-3}$
$ g_M^\Sigma $	$(0.94 \pm 0.02) \times 10^{-3}$	$(0.94 \pm 0.02) \times 10^{-3}$
$ g_E^\Lambda $	$(1.37 \pm 0.04) \times 10^{-3}$	$(0.6 \pm 0.1) \times 10^{-3}$
$ g_M^\Lambda $	$(1.64 \pm 0.03) \times 10^{-3}$	$(1.20 \pm 0.02) \times 10^{-3}$

shown in Fig. 3.6. We calculate the corresponding values of $|g_E|$, $|g_M|$, reported in Table 3.16 and shown in Fig. 3.7. The large sub-leading J/ψ amplitudes $|E_1|$, $|M_1|$ (see Table 3.15 and Fig. 3.6) are responsible for the inversion of the $|g_E^B|$, $|g_M^B|$ hierarchy (see the upper panel of Fig. 3.7). Different Λ and Σ^0 angular distributions can be explained using an effective model

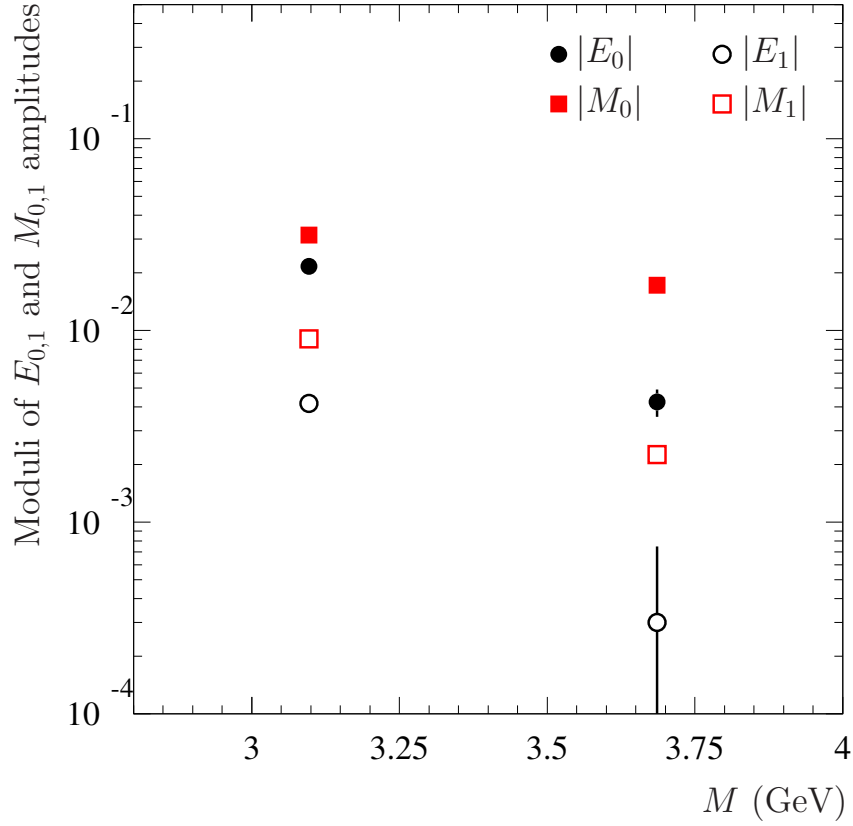


Figure 3.6: Moduli of the parameters from Table 3.15 as a function of the charmonium state mass M .

with the SU(3)-driven Lagrangian

$$\mathcal{L}_{\Sigma^0\bar{\Sigma}^0+\Lambda\bar{\Lambda}} = (G_0 + G_1)\Sigma^0\bar{\Sigma}^0 + (G_0 - G_1)\Lambda\bar{\Lambda}.$$

The interplay between leading G_0 and sub-leading G_1 contributions to the decay amplitudes determines signs and values of polarization parameters α_B .

In particular, the different behavior of the $J/\psi \rightarrow \Sigma^0\bar{\Sigma}^0$ angular distribution is due to the large values of the sub-leading amplitudes $|E_1|$ and $|M_1|$. It implies that the SU(3) mass breaking and the EM effects, which are responsible for these amplitudes, play a different role in the dynamics of the J/ψ and $\psi(2S)$ decays.

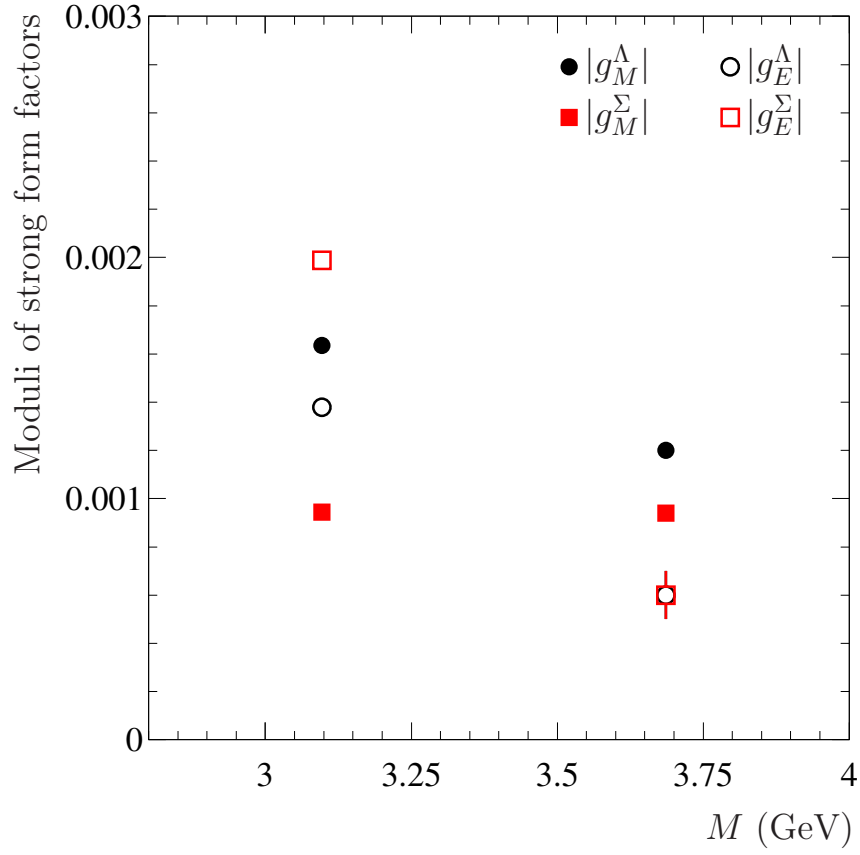


Figure 3.7: Moduli of the parameters from Table 3.16 as a function of the charmonium state mass M .

It is interesting to notice that a similar behavior has been observed also in the angular distributions of $\Sigma^0(1385)$ and $\Sigma^\pm(1385)$ measured by BESIII [128, 129].

Conclusions

Concerning the $J/\psi \rightarrow \pi^+\pi^-$ decay BaBar data suggests that it does not proceed only electromagnetically, i.e., $\text{BR}^{\text{PDG}} \neq \text{BR}^\gamma$, in particular BR^{PDG} and BR^γ differ for more than 4 standard deviations. Since the purely strong contribution is suppressed, being a G -parity violating decay, we explore the possibility of an unexpected large mixed strong-EM contribution, $gg\gamma$. Using a phenomenological model based on the Cutkosky rule, we calculate the imaginary part of the mixed strong-EM amplitude and hence a lower limit for the contribution to the total BR due to the $gg\gamma$ amplitude, $\text{BR}^{gg\gamma}$. The result agrees with the hypothesis that, at least for this particular decay with the minimum pion multiplicity in the final state, the mixed strong-EM contribution to the total BR is of the same order of the purely EM one, i.e., $13\% \text{BR}^\gamma \leq \text{BR}^{gg\gamma} \leq 37\% \text{BR}^\gamma$.

We study the theoretical modeling of the baryonic decays of the J/ψ meson, a subject that was modestly investigated about forty years ago and that is being revisited in the light of new data, especially from BESIII. In particular we consider the $J/\psi \rightarrow B\bar{B}$ decays, being B a spin-1/2 baryon of the SU(3) octet. The model is based on a hadronic Lagrangian with a SU(3)-flavor symmetry that is broken by specific sub-amplitudes of the process. These sub-amplitudes are identified with purely strong and purely EM Feynman diagrams and parameterized by free parameters. The model is completed with a mixed strong-EM sub-amplitude which is parameterized by the ratio R between the mixed and the purely strong sub-amplitudes, only for charged baryons, and with a relative phase between the EM and the strong sub-amplitudes. The obtained relative phase, $\varphi = (73 \pm 8)^\circ$, is compatible with

other results [120, 130]. For these decays we separate, for the first time, the strong, the EM and the mixed strong-EM contributions to the total BR and we give a prediction for $\text{BR}_{\Sigma^-\bar{\Sigma}^+}$, see Eq. (3.14), the only BR not yet measured and some $e^+e^- \rightarrow B\bar{B}$ cross sections at the J/ψ mass. In particular the $\text{BR}_{\Sigma^+\bar{\Sigma}^-}$, see Eq. (3.15), is predicted to be smaller than the corresponding PDG value. This fact is confirmed by a new independent preliminary analysis [118]. Finally we find that at the energy $\sqrt{q^2} \sim M_{J/\psi}$ the regime of QCD is not completely perturbative, in fact we obtain that the ratio R between the mixed strong-EM amplitude and the purely strong one is compatible with the reality hypothesis but is different from its perturbative QCD prevision, $R \sim -0.097 \neq R_{\text{pQCD}} \sim -0.030$. This fact can be seen also by looking at the behavior of the proton FF at the J/ψ mass, with a trend different from the power-law dependence predicted by perturbative QCD [131]. Moreover it is possible to explore higher energy values range, with $\sqrt{q^2} > M_{J/\psi}$, by studying particles heavier than the J/ψ meson, such as the $\psi(2S)$ one. In future more data will be available for further investigations, especially from the BESIII experiment that has just reached the World's largest J/ψ data sample.

Finally, in the case of the J/ψ and $\psi(2S)$ decays into $\Lambda\bar{\Lambda}$ and $\Sigma^0\bar{\Sigma}^0$, the angular distributions, measured by BESIII, show different behaviors. Such a difference can be explained in the framework of a model with an effective Lagrangian $\mathcal{L}_{\Sigma\Lambda} = (G_0 + G_1)\Sigma^0\bar{\Sigma}^0 + (G_0 - G_1)\Lambda\bar{\Lambda}$. We show that the interplay between dominant G_0 and sub-dominant G_1 contributions to the decay amplitudes is related to signs and values of the different polarization parameters α .

Appendix A

Notations and experimental data

A.1 Notations

In this thesis for the numerical values we consider an error with two significant figures in light of further manipulations.

We use also the following notations

QED	\longleftrightarrow	<i>Quantum Electrodynamics</i>
QCD	\longleftrightarrow	<i>Quantum Chromodynamics</i>
pQCD	\longleftrightarrow	<i>Perturbative QCD</i>
BR	\longleftrightarrow	<i>Branching Ratio</i>
PS	\longleftrightarrow	<i>Phase Space</i>
CM	\longleftrightarrow	<i>Center of Mass</i>
FF	\longleftrightarrow	<i>Form Factor</i>

We use the so-called natural units

$$\hbar = c = 1,$$

so that

$$[\text{length}] = \text{eV}^{-1}, \quad [\text{time}] = \text{eV}^{-1}, \quad [\text{speed}] = 1, \quad [\text{energy}] = \text{eV},$$

$$[\text{mass}] = \text{eV}, \quad [\text{momentum}] = \text{eV}, \quad [\text{action}] = 1, \quad [\text{surface}] = \text{eV}^{-2}$$

We use the following Minkowski metric tensor (flat space-time)

$$\eta^{\mu\nu} = \begin{pmatrix} 1 & 0 & 0 & 0 \\ 0 & -1 & 0 & 0 \\ 0 & 0 & -1 & 0 \\ 0 & 0 & 0 & -1 \end{pmatrix},$$

so that, for example,

$$x^\mu = (x^0, \vec{x}) = (x^0, x^1, x^2, x^3),$$

$$x_\mu = \eta_{\mu\nu} x^\nu = (x^0, -\vec{x}) = (x^0, -x^1, -x^2, -x^3),$$

$$x \cdot y = \eta_{\mu\nu} x^\mu y^\nu = x^\mu y_\mu = x_\mu y^\mu = x^0 y^0 - \vec{x} \cdot \vec{y} = x^0 y^0 - x^1 y^1 - x^2 y^2 - x^3 y^3.$$

We adopt also the following notations

$$\partial_\mu \equiv \frac{\partial}{\partial x^\mu}, \quad \partial^\mu \equiv \frac{\partial}{\partial x_\mu}, \quad \partial^2 \equiv \square \equiv \partial^\mu \partial_\mu,$$

A.2 Experimental data

In this appendix we report some experimental data, constants and values from PDG [28].

In particular in Tables A.1 we show masses and quantum numbers for some particles.

$$\alpha = \frac{1}{137.035\,999\,074(44)} = 7.297\,352\,5698(24) \times 10^{-3}.$$

$$1 = \hbar c = 197.326\,9718(44) \text{ MeV fm},$$

$$1 \text{ GeV} = 5.06773094(11) \text{ fm}^{-1},$$

$$1 \text{ GeV}^2 = 25.6818969(11) \text{ fm}^{-2},$$

$$1 \text{ GeV}^3 = 130.1489434(85) \text{ fm}^{-3}.$$

Table A.1: Data of some particles from PDG [28].

Lepton Mass (MeV)		Meson $I^G(J^{PC})$ Mass (MeV)		
e^-	$0.510998928 \pm 0.000000011$	π^\pm	$1^-(0^-)$	139.57018 ± 0.00035
μ^-	$105.6583715 \pm 0.0000035$	η	$0^+(0^{-+})$	547.862 ± 0.017
τ^-	1776.86 ± 0.12	η'	$0^+(0^{-+})$	957.78 ± 0.006
		ρ^0	$1^+(1^{--})$	775.26 ± 0.25
		f_1	$0^+(1^{++})$	1281.9 ± 0.5

Baryon $I(J^P)$		Mass (MeV)
p	$\frac{1}{2}(\frac{1}{2}^+)$	938.272081 ± 0.000006
n	$\frac{1}{2}(\frac{1}{2}^+)$	939.565413 ± 0.000006
Σ^+	$1(\frac{1}{2}^+)$	1189.37 ± 0.07
Σ^0	$1(\frac{1}{2}^+)$	1192.642 ± 0.024
Σ^-	$1(\frac{1}{2}^+)$	1197.449 ± 0.030
Λ	$0(\frac{1}{2}^+)$	1115.683 ± 0.006
Ξ^-	$\frac{1}{2}(\frac{1}{2}^+)$	1314.86 ± 0.20
Ξ^0	$\frac{1}{2}(\frac{1}{2}^+)$	1321.71 ± 0.07

In the International System of units we have the following expressions

elementary electric charge: $e = 1.602\,176\,565(35) \times 10^{-19} \text{ C},$

reduced Planck constant: $\hbar = 1.054\,571\,726(47) \times 10^{-34} \text{ J s},$

speed of light in vacuum: $c = 2.997\,924\,58 \times 10^8 \text{ m s}^{-1}.$

Appendix B

Decay width and branching ratio

Concerning a particular decay of the J/ψ meson there are two important quantities: its decay width (Γ) and the corresponding BR. These are related to Feynman total amplitude (\mathcal{A}) and the n -body phase space ($d\rho_n$) of the decay.

B.1 Phase space

The phase space for a n -body decay is

$$d\rho_n(P; p_1, \dots, p_n) = (2\pi)^4 \int \delta^4 \left(\sum_{i=1}^n p_i - P \right) \prod_{i=1}^n \frac{d^3 p_i}{(2\pi)^3 2E_i}, \quad (\text{B.1})$$

where P is the momentum of the decaying particle and p_1, \dots, p_n and E_1, \dots, E_n are, respectively, the momenta and the energies of the final state particles. Being a Lorentz invariant quantity it is possible to calculate it in the CM system where $P^\mu = (\sqrt{s}, 0, 0, 0)$, with $\sqrt{s} = M$, being M the mass of the decaying particle. Using this formula we have the following

particular cases:

$$\begin{aligned} d\rho_2(P; p_1, p_2) &= (2\pi)^4 \int \delta^4(p_1 + p_2 - P) \frac{d^3 p_1}{(2\pi)^3 2E_1} \frac{d^3 p_2}{(2\pi)^3 2E_2} \\ &= \frac{1}{(4\pi)^2} \int \delta(E_1 + E_2 - M) \delta^3(\vec{p}_1 + \vec{p}_2) \frac{d^3 p_1}{E_1} \frac{d^3 p_2}{E_2}, \end{aligned}$$

from which, using the masses of the two final state particles m_1 and m_2 ,

$$d\rho_2(M; m_1, m_2) = \frac{d\Omega}{32\pi^2} \sqrt{1 + \frac{(m_1^2 - m_2^2)^2}{M^4} - \frac{2(m_1^2 + m_2^2)}{M^2}},$$

where $p_{1,2} = (E_{1,2}, \vec{p}_{1,2})$ and $\vec{p}_1 = -\vec{p}_2$, with the following expressions for the energies

$$E_1 = \frac{M}{2} \left(1 + \frac{m_1^2}{M^2} - \frac{m_2^2}{M^2} \right), \quad E_2 = \frac{M}{2} \left(1 + \frac{m_2^2}{M^2} - \frac{m_1^2}{M^2} \right).$$

Moreover in the case of two particle in the final state with the same mass $m \equiv m_1 = m_2$, we put $p \equiv |\vec{p}_1| = |\vec{p}_2|$ and the phase space become

$$d\rho_2(M; m, m) = \frac{|\vec{p}|}{M} \frac{d\Omega}{16\pi^2}, \quad |\vec{p}| = \frac{M}{2} \beta, \quad \beta = \sqrt{1 - \frac{4m^2}{M^2}},$$

from which

$$d\rho_2(M; m, m) = \frac{\beta}{32\pi^2} d\Omega. \quad (\text{B.2})$$

For a three-body decay

$$d\rho_3 = \int \frac{d^3 k_1}{(2\pi)^3 2E_1} \frac{d^3 k_2}{(2\pi)^3 2E_2} \frac{d^3 k_3}{(2\pi)^3 2E_3} (2\pi)^4 \delta^4(P - p_1 - p_2 - p_3),$$

where p_1, p_2, p_3 are the four-momenta and E_1, E_2, E_3 the energies of the particles of the final state, in the CM frame, and P is the total four-momenta.

For the decay of the J/ψ meson into three particles of masses m_1, m_2, m_3 we can use the following expression [28] (valid in the case of a mean over spin states)

$$d\rho_3 = \frac{1}{(2\pi)^3} \frac{1}{16M_{J/\psi}^2} dp_{12}^2 dp_{23}^2,$$

where $M_{J/\psi}$ is the J/ψ mass, $p_{ij} \equiv p_i + p_j$ and with the following limits on p_{23}^2 and p_{12}^2

$$\begin{aligned}
(p_{23}^2)_{\min} &= \frac{(M_{J/\psi}^2 - m_1^2 + m_2^2 - m_3^2)^2}{4p_{12}^2} - \left(\sqrt{\frac{(p_{12}^2 - m_1^2 + m_2^2)^2}{4p_{12}^2} - m_2^2} \right. \\
&\quad \left. + \sqrt{\frac{(M_{J/\psi}^2 - p_{12}^2 - m_3^2)^2}{4p_{12}^2} - m_3^2} \right)^2, \\
(p_{23}^2)_{\max} &= \frac{(M_{J/\psi}^2 - m_1^2 + m_2^2 - m_3^2)^2}{4p_{12}^2} - \left(\sqrt{\frac{(p_{12}^2 - m_1^2 + m_2^2)^2}{4p_{12}^2} - m_2^2} \right. \\
&\quad \left. - \sqrt{\frac{(M_{J/\psi}^2 - p_{12}^2 - m_3^2)^2}{4p_{12}^2} - m_3^2} \right)^2, \\
(p_{12}^2)_{\min} &= (m_1 + m_2)^2, \quad (p_{12}^2)_{\max} = (M_{J/\psi} - m_3)^2.
\end{aligned}$$

In the case of a decay into three massless particles ($m_1 = m_2 = m_3 = 0$) the previous results become

$$\int d\rho_3 = \frac{1}{32\pi^3} \int_0^{M_{J/\psi}} dE_1 \int_{M_{J/\psi} - E_1}^{M_{J/\psi}} dE_2, \quad (\text{B.3})$$

with $E_1 + E_2 + E_3 = M_{J/\psi}$.

B.2 Decay width

The decay width for the decay of a particle of mass M into n particles can be calculated in its CM system and has the form

$$\Gamma(M \rightarrow n) = \frac{1}{2M} \int d\rho_n |\overline{\mathcal{A}(M \rightarrow n)}|^2,$$

where $\mathcal{A}(M \rightarrow n)$ is the Feynman amplitude of the decay. In particular for the decay of a bound state, as the J/ψ meson, we can calculate the decay width using two equivalent approach. Consider the case of the J/ψ meson ($c\bar{c}$ bound state) into a generic final state $|f\rangle$

of n particles. We can write

$$\Gamma(J/\psi \rightarrow |f\rangle) = \frac{1}{2M_{J/\psi}} \int d\rho_n \overline{|\mathcal{A}(J/\psi \rightarrow |f\rangle)|^2}, \quad (\text{B.4})$$

by using directly the decay amplitude of $J/\psi \rightarrow |f\rangle$ or

$$\Gamma(J/\psi \rightarrow |f\rangle) = \frac{4|\psi_{J/\psi}(0)|^2}{M_{J/\psi}^2} \int d\rho_n \overline{|\mathcal{A}_{\sqrt{s}=M_{J/\psi}}(c\bar{c} \rightarrow |f\rangle)|^2}. \quad (\text{B.5})$$

by using the amplitude of the scattering process $c\bar{c} \rightarrow |f\rangle$ and the absolute value of the radial wave function of the J/ψ at the origin $|\psi_{J/\psi}(0)|$ (related to probability that c and \bar{c} are at the origin). For a two-body decay into particles of the same mass m we have

$$\Gamma(J/\psi \rightarrow m, m) = \frac{\beta}{64\pi^2 M_{J/\psi}} \int d\Omega \overline{|\mathcal{A}(J/\psi \rightarrow m, m)|^2}, \quad (\text{B.6})$$

$$\Gamma(J/\psi \rightarrow m, m) = \frac{|\psi_{J/\psi}(0)|^2 \beta}{8\pi^2 M_{J/\psi}^2} \int d\Omega \overline{|\mathcal{A}_{\sqrt{s}=M_{J/\psi}}(c\bar{c} \rightarrow m, m)|^2} \quad (\text{B.7})$$

and

$$|\mathcal{A}(J/\psi \rightarrow m, m)|^2 = \frac{8|\psi_{J/\psi}(0)|^2}{M_{J/\psi}} |\mathcal{A}_{\sqrt{s}=M_{J/\psi}}(c\bar{c} \rightarrow m, m)|^2. \quad (\text{B.8})$$

B.3 Branching ratio

The BR for a general decay of a particle of mass M into a generic final state $|f\rangle$ is defined as

$$\text{BR}(M \rightarrow |f\rangle) = \frac{\Gamma(M \rightarrow |f\rangle)}{\Gamma_M}$$

where Γ_M is the total decay width of the decaying particle, i.e., the sum of all its decay widths. In the case of the J/ψ meson, using Eq. (B.6), we have the following useful result for the decay into two particle with the same mass m

$$\text{BR}(J/\psi \rightarrow m, m) = \frac{\beta}{64\pi^2 M_{J/\psi} \Gamma_{J/\psi}} \int d\Omega \overline{|\mathcal{A}(J/\psi \rightarrow m, m)|^2}. \quad (\text{B.9})$$

List of Figures

1.1	The level of charmonia [20].	9
1.2	The BESIII detector [76].	14
1.3	Feynman diagram for the process $e^+e^- \rightarrow B\bar{B}$	16
1.4	The three principal contributions to the decay $J/\psi \rightarrow \text{hadrons}$	20
1.5	Feynman diagram for the EM scattering process $c\bar{c} \rightarrow l^+l^-$	22
1.6	Feynman diagrams for the process $c\bar{c} \rightarrow \gamma\gamma\gamma$	24
1.7	Feynman diagram of the process $e^+e^- \rightarrow \psi \rightarrow B\bar{B}$, the red hexagon represents the $\psi B\bar{B}$ coupling.	25
1.8	Polarization parameter α for $\psi = J/\psi$ and for various baryon masses from 1.0 GeV to 3.0 GeV, as a function of the ratio $ g_E / g_M $	27
1.9	Ratio of the moduli of g_E and g_M for $\psi = J/\psi$ and for various baryon masses from 1.0 GeV to 3.0 GeV, as a function of the polarization parameter α	28
2.1	BABAR data on the $e^+e^- \rightarrow \pi^+\pi^-$ cross section and the fit (red line) from [101]. The vertical dashed line shows the J/ψ mass.	36
2.2	Application of the Cutkosky rule for the decay $J/\psi \rightarrow (gg\gamma)^* \rightarrow \pi^+\pi^-$	39
2.3	Feynman diagram for $\pi^+\pi^- \rightarrow \eta\gamma$ and $\pi^+\pi^- \rightarrow f_1\gamma$ mediated by the ρ^0 meson.	41
3.1	Feynman diagram for a typical process $e^+e^- \rightarrow J/\psi \rightarrow \Lambda\bar{\Lambda}$	55
3.2	Feynman diagrams for the three sub-amplitude of the decay $J/\psi \rightarrow B\bar{B}$	56

3.3	Ratios between the experimental input values of BRs and their best values obtained by minimizing the χ^2 of Eq. (3.13). The lower point, at the ordinate labelled width $\gamma \rightarrow p\bar{p}$, is the contribution due to EM BR of the proton, see Eq. (3.12).	66
3.4	Angular distribution of the baryon for the J/ψ decays into $\Lambda\bar{\Lambda}$ (upper panel) and $\Sigma^0\bar{\Sigma}^0$ (lower panel).	76
3.5	Angular distribution of the baryon for the $\psi(2S)$ decays into $\Lambda\bar{\Lambda}$ (upper panel) and $\Sigma^0\bar{\Sigma}^0$ (lower panel).	77
3.6	Moduli of the parameters from Table 3.15 as a function of the charmonium state mass M	80
3.7	Moduli of the parameters from Table 3.16 as a function of the charmonium state mass M	81

List of Tables

1.1	Principal charmonium states properties [28].	10
1.2	Principal parameters of BEPCII [77].	15
1.3	Mass and properties of spin-1/2 baryons from PDG [28].	30
2.1	Branching ratios data from PDG [28] for some of the larger BR of the J/ψ decays into mesons.	34
2.2	Branching ratios of a selection of intermediate decays [28].	39
2.3	Decay widths from Ref. [28].	47
2.4	Decay widths from Ref. [28].	50
3.1	Branching ratios data from PDG [28] for some of the larger BR of the J/ψ decays into baryons.	54
3.2	Amplitudes parametrization.	59
3.3	Branching ratios data from PDG [28] and BESIII experiment [116].	62
3.4	Values of the parameters from the χ^2 minimization.	64
3.5	Branching ratios from PDG [28] (second column), from parameters of Table 3.4 (third column) and their difference in units of the total error (fourth column).	65
3.6	Purely strong (second column), purely EM (third column) and mixed (fourth column) BRs.	68
3.7	Approximate values of moduli of the ratios between sub-amplitudes $\mathcal{A}_{B\bar{B}}^{\gamma}$ and $\mathcal{A}_{B\bar{B}}^{gg}$ (second column), and between $\mathcal{A}_{B\bar{B}}^{gg\gamma}$ and $\mathcal{A}_{B\bar{B}}^{gg}$ (third column).	68

3.8	Moduli of sub-amplitudes $\mathcal{S}_{B\bar{B}}$, $\mathcal{A}_{B\bar{B}}^\gamma$ and phase $\varphi_{B\bar{B}}$, defined in Eq. (3.9).	69
3.9	Non-resonant $e^+e^- \rightarrow B\bar{B}$ Born cross sections at $q^2 = M_{J/\psi}^2$	71
3.10	Amplitudes parameterization with a complex ratio R	72
3.11	Values of the parameters from the χ^2 minimization in the case of a complex ratio R	72
3.12	Branching ratios from PDG [28] (second column), from parameters of Table 3.11 (third column).	73
3.13	Purely strong (second column), purely EM (third column) and mixed (fourth column) BRs in the case of a complex ratio R	73
3.14	Branching ratios and polarization parameters from Ref. [116]. In particular the value of α_B for the decay $J/\psi \rightarrow \Lambda\bar{\Lambda}$ is from Ref. [109].	79
3.15	Moduli of the leading and sub-leading amplitudes.	79
3.16	Moduli of the strong Sachs FFs.	79
A.1	Data of some particles from PDG [28].	86

Acknowledgements

I would like to warmly thank my mentor and advisor, Prof. Simone Pacetti for guiding and supporting me over many years.

I would like to thank my advisor, Prof. Livio Fanò for all the support in these years.

I would like to thank my girlfriend Dr. Claudia Meazzini, for all her love and support.

I would like to thank my family for the support I have gotten over the years, especially my parents Alba and Giovanni.

I would like to thank all my colleagues and friends, the professors and researchers of the Physics and Geology Department and INFN section of Perugia, the BESIII collaboration members, especially the Italian group, for the time devoted to discussing physics and not.

I would also like to thank: Prof. Rinaldo Baldini Ferroli, for his precious support, Dr. Giulio Mezzadri for all useful discussions, and Dr. Ilaria Balossino, Prof. Monica Bertani, Dr. Diego Bettoni, Dr. Gianluigi Cibinetto, Dr. Francesca De Mori, Dr. Marco Destefanis, Dr. Riccardo Farinelli, Dr. Isabella Garzia, Dr. Michela Greco, Dr. Lia Lavezzi, Prof. Marco Maggiora, Prof. Simonetta Marcello, Dr. Stefano Spataro, Prof. Egle Tomasi-Gustafsson, Dr. Liang Yan, Dr. Kai Zhu.

Bibliography

- [1] M. Ablikim *et al.*, “Complete Measurement of the Λ Electromagnetic Form Factors,” *Phys. Rev. Lett.*, vol. 123, no. 12, p. 122003, 2019.
- [2] “Highlights, BESIII Accumulates 10 Billion J/ψ Events.” <http://bes3.ihep.ac.cn/doc/3313.html>. Accessed: 2019-10-10.
- [3] R. Baldini Ferroli, A. Mangoni, and S. Pacetti, “ G -parity violating amplitudes in the $J/\psi \rightarrow \pi^+\pi^-$ decay,” *Phys. Rev.*, vol. C98, no. 4, p. 045210, 2018.
- [4] M. Alekseev *et al.*, “A model to explain angular distributions of J/ψ and $\psi(2S)$ decays into $\Lambda\bar{\Lambda}$ and $\Sigma^0\bar{\Sigma}^0$,” *Chin. Phys.*, vol. C43, no. 2, p. 023103, 2019.
- [5] R. Baldini Ferroli, A. Mangoni, S. Pacetti, and K. Zhu, “Strong and electromagnetic amplitudes of the J/ψ decays into baryons and their relative phase,” *Phys. Lett.*, vol. B799, p. 135041, 2019.
- [6] M. Gell-Mann, “A Schematic Model of Baryons and Mesons,” *Phys. Lett.*, vol. 8, pp. 214–215, 1964.
- [7] G. Zweig, “An $SU(3)$ model for strong interaction symmetry and its breaking. Version 2,” in *DEVELOPMENTS IN THE QUARK THEORY OF HADRONS. VOL. 1. 1964 - 1978* (D. Lichtenberg and S. P. Rosen, eds.), pp. 22–101, 1964.

- [8] G. Zweig, “Fractionally charged particles and SU_6 ,” in *Symmetries in Elementary Particle Physics: International School of Physics Ettore Majorana, Erice, Italy, Aug 1964*, pp. 192–234, 1965.
- [9] P. Tarjanne and V. L. Teplitz, “SU (4) Assignments for the Vector Resonances,” *Phys. Rev. Lett.*, vol. 11, pp. 447–448, 1963.
- [10] Y. Hara, “Unitary triplets and the eightfold way,” *Phys. Rev.*, vol. 134, pp. B701–B704, 1964.
- [11] M. Gell-Mann, “The Eightfold Way: A Theory of strong interaction symmetry,” 1961.
- [12] M. Gell-Mann, “Nonleptonic weak decays and the eightfold way,” *Phys. Rev. Lett.*, vol. 12, pp. 155–156, 1964.
- [13] Y. Ne’eman, “Derivation of strong interactions from a gauge invariance,” *Nucl. Phys.*, vol. 26, pp. 222–229, 1961. [34(1961)].
- [14] M. Gell-Mann, “Symmetries of baryons and mesons,” *Phys. Rev.*, vol. 125, pp. 1067–1084, 1962.
- [15] J. D. Bjorken and S. L. Glashow, “Elementary Particles and SU(4),” *Phys. Lett.*, vol. 11, pp. 255–257, 1964.
- [16] S. L. Glashow, J. Iliopoulos, and L. Maiani, “Weak Interactions with Lepton-Hadron Symmetry,” *Phys. Rev.*, vol. D2, pp. 1285–1292, 1970.
- [17] M. K. Gaillard and B. W. Lee, “Rare Decay Modes of the K-Mesons in Gauge Theories,” *Phys. Rev.*, vol. D10, p. 897, 1974.
- [18] J. J. Aubert *et al.*, “Experimental Observation of a Heavy Particle J ,” *Phys. Rev. Lett.*, vol. 33, pp. 1404–1406, 1974.

- [19] J. E. Augustin *et al.*, “Discovery of a Narrow Resonance in e^+e^- Annihilation,” *Phys. Rev. Lett.*, vol. 33, pp. 1406–1408, 1974. [Adv. Exp. Phys.5,141(1976)].
- [20] K. Zhu, “Charmonium and Light Meson Spectroscopy,” in *Proceedings, 32nd International Symposium on Physics in Collision (PIC 2012): Strbske Pleso, Slovakia, September 12-15, 2012*, pp. 229–238, 2012.
- [21] C. Bacci *et al.*, “Preliminary Result of Frascati (ADONE) on the Nature of a New 3.1-GeV Particle Produced in e^+e^- Annihilation,” *Phys. Rev. Lett.*, vol. 33, p. 1408, 1974. [Erratum: *Phys. Rev. Lett.*33,1649(1974)].
- [22] W. Braunschweig *et al.*, “A measurement of large angle e^+e^- scattering at the 3100 MeV resonance,” *Phys. Lett.*, vol. 53B, pp. 393–396, 1974.
- [23] “<https://www.nobelprize.org/prizes/physics/1976/press-release/>.”
- [24] A. Khare, “The November J / ψ revolution: Twenty five years later,” *Curr. Sci.*, vol. 77, p. 1210, 1999.
- [25] S. Okubo, “Phi meson and unitary symmetry model,” *Phys. Lett.*, vol. 5, pp. 165–168, 1963.
- [26] J. Iizuka, K. Okada, and O. Shito, “Systematics and phenomenology of boson mass levels. 3,” *Prog. Theor. Phys.*, vol. 35, pp. 1061–1073, 1966.
- [27] S. Okubo, “Consequences of Quark Line (Okubo-Zweig-Iizuka) Rule,” *Phys. Rev.*, vol. D16, pp. 2336–2352, 1977.
- [28] M. Tanabashi *et al.*, “Review of Particle Physics,” *Phys. Rev.*, vol. D98, no. 3, p. 030001, 2018.
- [29] T. Appelquist, A. De Rujula, H. D. Politzer, and S. L. Glashow, “Charmonium Spectroscopy,” *Phys. Rev. Lett.*, vol. 34, p. 365, 1975.

- [30] G. S. Abrams *et al.*, “The Discovery of a Second Narrow Resonance in $e^+ e^-$ Annihilation,” *Phys. Rev. Lett.*, vol. 33, pp. 1453–1455, 1974. [Adv. Exp. Phys.5,150(1976)].
- [31] Z. Metreveli, “Charmonium Spectroscopy Below Open Flavor Threshold,” *eConf*, vol. C070805, p. 16, 2007.
- [32] G. Goldhaber, “From the ψ to Charmed Mesons,” *NATO Sci. Ser. B*, vol. 352, pp. 329–357, 1996.
- [33] G. Goldhaber *et al.*, “Observation in $e^+ e^-$ Annihilation of a Narrow State at 1865-MeV/ c^2 Decaying to $K \pi$ and $K \pi \pi \pi$,” *Phys. Rev. Lett.*, vol. 37, pp. 255–259, 1976.
- [34] J. P. Lansberg, “ J/ψ , ψ' and Υ production at hadron colliders: A Review,” *Int. J. Mod. Phys.*, vol. A21, pp. 3857–3916, 2006.
- [35] W. Braunschweig *et al.*, “ J/ψ and ψ' Decays Into Two Hadrons,” *Phys. Lett.*, vol. 63B, pp. 487–490, 1976.
- [36] B. Jean-Marie *et al.*, “Determination of the G Parity and Isospin of $\psi(3095)$ by Study of Multi-Pion Decays,” *Phys. Rev. Lett.*, vol. 36, p. 291, 1976.
- [37] A. A. Zholents *et al.*, “HIGH PRECISION MEASUREMENT OF THE ψ AND ψ' MESON MASSES,” *Phys. Lett.*, vol. 96B, pp. 214–216, 1980.
- [38] S. Van Der Meer, “Stochastic Cooling in the CERN Antiproton Accumulator,” *IEEE Trans. Nucl. Sci.*, vol. 28, pp. 1994–1998, 1981.
- [39] C. Baglin *et al.*, “ J/ψ Resonance Formation and Mass Measurement in Anti-proton - Proton Annihilations,” *Nucl. Phys.*, vol. B286, p. 592, 1987.

- [40] Ya. S. Derbenev, A. M. Kondratenko, S. I. Serednyakov, A. N. Skrinsky, G. M. Tumaikin, and Yu. M. Shatunov, “RADIATIVE POLARIZATION: OBTAINING, CONTROL, USING,” *Part. Accel.*, vol. 8, pp. 115–126, 1978.
- [41] J. D. Jackson and D. L. Scharre, “Initial State Radiative and Resolution Corrections and Resonance Parameters in e^+e^- Annihilation,” *Nucl. Instrum. Meth.*, vol. 128, p. 13, 1975.
- [42] K. Konigsmann, “LEPTONIC WIDTHS OF ψ AND UPSILON RESONANCES,” in *HADRONS, QUARKS AND GLUONS. PROCEEDINGS, HADRONIC SESSION OF THE 22ND RENCONTRES DE MORIOND, LES ARCS, FRANCE, MARCH 15-21, 1987*, pp. 343–350, 1987.
- [43] K. Konigsmann, “PRODUCTION, SPECTROSCOPY AND DECAYS OF HEAVY QUARK BOUND STATES,” in *6th Physics in Collision Chicago, Illinois, September 3-5, 1986*, 1986.
- [44] N. Brambilla *et al.*, “Heavy quarkonium physics,” 2004.
- [45] E. Eichten, K. Gottfried, T. Kinoshita, K. D. Lane, and T.-M. Yan, “Charmonium: The Model,” *Phys. Rev.*, vol. D17, p. 3090, 1978. [Erratum: *Phys. Rev.*D21,313(1980)].
- [46] E. Eichten and F. Feinberg, “Spin Dependent Forces in QCD,” *Phys. Rev.*, vol. D23, p. 2724, 1981.
- [47] T. Barnes, S. Godfrey, and E. S. Swanson, “Higher charmonia,” *Phys. Rev.*, vol. D72, p. 054026, 2005.
- [48] J. L. Richardson, “The Heavy Quark Potential and the Upsilon, J/ ψ Systems,” *Phys. Lett.*, vol. 82B, pp. 272–274, 1979.
- [49] G. Bhanot and S. Rudaz, “A New Potential for Quarkonium,” *Phys. Lett.*, vol. 78B, pp. 119–124, 1978.

- [50] E. Eichten and K. Gottfried, "Heavy Quarks in $e^+ e^-$ Annihilation," *Phys. Lett.*, vol. 66B, p. 286, 1977.
- [51] W. Celmaster, H. Georgi, and M. Machacek, "Potential Model of Meson Masses," *Phys. Rev.*, vol. D17, p. 879, 1978.
- [52] W. Celmaster and F. S. Henyey, "The Quark - Anti-quark Interaction at All Momentum Transfers," *Phys. Rev.*, vol. D18, p. 1688, 1978.
- [53] E. Eichten, K. Gottfried, T. Kinoshita, J. B. Kogut, K. D. Lane, and T.-M. Yan, "The Spectrum of Charmonium," *Phys. Rev. Lett.*, vol. 34, pp. 369–372, 1975. [Erratum: *Phys. Rev. Lett.* 36, 1276 (1976)].
- [54] D. B. Lichtenberg and J. G. Wills, "Heavy Meson Spectra With a New Phenomenological Potential," *Nuovo Cim.*, vol. A47, p. 483, 1978.
- [55] B. Margolis, R. Roskies, and N. De Takacsy, "POTENTIAL MODELS FOR HEAVY QUARKS AND ASYMPTOTIC FREEDOM," 1978.
- [56] B. Richter, "THE STANFORD STORAGE RING - SPEAR," *Kerntech.*, vol. 12, p. 531, 1970.
- [57] M. Allen *et al.*, "SPEAR: Status and Improvement Program.," in *Proceedings, 9th International Conference on the High-Energy Accelerators (HEACC 1974): Stanford, California, May 2-7, 1974*, pp. 37–42, 1974.
- [58] C. J. Biddick *et al.*, "Inclusive gamma-Ray Spectra from ψ (3095) and ψ' (3684)," *Phys. Rev. Lett.*, vol. 38, p. 1324, 1977.
- [59] A. Barbaro-Galtieri *et al.*, "Electron-Muon and electron-Hadron Production in $e^+ e^-$ Collisions," *Phys. Rev. Lett.*, vol. 39, p. 1058, 1977.

- [60] F. Amman *et al.*, “Adone - The Frascati 1.5 GeV Electron Positron Storage Ring,” in *Proceedings, 5th International Conference on High-Energy Accelerators, HEACC 1965: Frascati, Italy, September 09–16, 1965*, pp. 703–707, 1965.
- [61] F. Amman *et al.*, “Two-beam operation of the 1.5 GeV electron-positron storage ring adone,” *Lett. Nuovo Cim.*, vol. 1S1, pp. 729–737, 1969. [Lett. Nuovo Cim.1,729(1969)].
- [62] W. W. Ash, G. T. Zorn, and B. Bartoli, “Experimental Study of the New 3.1 GeV Particle by e^+e^- Collision at #technADONE,” *Lett. Nuovo Cim.*, vol. 11, p. 705, 1974.
- [63] K. Steffen, “Final parameters and status of desy double storage rings,” in *Proceedings, 7th International Conference on High-energy Accelerators, HEACC 1969, v.2: Yerevan, USSR, August 27 – September 02, 1969*, vol. 2, pp. 60–80, 1969.
- [64] J. Le Duff *et al.*, “DORIS, Present Status and Future Plans,” in *Proceedings, 9th International Conference on the High-Energy Accelerators (HEACC 1974): Stanford, California, May 2-7, 1974*, pp. 43–48, 1974.
- [65] H. J. Besch, H. W. Eisermann, B. Lohr, G. Noldeke, M. Tonutti, R. Wilcke, H. Kowalski, H. J. Von Eyss, and H. Von Der Schmitt, “Measurement of J/ψ Decays Into Channels Containing Charged and Neutral Anti-nucleons,” *Z. Phys.*, vol. C8, pp. 1–5, 1981.
- [66] Z. Arzelier *et al.*, “The Orsay Compensated Colliding Beam Rings (DCI),” *eConf*, vol. C710920, p. 150, 1971.
- [67] P. Marin, “Design And Status Of Dci,” in *Proceedings, 9th International Conference on the High-Energy Accelerators (HEACC 1974): Stanford, California, May 2-7, 1974*, pp. 49–52, 1974.
- [68] J. E. Augustin *et al.*, “Measurement of $e^+e^- \rightarrow e^+e^-$ and $e^+e^- \rightarrow \mu^+\mu^-$ at SPEAR,” *Phys. Rev. Lett.*, vol. 34, p. 233, 1975.

- [69] R. Brandelik *et al.*, “RESULTS FROM DASP ON E^+E^- ANNIHILATION BETWEEN 3.1-GEV AND 5.2-GEV,” *Z. Phys.*, vol. C1, pp. 233–256, 1979.
- [70] W. Bartel *et al.*, “Measurement of the Branching Ratios for the Decays $J/\psi \rightarrow \rho + \pi$ and $J/\psi \rightarrow \gamma + \eta'$,” *Phys. Lett.*, vol. 64B, pp. 483–487, 1976.
- [71] J. Burmester *et al.*, “The Total Hadronic Cross-Section for e^+e^- Annihilation Between 3.1-GeV and 4.8-GeV Center-Of-Mass Energy,” *Phys. Lett.*, vol. 66B, pp. 395–400, 1977.
- [72] M. Oreglia *et al.*, “A Study of the Reaction $\psi' \rightarrow \gamma \gamma J/\psi$,” *Phys. Rev.*, vol. D25, p. 2259, 1982.
- [73] G. S. Abrams *et al.*, “Measurement of the Radiative Width of the η' in Two Photon Interactions at SPEAR,” *Phys. Rev. Lett.*, vol. 43, p. 477, 1979.
- [74] J. E. Augustin *et al.*, “Dm2: A Magnetic Detector for the Orsay Storage Ring DCI,” *Phys. Scripta*, vol. 23, pp. 623–633, 1981.
- [75] P. Zweber, “Charm Factories: Present and Future,” *AIP Conf. Proc.*, vol. 1182, pp. 406–409, 2009.
- [76] C.-Z. Yuan and S. L. Olsen, “The BESIII physics programme,” *Nature Rev. Phys.*, vol. 1, no. 8, pp. 480–494, 2019.
- [77] M. Ablikim *et al.*, “Design and Construction of the BESIII Detector,” *Nucl. Instrum. Meth.*, vol. A614, pp. 345–399, 2010.
- [78] J. G. Korner, “The $N - \Delta$ Transition Form-factor and Anomalous ψ Decays Into Octet Decuplet Baryon - Anti-baryon Pairs,” *Z. Phys.*, vol. C33, p. 529, 1987.
- [79] L. Kopke and N. Wermes, “ J/ψ Decays,” *Phys. Rept.*, vol. 174, p. 67, 1989.
- [80] M. Claudson, S. L. Glashow, and M. B. Wise, “Isospin Violation in $J/\psi \rightarrow$ Baryon Anti-baryon,” *Phys. Rev.*, vol. D25, p. 1345, 1982.

- [81] C. Bini, “Final results of a new measurement of the J/ψ decays in nucleon antinucleon pairs,” *Nucl. Phys. Proc. Suppl.*, vol. 75, pp. 195–198, 1999. [195(1999)].
- [82] T. Appelquist and H. D. Politzer, “Orthocharmonium and e^+e^- Annihilation,” *Phys. Rev. Lett.*, vol. 34, p. 43, 1975.
- [83] M. S. Chanowitz, “Comment on the Decay of $\psi(3.1)$ Into Even G - Parity States,” *Phys. Rev.*, vol. D12, p. 918, 1975.
- [84] L. B. Okun and M. B. Voloshin, “On the Charmonium Decays,” 1976.
- [85] T. Appelquist and H. D. Politzer, “Heavy Quarks and Longlived Hadrons,” *Phys. Rev.*, vol. D12, p. 1404, 1975.
- [86] T. Appelquist, R. M. Barnett, and K. D. Lane, “Charm and Beyond,” *Ann. Rev. Nucl. Part. Sci.*, vol. 28, pp. 387–499, 1978.
- [87] P. B. Mackenzie and G. P. Lepage, “QCD corrections to the gluonic width of Υ meson,” *AIP Conf. Proc.*, vol. 74, pp. 176–192, 1981.
- [88] W. Kwong, J. L. Rosner, and C. Quigg, “Heavy Quark Systems,” *Ann. Rev. Nucl. Part. Sci.*, vol. 37, pp. 325–382, 1987.
- [89] W. Kwong, P. B. Mackenzie, R. Rosenfeld, and J. L. Rosner, “Quarkonium Annihilation Rates,” *Phys. Rev.*, vol. D37, p. 3210, 1988.
- [90] R. Barbieri, R. Gatto, and E. Remiddi, “QCD Radiative Corrections to Hyperfine Splitting in Quarkonium,” *Phys. Lett.*, vol. 106B, p. 497, 1981.
- [91] R. Van Royen and V. F. Weisskopf, “Hadron Decay Processes and the Quark Model,” *Nuovo Cim.*, vol. A50, pp. 617–645, 1967. [Erratum: *Nuovo Cim.*A51,583(1967)].
- [92] E. D. Bloom and C. Peck, “Physics with the Crystal Ball Detector,” *Ann. Rev. Nucl. Part. Sci.*, vol. 33, pp. 143–197, 1983.

- [93] G. Salzman, “Neutron-Electron Interaction,” *Phys. Rev.*, vol. 99, pp. 973–979, 1955.
- [94] F. J. Ernst, R. G. Sachs, and K. C. Wali, “Electromagnetic form factors of the nucleon,” *Phys. Rev.*, vol. 119, pp. 1105–1114, 1960.
- [95] K. Zhu, X.-H. Mo, and C.-Z. Yuan, “Determination of the relative phase in ψ' and J/ψ decays into baryon and antibaryon,” *Int. J. Mod. Phys.*, vol. A30, no. 25, p. 1550148, 2015.
- [96] G. López Castro, J. L. Lucio M., and J. Pestieau, “Tests of flavor symmetry in J/ψ decays,” *AIP Conf. Proc.*, vol. 342, pp. 441–448, 1995.
- [97] H. E. Haber and J. Perrier, “A Model Independent Analysis of Hadronic Decays of J/ψ and η_c (2980),” *Phys. Rev.*, vol. D32, p. 2961, 1985.
- [98] N. Morisita, I. Kitamura, and T. Teshima, “ J/ψ Decays and the Pseudoscalar Meson Mixing,” *Phys. Rev.*, vol. D44, pp. 175–181, 1991.
- [99] J. Milana, S. Nussinov, and M. G. Olsson, “Does $J/\psi \rightarrow \pi^+\pi^-$ fix the electromagnetic form-factor $F_\pi(t)$ at $t = M^2(J/\psi)$?” *Phys. Rev. Lett.*, vol. 71, pp. 2533–2536, 1993.
- [100] R. B. Ferroli *et al.*, “A new G -parity violating amplitude in the J/ψ decay?,” *Phys. Rev.*, vol. D95, no. 3, p. 034038, 2017.
- [101] J. P. Lees *et al.*, “Precise Measurement of the $e^+e^- \rightarrow \pi^+\pi^-(\gamma)$ Cross Section with the Initial-State Radiation Method at BABAR,” *Phys. Rev.*, vol. D86, p. 032013, 2012.
- [102] B. Aubert *et al.*, “The $e^+e^- \rightarrow \pi^+\pi^-\pi^+\pi^-$, $K^+K^-\pi^+\pi^-$, and $K^+K^-K^+K^-$ cross sections at center-of-mass energies 0.5-GeV - 4.5-GeV measured with initial-state radiation,” *Phys. Rev.*, vol. D71, p. 052001, 2005.

- [103] B. Aubert *et al.*, “The $e^+e^- \rightarrow 3(\pi^+\pi^-), 2(\pi^+\pi^-\pi^0)$ and $K^+K^-2(\pi^+\pi^-)$ cross sections at center-of-mass energies from production threshold to 4.5-GeV measured with initial-state radiation,” *Phys. Rev.*, vol. D73, p. 052003, 2006.
- [104] G. J. Gounaris and J. J. Sakurai, “Finite width corrections to the vector meson dominance prediction for $\rho \rightarrow e^+e^-$,” *Phys. Rev. Lett.*, vol. 21, pp. 244–247, 1968.
- [105] R. E. Cutkosky, “Singularities and discontinuities of Feynman amplitudes,” *J. Math. Phys.*, vol. 1, pp. 429–433, 1960.
- [106] S. Pacetti, “Study of the $\phi\pi^0$ transition form factor,” *Nucl. Phys.*, vol. A919, pp. 15–31, 2013.
- [107] A. S. Rudenko, “ $f_1(1285) \rightarrow e^+e^-$ decay and direct f_1 production in e^+e^- collisions,” *Phys. Rev.*, vol. D96, no. 7, p. 076004, 2017.
- [108] J. P. Lees *et al.*, “Study of the $e^+e^- \rightarrow K^+K^-$ reaction in the energy range from 2.6 to 8.0 GeV,” *Phys. Rev.*, vol. D92, no. 7, p. 072008, 2015.
- [109] M. Ablikim *et al.*, “Polarization and Entanglement in Baryon-Antibaryon Pair Production in Electron-Positron Annihilation,” *Nature*, 2019.
- [110] S. J. Brodsky, G. P. Lepage, and S. F. Tuan, “Exclusive Charmonium Decays: The $J/\psi(\psi') \rightarrow \rho\pi, K^*\bar{K}$ Puzzle,” *Phys. Rev. Lett.*, vol. 59, p. 621, 1987.
- [111] S. J. Brodsky and G. P. Lepage, “Helicity Selection Rules and Tests of Gluon Spin in Exclusive QCD Processes,” *Phys. Rev.*, vol. D24, p. 2848, 1981.
- [112] V. L. Chernyak and I. R. Zhitnitsky, “Nucleon Wave Function and Nucleon Form-Factors in QCD,” *Nucl. Phys.*, vol. B246, pp. 52–74, 1984.
- [113] R. Baldini, C. Bini, and E. Luppi, “Measuring the phase of the J/ψ strong decay amplitudes,” *Phys. Lett.*, vol. B404, pp. 362–368, 1997.

- [114] M. Ablikim *et al.*, “Study of $J/\psi \rightarrow p\bar{p}$ and $J/\psi \rightarrow n\bar{n}$,” *Phys. Rev.*, vol. D86, p. 032014, 2012.
- [115] J. Jousset *et al.*, “The $J/\psi \rightarrow$ Vector + Pseudoscalar Decays and the η , η' Quark Content,” *Phys. Rev.*, vol. D41, p. 1389, 1990.
- [116] M. Ablikim *et al.*, “Study of J/ψ and $\psi(3686)$ decay to $\Lambda\bar{\Lambda}$ and $\Sigma^0\bar{\Sigma}^0$ final states,” *Phys. Rev.*, vol. D95, no. 5, p. 052003, 2017.
- [117] M. Ablikim *et al.*, “Study of $e^+e^- \rightarrow p\bar{p}$ via initial state radiation at BESIII,” *Phys. Rev.*, vol. D99, no. 9, p. 092002, 2019.
- [118] L. Y. et al., “Study of $J\psi$ and $\psi(3686) \rightarrow \Sigma^+\bar{\Sigma}^-$.” BESIII Collaboration Internal Document - Bes Analysis Memo 00272, August 2019.
- [119] R. Baldini *et al.*, “Measurement of $J/\psi \rightarrow N\bar{N}$ branching ratios and estimate of the phase of the strong decay amplitude,” *Phys. Lett.*, vol. B444, pp. 111–118, 1998.
- [120] M. Ablikim *et al.*, “First observation of the isospin violating decay $J/\psi \rightarrow \Lambda\bar{\Sigma}^0 + c.c.$,” *Phys. Rev.*, vol. D86, p. 032008, 2012.
- [121] M. Ablikim *et al.*, “Study of J/ψ decays to $\Lambda\bar{\Lambda}$ and $\Sigma^0\bar{\Sigma}^0$,” *Phys. Lett.*, vol. B632, pp. 181–186, 2006.
- [122] D. Pallin *et al.*, “Baryon Pair Production in J/ψ Decays,” *Nucl. Phys.*, vol. B292, p. 653, 1987.
- [123] M. Ablikim, M. N. Achasov, O. Albayrak, and D. J. Ambrose, “Determination of the number of ψ' event at BESIII,” *Chin. Phys.*, vol. C37, p. 063001, 2013.
- [124] B. Aubert *et al.*, “Study of $e^+e^- \rightarrow \Lambda\bar{\Lambda}$, $\Lambda\bar{\Sigma}^0$, $\Sigma^0\bar{\Sigma}^0$ using initial state radiation with BABAR,” *Phys. Rev.*, vol. D76, p. 092006, 2007.

-
- [125] T. K. Pedlar *et al.*, “Branching fraction measurements of $\psi(2S)$ decay to baryon-antibaryon final states,” *Phys. Rev.*, vol. D72, p. 051108, 2005.
- [126] M. Ablikim *et al.*, “Measurements of $\psi(2S)$ decays to octet baryon-antibaryon pairs,” *Phys. Lett.*, vol. B648, pp. 149–155, 2007.
- [127] S. Dobbs, A. Tomaradze, T. Xiao, K. K. Seth, and G. Bonvicini, “First measurements of timelike form factors of the hyperons, $\Lambda^0, \Sigma^0, \Sigma^+, \Xi^0, \Xi^-,$ and Ω^- , and evidence of diquark correlations,” *Phys. Lett.*, vol. B739, pp. 90–94, 2014.
- [128] M. Ablikim *et al.*, “Study of J/ψ and $\psi(3686) \rightarrow \Sigma(1385)^0 \bar{\Sigma}(1385)^0$ and $\Xi^0 \bar{\Xi}^0$,” *Phys. Lett.*, vol. B770, pp. 217–225, 2017.
- [129] M. Ablikim *et al.*, “Study of ψ decays to the $\Xi^- \bar{\Xi}^+$ and $\Sigma(1385)^\mp \bar{\Sigma}(1385)^\pm$ final states,” *Phys. Rev.*, vol. D93, no. 7, p. 072003, 2016.
- [130] D.-H. Wei, “The $SU(3)$ symmetry breaking in J/ψ decays,” *J. Phys.*, vol. G36, p. 115006, 2009.
- [131] E. Tomasi-Gustafsson and M. P. Rekalo, “Search for evidence of asymptotic regime of nucleon electromagnetic form-factors from a compared analysis in space- and time - like regions,” *Phys. Lett.*, vol. B504, pp. 291–295, 2001.